JOINT TRANSPORTATION
RESEARCH PROGRAM
INDIANA DEPARTMENT OF TRANSPORTATION
AND PURDUE UNIVERSITY

Laser Mobile Mapping Standards and Applications in Transportation

Steven D. Johnson, James S. Bethel,
Chisaphat Supunyachotsakul, Scott Peterson

SPR-3706 • Report Number: FHWA/IN/JTRP-2016/01 • DOI: 10.5703/1288284316164

RECOMMENDED CITATION

Johnson, S. D., Bethel, J. S., Supunyachotsakul, C., & Peterson, S. (2016). *Laser mobile mapping standards and applications in transportation* (Joint Transportation Research Program Publication No. FHWA/IN/JTRP-2016/01). West Lafayette, IN: Purdue University. http://dx.doi.org/10.5703/1288284316164

AUTHORS

Steven D. Johnson, PhD
Associate Professor of Civil Engineering
Lyles School of Civil Engineering
Purdue University
(765) 494-0786
steven@ecn.purdue.edu
Corresponding Author

James S. Bethel, PhD
Associate Professor of Civil Engineering
Lyles School of Civil Engineering
Purdue University

Chisaphat Supunyachotsakul
Graduate Research Assistant
Lyles School of Civil Engineering
Purdue University

Scott Peterson
Assistant Professor
Department of Civil and Geomatics Engineering
California State University, Fresno

JOINT TRANSPORTATION RESEARCH PROGRAM

The Joint Transportation Research Program serves as a vehicle for INDOT collaboration with higher education institutions and industry in Indiana to facilitate innovation that results in continuous improvement in the planning, design, construction, operation, management and economic efficiency of the Indiana transportation infrastructure. https://engineering.purdue.edu/JTRP/index_html

Published reports of the Joint Transportation Research Program are available at http://docs.lib.purdue.edu/jtrp/.

NOTICE

COPYRIGHT

Print ISBN: 978-1-62260-400-5
ePUB ISBN: 978-1-62260-401-2

TECHNICAL REPORT STANDARD TITLE PAGE

1. Report No.	2. Government Accession No.	3. Recipient's Catalog No.
FHWA/IN/JTRP-2016/01		

4. Title and Subtitle	5. Report Date
Laser Mobile Mapping Standards and Applications in Transportation	November 2015
	6. Performing Organization Code

7. Author(s)	8. Performing Organization Report No.
Steven D. Johnson, James S. Bethel, Chisaphat Supunyachotsakul, Scott Peterson	FHWA/IN/JTRP-2016/01

9. Performing Organization Name and Address	10. Work Unit No.
Joint Transportation Research Program Purdue University 550 Stadium Mall Drive West Lafayette, IN 47907-2051	
	11. Contract or Grant No. SPR-3706

12. Sponsoring Agency Name and Address	13. Type of Report and Period Covered
Indiana Department of Transportation State Office Building 100 North Senate Avenue Indianapolis, IN 46204	Final Report
	14. Sponsoring Agency Code

15. Supplementary Notes
Prepared in cooperation with the Indiana Department of Transportation and Federal Highway Administration.

16. Abstract

This report describes the work that was done to support the development of a chapter for the INDOT Survey Manual on Mobile Mapping. The work includes experiments that were done, data that was collected, analysis that was carried out, and conclusions that were drawn about accuracy of Mobile Terrestrial Laser Scanning (MTLS) systems. The resulting Manual chapter, located in the appendix, defines standards and procedures for preparing, collecting, editing, delivering, exploiting, and archiving electronic mapping data that is created for Indiana Department of Transportation (INDOT). The purpose of the standards and procedures within this manual is to obtain statewide uniformity within the INDOT combined Aerial/Ground Survey process, to establish and maintain MTLS Standards for INDOT and contracted consultants, and allow for all of the project data to be effectively managed from conception to completion. These standards apply to all projects delivered to INDOT by contracted consulting firms, or exchanged internally within INDOT or between state agencies. The standards and procedures are the result of mobile terrestrial laser scanning surveys of two test sites - one urban and one freeway - created for this project. After establishing reference control points on the sites, each site was surveyed by four mobile terrestrial laser scanning vendors. The results from the vendor data over the test sites, in addition to information in published literature, are the basis for the specifications manual. The proposed chapter for the Survey Manual is in Appendix E of this report.

17. Key Words	18. Distribution Statement
Mobile Terrestrial Laser Scanning, accuracy evaluation, mobile LiDAR	No restrictions. This document is available to the public through the National Technical Information Service, Springfield, VA 22161.

19. Security Classif. (of this report)	20. Security Classif. (of this page)	21. No. of Pages	22. Price
Unclassified	Unclassified	93	

Form DOT F 1700.7 (8-69)

EXECUTIVE SUMMARY

LASER MOBILE MAPPING STANDARDS AND APPLICATIONS IN TRANSPORTATION

Introduction

The objective of this project was to develop a draft INDOT Manual for laser mobile mapping. One urban street test site and one rural highway test site were selected and reference control points were established. The test sites were mapped by four commercial mobile mapping vendors. From the test site scanning results, a performance-based process for evaluating vendor results was demonstrated, and quality assurance and quality control procedures were developed and incorporated in a proposed manual for laser mobile mapping.

Findings

Our findings include specifications and procedures for performance-based evaluation of mobile mapping vendors, both design-grade and asset-grade scanning systems, and processes for measuring and evaluating absolute accuracy and relative accuracy.

The following table summarizes the accuracies obtained by both design and asset grade mobile mapping systems (at the 95% probability level). Be aware of this 95% value when comparing our results with others in the literature, which may be in terms of Root Mean Squares Error (RMSE) or standard deviation (68% probability level).

95% Critical values for testing MMS results.

MMS Grade	Absolute Accuracy		Relative Accuracy (over small area)
	Horizontal (cm)	Vertical (cm)	Vertical (cm)
Design	<8	<5	<5
Asset	<18	<24	<6

In addition, components of a quality assurance and quality control plan for a mobile scanning project are discussed. Other specific findings, too numerous to fully discuss here, include absolute and relative accuracy statistics for each of the four vendors, accuracy statistics for a bridge clearance measurement, effects of different scanning rate settings, and driving techniques.

Implementation

One or more test sites may be established by INDOT with known mapping project control points and known validation checkpoints, or INDOT could continue to use the project test sites in West Lafayette. The vendors would then scan the test site and deliver a final point cloud that is adjusted to the project control. The coordinates of the validation points withheld from the adjustment would be extracted from the point cloud and tested for accuracy. Painted targets on the roadway or geometric target objects mounted on tripods along the roadway or other feature points may be used. Algorithms and computer code have been developed for INDOT to accurately and semi-automatically extract the validation point coordinates.

CONTENTS

ABBREVIATIONS

DMI	Distance Measurement Indicator
GNSS	Global Navigation Satellite Systems
HI	Height of Instrument
IMU	Inertial Measurement Unit
INDOT	Indiana Department of Transportation
LiDAR	Light Detection and Ranging
MMS	Mobile Mapping System
MTLS	Mobile Terrestrial Laser Scanning
RMSE	Root Mean Squares Error
RTK	Real Time Kinematic
SPCS	State Plane Coordinate System
STLS	Static Terrestrial Laser Scanning

LIST OF TABLES

LIST OF FIGURES

1. INTRODUCTION

1.1 Background and Problems

Light Detection and Ranging (LiDAR) is a technology that uses a laser scanner to obtain local information about the positions and reflectivities of the objects being surveyed. A basic LiDAR device combines a ranging instrument, a beam steering mechanism, and a sampling capability to produce discrete points in the surrounding 3D space. The fundamental result of this technique is known as the "point cloud." This point cloud contains three dimensional position and intensity data (X, Y, Z, I). The intensity data gives information about the reflectivity of the survey object surfaces under that scanning environment.

Mobile Terrestrial Laser Scanning (MTLS) is a technology that combines LiDAR, optical cameras, a Global Navigation Satellite System (GNSS) receiver, Inertial Measurement Unit (IMU), Distance Measurement Indicator (DMI, a vehicle wheel revolution counter) as well as other devices. The combined system produces a registered geospatial dataset from these instruments mounted on moving terrestrial vehicle. The moving vehicle can be a van, a Sport Utility Vehicle (SUV), truck, boat, or rail vehicle as dictated by the scanning requirements. The Mobile Terrestrial Laser Scanner (MTLS) is often referred to as a Mobile Laser Scanner (MLS) and may also be referred to as a Mobile Mapping System (MMS).

Mobile Terrestrial Laser Scanning (MTLS) or Mobile Mapping System (MMS) Technology is emerging today as a popular choice for mapping in transportation rights of way. Advances in laser scanning and positioning instruments allow a scene to be rapidly scanned resulting in rich 3D point clouds and their associated reflectance or intensity information.

MMS technology is widely used as the survey method in many engineering and science applications. Nowadays, MMS technology is a very popular survey method for transportation applications (see Williams, Olsen, Roe, & Glennie, 2013); however, as of March 2015 there are only a few MMS Specifications Manuals or MMS Standards developed by the Transportation Research Board of the National Academies (Olsen et al., 2013) and state Departments of Transportation—for example, California (Caltrans, 2011) and Florida (FDOT, 2012). Similar documents have also been written by other agencies and private companies (see Austroads, Ltd. (2014), Certainty 3D (2012), and Continental Mapping Consultants, Inc. (2013)). Existing MMS Specifications Manuals or Standards of peer states and other parties are somewhat useful but not always applicable or appropriate with the continual advances of MTLS technology. This is because most of the existing MMS Specifications Manuals or Standards are written from the operation-based or procedural point of view, suggesting that vendors perform MMS data collection by following lists of suggested operational procedures. Many of their suggestions are obsolete and many of the technically related numbers or values are suggested to be adopted without reported justification.

Since agencies without well-established MMS Specifications Manuals or Standards must rely only on vendor proposals, the Indiana Department of Transportation (INDOT) has seen the importance of having its own MMS Specifications Manual developed for the emerging use of MMS technology as an accepted survey method for transportation applications.

Another important aspect to consider for MTLS technology is the quantification of its accuracy. Some transportation applications require very high absolute accuracy whereas in some applications a high relative accuracy sufficient. As such, to ensure the quality of the MMS survey point clouds as well as their derived products, quantifying accuracy of MMS surveys is essential. The aforementioned needs for INDOT to have its own specifications manual and the justification of those specifications, constitutes the objective of this project.

1.2 Problem Statement

INDOT requires a chapter in its Survey Manual covering Mobile Mapping Systems. We must design and carry out a series of experiments using commercial data providers, to justify the numerical and procedural recommendations in that chapter.

2. PROJECT OBJECTIVE / PURPOSE

The objective of this project is to develop the **Mobile Terrestrial Laser Scanning (MTLS) Specifications Manual** for INDOT. It is to be expected that the developed MTLS Specifications Manual, once finalized, will be part of the INDOT Survey Design Manual. It will serve as the reference for INDOT's communication with contractors for projects exploiting MTLS technology. It has been foreseen that the use of the developed MTLS Specifications Manual will allow for all of the project data to be effectively managed from conception to completion.

The project team has agreed on the strategy that the developed MTLS Specifications Manual will be performance driven rather than procedural or operation-based. This makes sense because LiDAR and related system sensors continue to evolve and improve, rendering specific operational procedures quickly obsolete. This will hopefully enhance the usefulness and longevity of the accompanying, proposed manual chapter.

A supporting objective of this project is to construct a test facility for use in the evaluation of commercial Mobile Mapping System accuracy. The motivation for constructing the test site is to establish a common, objective criterion for evaluation of accuracy and performance among the vendors chosen to provide data. Many technically related numbers or values to be presented in the MTLS Specifications Manual are obtained and justified through the results of accuracy evaluation of the MMS data collected on the test site.

From the aforementioned description we can summarize the objectives of this project as:

1. To establish a test site and testing procedures for use in the evaluation of commercial Mobile Mapping Systems (MMS) accuracy.
2. To develop the Mobile Terrestrial Laser Scanning (MTLS) Specifications Manual for INDOT, which is proposed to be incorporated into the Survey Design Manual.

3. WORK PLAN

In this section the overall ideas of how the project objectives are to be achieved will be presented. This is mainly to give readers the big picture about tasks and procedures which are required to be performed in order to arrive at the written MTLS Specifications Manual. These tasks mainly consist of evaluating actual commercial data collected on the test site.

Based on the objectives of this project the main tasks of the project are grouped into 2 parts as follows:

1. Collect, analyze, and evaluate commercial MMS data on the test site.
2. Develop the Mobile Terrestrial Laser Scanning (MTLS) Specifications Manual. It is a separate document from this report and will, itself, serve as the manual or the reference for the use of MTLS technology. This written MTLS Specifications Manual for INDOT can be found in Appendix E.

It is important to reemphasize that the outcomes in part 1, which are the findings and knowledge obtained from the use of the developed test site, are essential in the development of the MTLS Specifications Manual. This is because many of the technically related numbers and values as well as some other insights presented in the MTLS Specifications Manual are substantiated and justified through these findings.

The MTLS Specifications Manual, which is a separate document, is attached in Appendix E. Therefore most of the contents of this document are devoted to the tasks in part 1.

3.1 Test Site Planning

In this section, an overview of tasks related to the design and use of the test site will be covered.

In order for the test site to serve the purpose of evaluating accuracy, it had to be designed considering a number of related factors. These factors represented different environmental conditions, equipment characteristics, or operating procedures which might plausibly affect accuracies. The following factors were chosen to be included in the study. They were not necessarily included as formal factors in an experiment design, but rather were included to make sure that representative conditions were present in the testing.

- Two different types of roadway environments:
  1. Highway or freeway style roadway; and
  2. Urban style roadway where the driving neighborhoods are commercial buildings, residences, and other urban features.
- Different grade of MMS used (conventionally known as design grade and asset grade).
- Different data collection driving technique.
- Different selectable data collection (sampling) rate.

The above mentioned factors are considered in designing/selecting the test sites, as well as in the designing of the data collection operational procedures and settings.

3.1.1 Test Site

The test site for this project is actually two separate sites that represent different types of roadway environments. The first site is an open freeway setting that includes an overpass railroad bridge. It is along the new US 231 bypass west of West Lafayette (passing the Purdue University Airport). This site is referred to here as "231Route" for short. It is approximately 2.93 km (1.82 mi.) long. The second site is set in an urban setting, in the vicinity of the INDOT Research Facility in West Lafayette. This site is referred to here as "INDOTLoop." It is approximately 3.15 km (1.96 mi.) long. Image maps of these two sites (231Route and INDOTLoop) can be found in Figures 3.1 and 3.3, respectively. The overpass railroad bridge on the 231Route is shown in Figure 3.2. The data collections are performed on both sites (231Route and INDOTLoop).

3.2 Tasks Performed to Arrive at MTLS Specifications Manual

Many procedures and tasks are necessary to support the development of the Mobile Terrestrial Laser Scanning (MTLS) Specifications Manual for INDOT. The development of this Manual has involved the tasks as listed below.

Task 1: Review existing INDOT mapping requirements and mapping specifications which make use of legacy technologies

Task 2: Consider mobile mapping applications of interest to INDOT

Task 3: Examine and synthesize mapping specifications and mobile mapping guidelines from peer states and related agencies

Task 4: Develop test site to be used in evaluation process of mobile mapping technology and its accuracy, develop analysis tools

Task 5: Evaluate the accuracy of mobile mapping data through the use of test site and the developed accuracy evaluating procedures

Task 6: Develop content for MTLS Specifications or Standards from all of the above sources

Tasks 1, 2, and 3 were performed in a parallel fashion and they can be considered as a literature review type of work. This consisted of studying and reviewing existing mobile mapping standards and their related

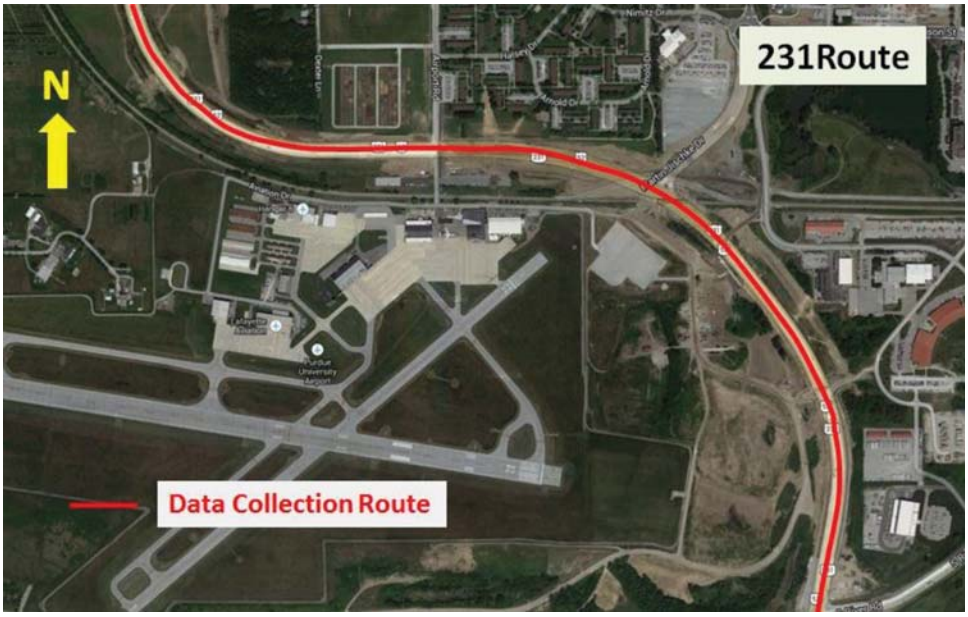

Figure 3.1 The 231Route.

documents. Interviews with numerous officials in various departments of INDOT (design, bridges, safety, construction, etc.) have also been conducted to get some indication about mobile mapping applications of potential interest to INDOT. Task 6 was started once some information had been gathered through the performance of Tasks 1, 2, and 3. Tasks 4 and 5 were then started in order to make the Test site ready for the MMS data collection process. Task 6 continued to be addressed during the performance of Tasks 4 and 5. Once the test site was finalized and the MMS data collection processes have been completed, the Task 5 was then begun. The results, findings and knowledge gained through the performance of Tasks 4 and 5 are incorporated in the contents of MTLS Specifications Manual; the manual was refined and updated throughout the project.

Figure 3.2 Bridge overpass on 231Route.

3.3 Data Collection Planning

As discussed in section 3.1, the factors affecting accuracy of the MMS data will be investigated and studied through the datasets obtained from MMS data collection on the test site. We approached a number of vendors who provide MMS services, trying to get low cost data in exchange for sharing our test results. Our thinking was to just ask them to scan the sites as they normally would for a regular customer, without any guidelines from us on operations, etc. An exception was made to make sure that we had examples of different driving techniques, different sampling frequencies, and different nominal data qualities (design vs. asset grade). We knew that most vendors would want control points to register their data, so we planned to provide coordinates of painted control targets on the pavement surface to satisfy this requirement. In addition we wanted to have withheld control also known as checkpoints or validation points for our own analysis. Detailed descriptions of all of this will be presented in subsequent sections.

3.4 Mobile Mapping System Used for Data Collection

Since the grade of MMS is one of the factors that affect the accuracy of MMS data, it is crucial to evaluate the accuracy of MMS data collected from different grades of mobile mapping systems. In this project four different MMS vendors with two different grades have been deployed in data collection at the test site. The actual name of each system and vendor are withheld in this report (the information will be made available to the INDOT Study Advisory Committee) to fulfill our assurances to the vendors. The names in column one of Table 3.1 will be used in this document, in place of the vendor/system names. Table 3.1 summarizes the

Figure 3.3 The INDOTLoop.

information about the mobile mapping systems used for the data collection in this project.

3.5 Control Surveys and Point Signalization

The control points and validation points were placed along on both the 231Route and the INDOTLoop. These control and validation points, having been signalized, were captured during the MMS data collection (during MMS scanning).

3.5.1 Control Points (Painted on Asphalt)

The high contrast black and white pavement markings were painted along the 231Route and INDOTLoop. These marks we refer to as painted targets and they serve as the control points in MMS data collection. The project team has generated two different patterns of painted targets which are the cross pattern of size 30″ x 30″ and the square pattern of size 30″, as shown in Figures 3.4 and 3.5, respectively. In all cases the surveyed point was a nail at the center of the target pattern. We subsequently used least squares matching to align a template with the intensity image. Some people have complained that it would be better to use a corner rather than the center of the target. Long histories in photogrammetry of aligning such targets by least squares matching have shown it to be a very accurate and reliable method. This is so because one uses all of the edges or gradients of the target shape, not just two edges. Further, this is done automatically, eliminating any biases from manual measurement.

The painted targets are designed to achieve high contrast to benefit control point positioning in the scanned point cloud during data processing. Black color paint was used for the background of the target while the target in cross and square shape are painted in white, with the designated size. The size of the painted background is not critical as long as it is big enough to produce a good intensity response in the point cloud. For this project, the black backgrounds were painted with a size of one meter by one meter.

These targets are well distributed along the test site routes to form a good network of control points to be used for processing collected MMS data (by the

TABLE 3.1
Summary of MMS used for data collection.

MMS Reference Name	System Grade	Data Collection Date	Remarks
Design Grade 1	Design	10/17/2014	
Design Grade 2	Design	08/26/2014	System calibration problem
Design Grade 2	Design	01/27/2015	The data collection on 01/27/2015 is the re-drive to replace the one collected on 08/26/2014 that had calibration issues
Asset Grade 1	Asset	07/09/2014	
Asset Grade 2	Asset	12/09/2014	

Figure 3.4 Painted target with cross pattern.

vendor). The choice of target pattern to be painted on each location of control point is somewhat random without any specific pattern. The distribution of control point locations on the test site and their reference names are depicted in Figures 3.9 and 3.10 for the 231Route and INDOTLoop, respectively.

Figure 3.5 Painted target with square pattern.

On the 231Route there are a total of seven control points (T1-T7), four of them are painted in the square pattern while the other three are in the cross pattern. For the case of the INDOTLoop, there are total of nine control points (T8-T16), four of them are painted in the square pattern while the other five are in the cross pattern.

All of the control point positions have been independently surveyed by using GNSS (Global Navigation Satellite System) with the Real Time Kinematic (RTK) technique (Using the INCORS reference stations). They were surveyed multiple times, with times of day chosen for constellation diversity. The coordinates of all control points (painted targets) in the State Plane Coordinate System (west zone) and their ellipsoid heights were made available for all MMS vendors to be used in any steps of their MMS data processing. Note that if we were to do this project over again we would probably have chosen to get the vertical by leveling, and ask the vendors to provide orthometric heights, as this is the mode they would be working for INDOT. As it is all heights are ellipsoid heights in NAD83.

3.5.2 Validation Point (Tripod Mounted)

In MMS surveying some of the features of interest for the survey are not on the paved roadway surface close to the mobile mapping vehicle. As such, validating the accuracy of the point cloud data off of the roadway is important. A way is needed to capture a point feature off of the roadway in a position where a target on the ground surface would not be visible to the scanner. In this case the project team has elected to use geometric 3D targets of sphere and cube shape as the validation points.

These 3D geometric targets are constructed by the project team with the use of available materials. The sphere targets are constructed from an injection molded spherical light fixtures of 14″ diameter. The sphere bases are fixed with customized aluminum mounting brackets with a tapped hole at the bottom for attaching to a conventional tribrach. The cube target is constructed from wood panels fastened together forming the cube shape target with a size of 12″. Figures 3.6 and 3.7 depict the sphere with its mounting bracket and cube target, respectively. We did verify, using a static, terrestrial laser scanner, that the eight sphere targets were consistent in size and shape at the 2 mm level.

It was concluded by the project team that the construction of 3D sphere target is much simpler than the cube target, especially when considering the need for many such targets to be used in the data collection. Another drawback of the cube target is that when placing it on tripod, extra attention is needed to ensure that the orientation of the cube makes it possible for at least three faces of the cube to be scanned by the MMS. For the case of sphere target, the orientation of the sphere is irrelevant, since of course it is spherically symmetric. Therefore the geometric target with sphere shape seems to be a better choice compared to the cube.

Figure 3.6 Sphere target.

The project team constructed eight such sphere targets, so we could fully occupy one route with validation points. This necessitated moving the validation targets before commencing scan for the second route.

Figure 3.7 Cube target.

The cube target was not be used in any procedures or steps of the MMS data accuracy evaluation for this project. Nevertheless we place it on the routes to be scanned so that, perhaps at a later time, we can evaluate the issues involved with using it for validation.

For this project, eight sphere targets and one cube target are placed off the road shoulder (see Figure 3.8) along the test site on both routes in the well distributed way forming a network of validation points. The distribution of validation points and their assigned names are depicted in Figures 3.9 and 3.10 for the 231Route and INDOTLoop, respectively.

All of the validation points have been independently surveyed by using GNSS with Real Time Kinematic (RTK) technique. The coordinates of all the validation points in the State Plane Coordinate System (west zone) and their ellipsoidal heights were withheld from the vendors. Therefore we could use them for data accuracy evaluation. The distribution of validation points on the test site and their reference names are depicted in Figures 3.9 and 3.10 for the 231Route and the INDOTLoop, respectively.

In the 231Route there are a total of eight sphere target validation points (S1-S8), the cube target is placed and referred as C1 in Figure 3.9 even though it was not used in the accuracy evaluation for this project. For the case of INDOTLoop, there are a total of eight sphere validation points referred to as S9–S16. The prior comment about cube target is applied here as well.

Figure 3.8 Validation point placed off road shoulder.

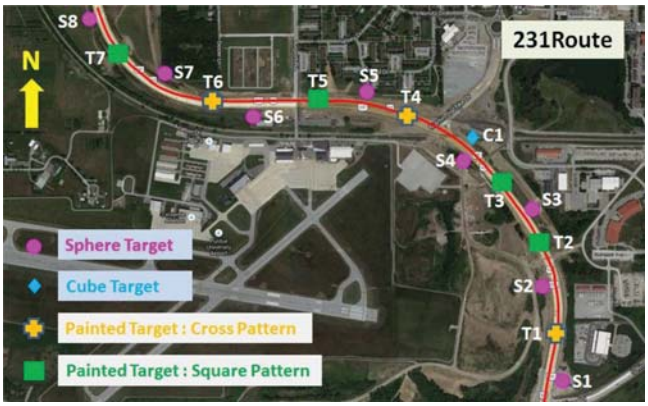

Figure 3.9 The distribution of control and validation points on 231Route.

Figure 3.10 The distribution of control and validation points on INDOTLoop.

4. COLLECTION OF DATA

In this section the details about collection of data will be covered. These include (1) the surveyed control data which includes both the control and validation points, (2) the setup of the GNSS base stations during the MMS scanning, (3) the collection strategy for MMS data using different mobile mapping systems, and (4) the scanned bridge (overpass on the 231Route) dataset obtained from the Static Terrestrial Laser Scanning (STLS) system.

4.1 Survey Control Data

As discussed in section 3.5, the painted targets on the asphalt (or concrete) in the shape of a cross and a square (see Figures 3.9 and 3.10) serve as the control points in this project. The 3D geometric targets (spheres) serve as the validation points in the process of MMS data accuracy evaluation.

The coordinates in the State Plane Coordinate System (SPCS) of 1983 and their elevations in terms of the ellipsoidal heights of these control points (T1-T7 for 231Route and T8-T16 for INDOTLoop) and validation points (S1-S8 for 231Route and S9-S16 for INDOTLoop) are independently surveyed by using GNSS (Global Navigation Satellite System) with Real Time Kinematic (RTK) technique. The coordinates of the control points are tabulated in Table 4.1 while the ones of validation points are tabulated in Table 4.2. The project team has made coordinates of the setup control points available for the vendors who agreed to perform the data collection at the test site to be used in any steps of their MMS data processing, while the coordinates of the setup validation points are withheld from the vendors for the accuracy evaluation processes to be performed by the project team.

TABLE 4.1
The planimetric coordinates in SPCS (west zone) and ellipsoidal heights of the control points for this project.

Test Site	Control Point Name	Pattern	Easting (E) (m)	Northing (N) (m)	Elevation (h) (m)
231Route	T1	Cross	913919.411	573135.327	170.556
	T2	Square	913833.451	573475.744	174.129
	T3	Square	913693.131	573662.637	175.055
	T4	Cross	913433.859	573868.266	176.447
	T5	Square	913018.865	573937.302	187.096
	T6	Cross	912705.496	573934.607	186.719
	T7	Square	912352.849	574092.968	186.579
INDOTLoop	T8	Cross	913182.382	578331.451	215.437
	T9	Square	913026.955	578570.905	212.703
	T10	Cross	912972.037	578993.181	213.354
	T11	Square	913071.342	579185.640	211.289
	T12	Cross	913196.240	579263.607	211.549
	T13	Square	913135.469	579265.479	211.517
	T14	Cross	913462.906	579001.649	211.849
	T15	Square	913474.051	578598.419	217.227
	T16	Cross	913474.622	578174.686	217.409

TABLE 4.2
The planimetric coordinates in SPCS of 1983 and ellipsoidal heights of the setup validation points of this project.

Test Site	Validation Point Name	Pattern	Easting (E) (m)	Northing (N) (m)	Elevation (h) (m)
231Route	S1	Sphere	913898.492	572908.244	166.374
	S2	Sphere	913897.112	573264.548	171.901
	S3	Sphere	913784.294	573571.427	174.543
	S4	Sphere	913622.253	573720.365	174.637
	S5	Sphere	913167.782	573953.064	186.072
	S6	Sphere	912790.581	573917.508	186.587
	S7	Sphere	912484.231	574004.643	185.120
	S8	Sphere	912261.312	574217.243	187.418
INDOTLoop	S9	Sphere	913372.904	578087.309	217.476
	S10	Sphere	913229.567	578263.011	215.964
	S11	Sphere	913109.996	578463.251	214.261
	S12	Sphere	912977.117	578703.722	213.204
	S13	Sphere	912917.393	579162.528	211.646
	S14	Sphere	913392.229	579134.455	212.011
	S15	Sphere	913484.352	578741.393	214.355
	S16	Sphere	913457.593	578387.289	215.740

4.2 GNSS Base Stations

For the vendor MMS data processing, we provided a GNSS base station in the vicinity of each route. Sometimes the vendor chose to set up their own base station, sometimes not. The project team has set up three GNSS base stations (Topcon GR5) around the test site. These were collecting pseudorange and phase observables during the whole time of data collection by each vendor. The geodetic coordinates of the three base stations used during the data collection process are shown in Table 4.3. All base station locations lie in open areas with unobstructed sky-views and the distances between them form short baselines. The observations from these three GNSS base stations around the test site, in the form of RINEX files, are delivered to all vendors for MMS data post processing purpose.

4.3 Mobile Mapping System (MMS) Data Collection Strategy

As discussed in sections 3.2 and 3.3, factors which influence accuracy include the grade of the MMS, the driving technique, and the data collection rate or the sampling rate which is selectable. The project team has decided to also take the aforementioned factors into account.

The effects of these factors (driving technique and sampling rate) were investigated and studied through a data collection by one single vendor. As such, the vendor designated "Design Grade 1" has been requested to exploit different data collection strategies or settings as listed below during the process of MMS data collection.

1. *Setting 1:* Use the 231Route to study the effect of sampling rate by utilizing a different sampling rate in each of the sessions of normal driving:
   a. Collect data on 231Route with the sampling rate of 250 KHz. (sampling rate means numbers of measurement/sec, e.g. 250 KHz is 250000 measurements/sec)
   b. Collect data on the 231Route with sampling rate of 500 KHz.
2. *Setting 2:* Use INDOTLoop to study the effect of data collection driving technique by deploying a single fixed data sampling rate of 250 KHz for different driving techniques.
   a. Collect data on INDOTLoop with the so-called "Acceleration Collection" technique. Acceleration Collection

TABLE 4.3
The geodetic coordinates of the setup base station during MMS data collection.

Base Station Name	Longitude (dd mm ss.sssss)	Latitude (dd mm ss.sssss)	Ellipsoidal Height (h) (m)	Point Location Description
PENC	86 54 53.51293 W	40 25 49.51199 N	182.849	On roof top of Civil Eng. building of Purdue University, West Lafayette, IN
Q94	86 55 52.80697 W	40 25 00.66256 N	152.015	At Purdue University Airport, West Lafayette, IN
C0085	86 55 33.96929 W	40 27 30.28914 N	182.313	INDOT benchmark, at INDOT facility, West Lafayette, IN

keeps the scanner working during all turns. This is a conventional way of driving along the roadways during the data collection process without stopping the vehicle.

b. Collect data on INDOTLoop with the so-called "No Acceleration Collection" technique. No Acceleration Collection has the scanner working only on straight or gently curving trajectories. This is a way of driving which avoids accelerations by driving through intersections, turning off collection, repositioning the vehicle, restarting the collection, and driving again through the intersection in new direction.

Figures 4.1 and 4.2 depict the Acceleration Collection technique and the No Acceleration Collection technique on the INDOTLoop, respectively.

Figure 4.1 shows the driving trajectory (route) of the Acceleration Collection technique. As suggested by its name, this technique allows the MMS to simultaneously collect the data while the vehicle is driven continuously along the scanning route. In contrast, Figure 4.2 shows the discontinuous driving trajectory (routes) of the No Acceleration Collection technique. With this driving technique the scanning is stopped at the end of each trajectory path and started again at the beginning of the next trajectory path. The purpose of driving in such way is to avoid the situation the system collects data while the vehicle making a sharp turn. The motivation for this (admittedly more cumbersome) approach is that vendors have noticed a significant increase in data noise in the vicinity of sharp turns. Possibly the IMU/INS is not tracking position and attitude so accurately in these cases. The project team has decided to investigate this factor; therefore both driving techniques are exercised.

Figure 4.1 One round of driving with Acceleration Collection technique over INDOTLoop.

Figure 4.2 One round of driving with No Acceleration Collection technique over INDOTLoop.

The effect of the variable scanning rate (sampling rate) and the driving technique are studied through the data collection only by MMS Design Grade 1 following the settings as discussed above. For other mobile map-ping systems (Design Grade 2, Asset Grade 1, and Asset Grade 2) the data collections on test site (231Route and INDOTLoop) were done using the conventional settings used by the vendor. Information about the MMS data obtained from different systems used in this project is summarized in Table 4.4.

4.4 Bridge Scanned from Static Terrestrial Laser Scanning (STLS) System

During accuracy evaluation of the data, both absolute and relative accuracies will be evaluated. The

TABLE 4.4
Summary of the collected MMS data of this project.

MMS Reference Name	Dataset Reference Name	Number of Points in the Scan
Design Grade 1	231Route 250KHz of Design Grade 1	86,443,632
	231Route 500KHz of Design Grade 1	170,223,144
	INDOTLoop Acceleration Collection of Design Grade 1	149,396,436
	INDOTLoop No Acceleration Collection of Design Grade 1	160,824,200
Design Grade 2	231Route of Design Grade 2	382,154,349
	INDOTLoop of Design Grade 2	359,155,000
Asset Grade 1	231Route of Asset Grade 1	16,873,445
	INDOTLoop of Asset Grade 1	21,934,484
Asset Grade 2	231Route of Asset Grade 2	212,911,931
	INDOTLoop of Asset Grade 2	451,820,570

detail about accuracy evaluation procedures will not be covered here (see Chapter 6 for that). However there is a part of the relative accuracy evaluation procedure that involves the comparison of the bridge clearances (bridge overpass on 231Route) derived from MMS data against the ones obtained by a higher accuracy survey method which in this case is the survey of the bridge by using Static Terrestrial Laser Scanning (STLS) system. Therefore in this section of the Data Collection chapter the laser scanning of the bridge overpassing 231Route by using the STLS system will be addressed.

The bridge (it carries a railroad track) passing over the 231Route, as shown in Figure 3.2, is scanned during the data collection on 231Route by all of the vendors. This bridge is also separately scanned by STLS system. The static terrestrial laser scanner used was the "ScanStation 2" of Leica Geosystems. Our experience has been, at these ranges, that this instrument is accurate to a fraction of a centimeter. The scan result from the STLS system should be more accurate than the mobile systems since there is no motion involved. In order to verify that the scan result from the STLS system can be used as the reference data in this portion of the MMS relative accuracy evaluation processes, a separate experiment, as fully described in Appendix C, was conducted to verify scale of the scanned point cloud from STLS system. The results from experiment proved no significant scale errors in the scanned point cloud from STLS system; therefore we were justified to use this point cloud as a reference to evaluate the bridge clearances extracted from the MMS data.

To fully cover the detail of the bridge in order to obtain bridge clearance measurements from the scanned point cloud, the bridge cannot be scanned or captured by single position of the static scanner. In this case the laser scanner is placed at two different positions, one at the west side and the other at the east side. The scanning is performed at each scan position capturing (scanning) the bridge from two different viewpoints as shown in Figures 4.3 and 4.4.

Figures 4.3 and 4.3 show the (colorized) scanned point clouds of the bridge from the two different instrument positions.

A registration process is needed in order to combine point clouds from two different scan positions into one single unified point cloud. The overlap between the scanned scenes is needed for the registration process.

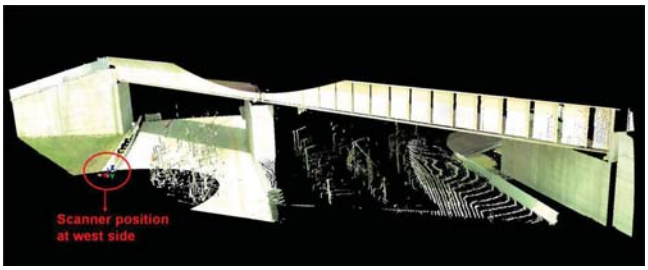

Figure 4.3 The scanned point cloud of the bridge from the scanner positioned at west side.

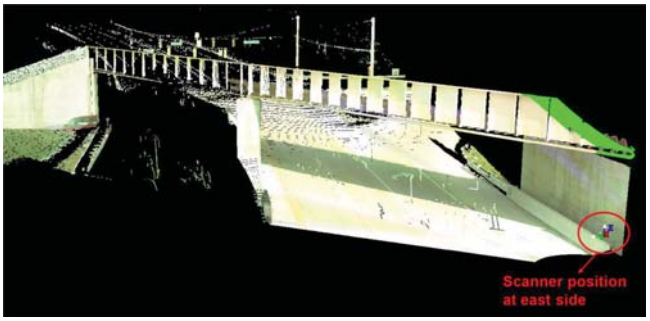

Figure 4.4 The scanned point cloud of the bridge from the scanner positioned at east side.

Figure 4.5 The merged point cloud with grayscale intensities of the bridge on 231Route scanned by STLS system (Leica ScanStation 2).

As shown in Figures 4.3 and 4.4, the scanned point clouds from the two different scan positions have substantial overlap.

In this case the point clouds from the two different scan positions are registered through the use of the Cyclone software. This software employs a rigid body transformation (six parameters) for the registration process. The process is referred to as "Cloud to Cloud" registration. In the Cloud to Cloud registration process, the selected common scanned points appearing in both clouds are used for setting up the initial approximation of the alignment between clouds. The parameters representing the alignment between the two scanned clouds are adjusted through the iterations based on the Iterative Closet Point (ICP) algorithm. Since the point cloud registration process is not the focus of this project study, the details of the registration process will not be covered here.

Once the registration process is complete, the result is a single unified point cloud representing the bridge as shown in Figure 4.5. The intensities here are displayed in a grayscale mode. This point cloud is then ready to be brought into the bridge clearance determination process in order to obtain the reference bridge clearance values. These will then be used to evaluate the data collected from the mobile platforms.

5. PRE-ANALYSIS OF DATA

After the MMS data collection was done, the next step was to bring all the collected 10 MMS datasets

(see Table 4.4 for summary of the collected MMS data) into analysis, to evaluate their accuracies in both absolute and relative sense. The absolute and relative accuracy of each MMS dataset is evaluated through the use of validation points (sphere targets) distributed over the test site. The methodologies for accuracy evaluation are described in detail in Chapter 6, Analysis of Data. In this section an overview of the tasks in data analysis will be addressed. This will give the reader a big picture about the steps needed from the start (the scanned point clouds) to the end (results of the MMS data accuracy evaluation).

5.1 Working Scheme Overview

In this section an overview of the workflow will be presented. It is to give the reader the big picture of how the scanned data are analyzed and evaluated. Figure 5.1 presents the overview of the project workflow. Brief details of the methodologies behind each working step will be given here.

The first task (referred as Step 1) that needs to be done is the calibration of the constructed sphere targets. The results from the calibration procedure give insight about sphere quality and consistency. It is necessary to perform Step 1 (sphere target calibration), as its outcome provides the required values (radius, offsets) to be used in the next step which is referred as Step 2 (automatic sphere detection procedures). The details of procedures used in Step 1 are separately described in section 5.2.

For the tasks in dashed rectangle (see Figure 5.1), they are performed per dataset. This means each of the datasets (see Table 4.4) is individually processed from Step 2 through Step 4.

For each dataset, Step 2 can be started with the information (some required values) obtained from Step 1 in conjunction with the independently surveyed coordinates of validation points known as the "Reference Validation Point Coordinates" (denoted here as (E_{Ref}, N_{Ref}, h_{Ref})) of all 8 validation points on each route (see Table 4.2). Once the procedures in Step 2 are completed, the results are the coordinates of the validation points detected from the scanned point clouds known as "Detected Validation Point Coordinates" (denoted here as (E_{Det}, N_{Det}, h_{Det})). Details of procedures used in Step 2 are separately described in section 6.1.

The Detected Validation Point Coordinates (E_{Det}, N_{Det}, h_{Det}) of each dataset and the reference ones (Reference Validation Point Coordinates (E_{Ref}, N_{Ref}, h_{Ref})) which have been independently surveyed by using GNSS/RTK are compared for absolute and relative accuracy using the procedures of Step 3 and Step 4 respectively. The details of procedures used in Step 3 and Step 4 are described in Chapter 6.

5.2 Sphere Target Calibration Procedures

Many details of the sphere calibration process have been placed in Appendix A. As has been mentioned earlier the sphere targets are constructed from injection molded spherical light fixtures of 14″ diameter. Each of the sphere bases is fixed to a customized aluminum mounting bracket with tapped hole at the bottom for attaching to an adaptor on a tribrach. In the evaluation of accuracy, the coordinates of validation points

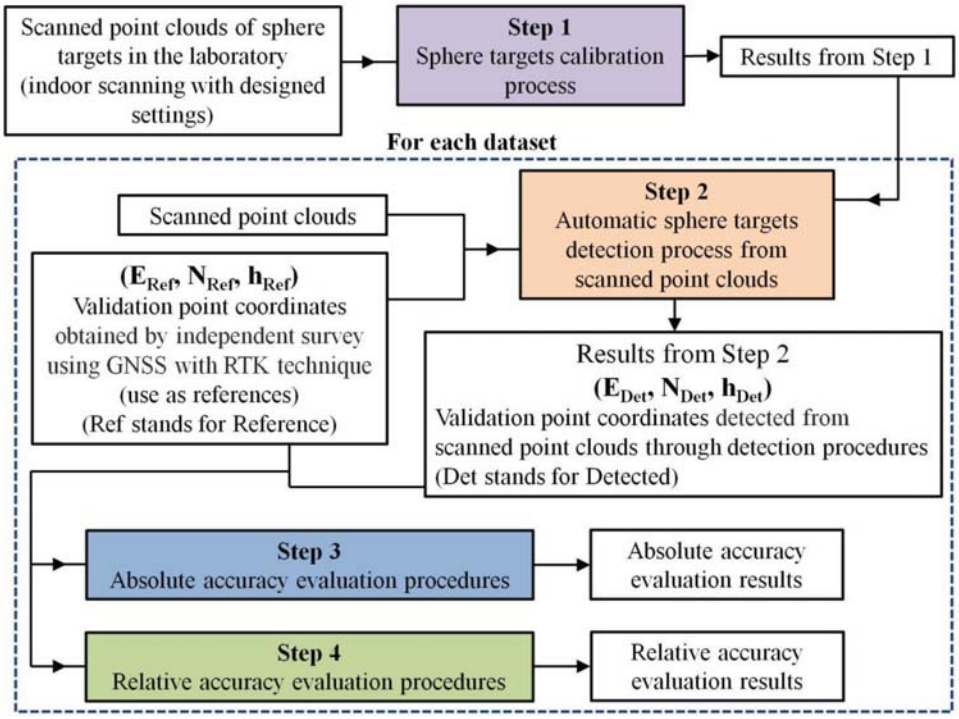

Figure 5.1 Diagram of the workflow for accuracy analysis.

independently surveyed by using GNSS with RTK technique are used as the references and are compared with the coordinates of the corresponding points detected from the scanned point clouds (known as (E_{Det}, N_{Det}, h_{Det})).

Figure 5.2 depicts the position of (E_{Det}, N_{Det}, h_{Det}) in the scanned point clouds. It should be noted that the coordinates of validation points (E_{Det}, N_{Det}, h_{Det}) obtained from the scanned point clouds are not directly detected in the automatic detection procedures. The results of the detection algorithm are instead the coordinates of the sphere center denoted as (Esc_{Det}, Nsc_{Det}, hsc_{Det}) throughout the document. The detected sphere center (Esc_{Det}, Nsc_{Det}, hsc_{Det}) needs to be related to the coordinates of validation point on the ground (E_{Det}, N_{Det}, h_{Det}) via a calibrated offset from sphere center to mounting bracket base, the so-called offset distance "D" (obtained from Step 1), and the measured HI (height of instrument) of the setup. The mentioned relationship can be expressed as in Equation 5.1 and is depicted in Figure 5.3

$$\begin{bmatrix} E_{Det} \\ N_{Det} \\ h_{Det} \end{bmatrix} = \begin{bmatrix} Esc_{Det} \\ Nsc_{Det} \\ hsc_{Det} \end{bmatrix} - \begin{bmatrix} 0 \\ 0 \\ HI + D \end{bmatrix} \quad (5.1)$$

Since an accurate value of the offset distance D cannot be directly measured, therefore it can only be obtained indirectly through the calibration process (Step 1). The project team has designed the calibration process and applied it to all sphere targets (8 of them) to obtain the offset distance D. The steps in the calibration process are listed as follows:

1. Using a high accuracy Static Terrestrial Laser Scanner (ScanStation2 of Leica Geosystems), scan the sphere targets located on a flat surface. Scan all of the spheres from at least two scanning positions to ensure good coverage of the sphere surfaces.

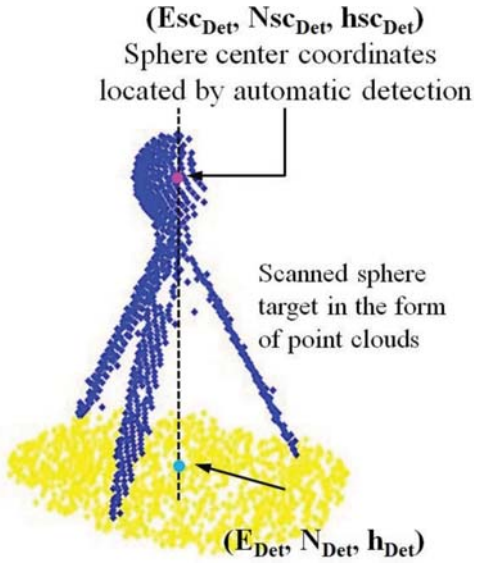

Figure 5.2 Validation point in the point cloud.

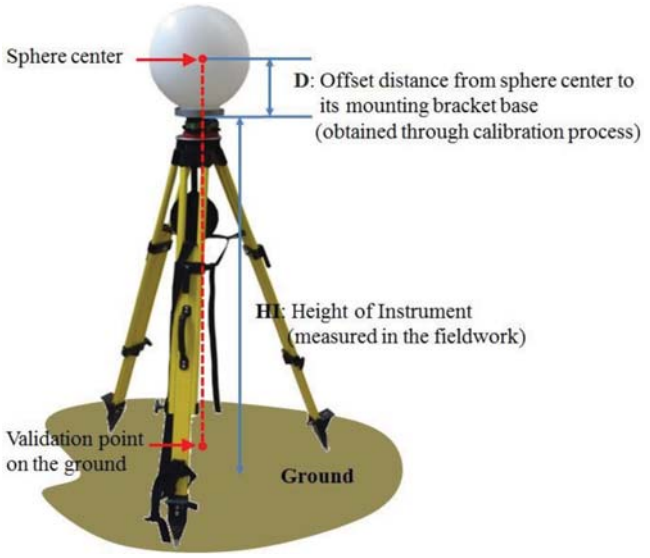

Figure 5.3 The Relationship of Detected Sphere Center and Validation Point on the ground.

2. Recover the sphere points of each sphere and fit, via Least Squares, those points to a sphere model, carrying sphere center coordinates and radius as parameters. From this step the sphere center is located.
3. Recover points constituting flat surface on which spheres are placed and fit those points to plane model carry normal vectors of planes as parameters. From this step, the plane is located.
4. For a sphere, compute the perpendicular distance between located sphere center and plane which is the offset distance from the sphere center to its base.
5. Averaging over the computed perpendicular distances for all spheres, get the final representative offset distance (the distance from sphere center to its base) for using in all sphere known as offset distance "D." The differences between individual spheres are negligible.

From the calibration process, the offset distance D is computed as 0.194 m $\pm$ 0.001 m. The recovered sphere radius averaging from all spheres is computed as 0.177 m $\pm$ 0.0004 m. The standard deviation of $\pm$0.0004 m in the recovered radius values reflects the good quality and consistency or uniformity of the sphere targets which were intended as light fixtures. It can be implied that the sphere light fixtures are accurately produced as the recovered sphere radius and the one listed in manufacture report (0.1778 m (7″)) are insignificantly different. The standard deviation of $\pm$ 0.0004 m of sphere radius value simply represents the noise in the scanning process. The noise in the scanning process is also shown in the standard deviation of the recovered offset distance D of the size of $\pm$ 0.001 m. More details about the sphere calibration process can be found in the Appendix A.

6. ANALYSIS OF DATA

According to the project workflow as summarized in Figure 5.1, it is to be noted that the analysis of MMS

data is started with Step 2 where the scanned sphere targets are detected from the scanned point clouds obtained by MMS. The absolute and relative accuracy of the collected MMS data are evaluated through the use of validation points (sphere targets) placed over the test site. The designed methodologies for MMS data accuracy evaluation will be described in detail as follows.

6.1 Automatic Sphere Target Detection Procedures

The automatic sphere target detection process denoted as Step 2 in the workflow diagram presented in Figure 5.1 involves use of our developed algorithm to detect the sphere center from the scanned point clouds. In the algorithm, there are many procedures and steps before the final sphere center of each sphere target is located. In this section the specifics of this algorithm will be addressed. The procedures will be described for the case of one sphere target only for the ease of explanation. The same identical logic and steps are also applied to the other sphere targets found in the MMS point cloud. For a sphere target the procedures in this sphere center detection algorithm can be shown in the diagram of Figure 6.1.

1. Get the data subset, so-called Cutlevel 1. Start from the known coordinate of a validation point (denoted as (E_{Ref}, N_{Ref}, h_{Ref})) obtained from independent survey by using GNSS/ RTK and then offsetting it up to the virtual sphere center with the known fixed distance offset "D" and the corresponding set up HI (see Figure 5.3). Extract all the points that fall within the cube box extent of predefined size "B" where the center of the drawn cube box is the previously computed virtual sphere center. All the points extracted from this step are denoted as "Cutlevel 1." The cube box size "B" is an algorithm parameter and it can be changed to extract more or fewer numbers of points. In this project the cube box size B is selected to be equal to 1 meter.

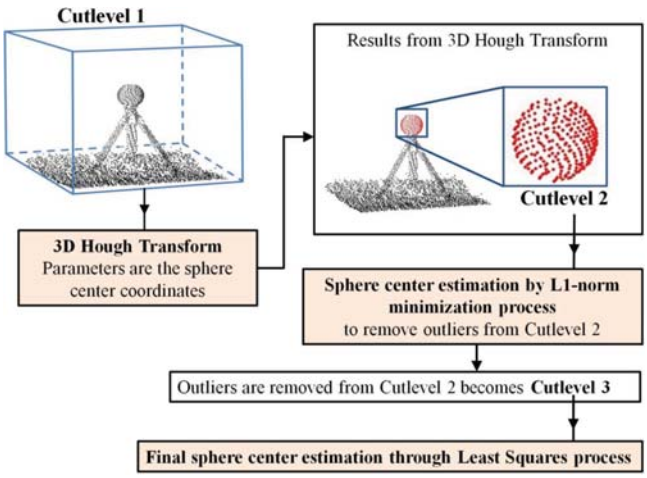

Figure 6.1 Diagram showing an overview of automatic sphere target detection algorithm.

2. Get the data subset, so-called Cutlevel 2. A 3D Hough transform carrying the sphere center as parameters is applied to points in Cutlevel 1. In the 3D Hough transform, the voting is performed in a discretized parameter space of possible sphere centers values. The number of parameters cells and the cell size are algorithm parameters in this process. In this case, the parameter cells are drawn from the computed virtual sphere center with the dimension of 51 and 101 cells for Design Grade and Asset Grade MMS, respectively, in all directions with the cell size of 2 cm. This always includes the actual sphere center being sought. As with other applications of the Hough transform method, the parameter cells (which in this case are the cells of all possible sphere center values) which possess the highest vote is the one selected to be the detected sphere center. Once the sphere center is detected by Hough transform, the points that constitute the sphere surface are extracted by including any points that fall within the threshold distance "d" from sphere surface created by the detected sphere center resulted from Hough transform process. The extracted points mentioned above constitute "Cutlevel 2," and the threshold distance "d" is an algorithm parameter in this process. In actual application the threshold distance "d" is set equal to 3 cm, this allows points that constitute the sphere surface to be consistently recovered.

3. Get the so-called Cutlevel 3 by removing some points with large noise magnitude in Cutlevel 2. The points in Cutlevel 2 which have large discrepancies from the sphere model can be thought of as the outliers of the sphere surface. The purpose of this step is to remove those outliers so that the detected sphere center from the previous step can be refined. In this case the sphere center is located in a robust fashion through estimation via L1-norm minimization applied to points in the Cutlevel 2. The main purpose of applying L1-norm minimization estimation is to detect the points which have large errors in estimation process (sphere model fitting). Those points with large fitting residuals are the outliers and therefore must be removed. The remaining sphere points after the outliers are removed are denoted as "Cutlevel 3."

4. Final estimation of the sphere center through conventional Least Squares method. Once the outliers have been removed resulting in the sphere points in Cutlevel 3, the sphere center is then finally estimated through a conventional, nonlinear Least Squares process. This entire procedure has the advantage of being robust to several sources of non-random noise which can occur in the laser scanning process.

6.2 Absolute Accuracy Evaluation of MMS Data

Referring to the workflow diagram in Figure 5.1, once the coordinates of the validation points in the point cloud (known as (E_{Det}, N_{Det}, h_{Det})) are successfully determined through the prior steps, they are compared to their corresponding coordinates from the GNSS/RTK survey (known as (E_{Ref}, N_{Ref}, h_{Ref})). The results from the comparisons reflect absolute accuracy of the MMS point cloud. This section describes how the absolute accuracy of an MMS dataset is evaluated and how the statistical descriptors of the comparison are constructed.

For a validation point "i," the detected coordinates of the validation point on the ground are denoted as $(E_{Det}, N_{Det}, h_{Det})_i$ or $[E_{Det}, N_{Det}, h_{Det}]_i^T$. The reference coordinates of validation point "i" are denoted as $(E_{Ref}, N_{Ref}, h_{Ref})_i$ or $[E_{Ref}, N_{Ref}, h_{Ref}]_i^T$. These represent the coordinates of the validation point independently surveyed by using GNSS/RTK. For each route there are total of 8 validation points. They are S1-S8 for 231Route and S9-S16 for INDOTLoop.

The absolute accuracy evaluations are performed dataset-wise (refer to Table 4.4 for all 10 datasets of this project) which means for each dataset there will be a set of its own absolute accuracy evaluation results and the related statistics. As such, in this section the absolute accuracy evaluation procedures are described only for a single dataset as an example, the same routine also applies to the other datasets.

For a dataset the following values are computed as listed in Equation 6.1 through Equation 6.13. The subscript "i" refers to the i^{th} point.

$$\begin{bmatrix} dE \\ dN \\ dh \end{bmatrix}_i = \begin{bmatrix} E_{Det} \\ N_{Det} \\ h_{Det} \end{bmatrix}_i - \begin{bmatrix} E_{Ref} \\ N_{Ref} \\ h_{Ref} \end{bmatrix}_i \tag{6.1}$$

$$dP_i = \sqrt{dE_i^2 + dN_i^2} \tag{6.2}$$

$$dQ_i = \sqrt{dE_i^2 + dN_i^2 + dh_i^2} \tag{6.3}$$

$$dE_{Avg} = \frac{\sum_{i=1}^{8} dE_i}{8} \tag{6.4}$$

$$dN_{Avg} = \frac{\sum_{i=1}^{8} dN_i}{8} \tag{6.5}$$

$$dh_{Avg} = \frac{\sum_{i=1}^{8} dh_i}{8} \tag{6.6}$$

$$dP_{Avg} = \frac{\sum_{i=1}^{8} dP_i}{8} \tag{6.7}$$

$$dQ_{Avg} = \frac{\sum_{i=1}^{8} dQ_i}{8} \tag{6.8}$$

$$RMSE_E = \sqrt{\frac{\sum_{i=1}^{8} dE_i^2}{8}} \tag{6.9}$$

$$RMSE_N = \sqrt{\frac{\sum_{i=1}^{8} dN_i^2}{8}} \tag{6.10}$$

$$RMSE_h = \sqrt{\frac{\sum_{i=1}^{8} dh_i^2}{8}} \tag{6.11}$$

$$RMSE_P = \sqrt{(RMSE_E)^2 + (RMSE_N)^2} \tag{6.12}$$

$$RMSE_Q = \sqrt{(RMSE_E)^2 + (RMSE_N)^2 + (RMSE_h)^2} \tag{6.13}$$

The values dE_i, dN_i, and dh_i are the discrepancy between coordinates of validation points "i" detected from point cloud and the reference one in Easting (E), Northing (N) of the State Plane Coordinate System, and in elevation (h), respectively.

The value dP_i is the different in planimetric position (2D) between detected coordinates of validation point "i" from point cloud and its reference one, while dQ_i is the one for the case of 3D position. The absolute accuracy of the MMS data along a particular axis is expressed in terms of the root mean square errors (RMSE) in Easting (E), Northing (N) and Elevation (h). The absolute accuracy in combined planimetric position (2D) and the one of 3D position are expressed

in terms of $RMSE_P$ and $RMSE_Q$, respectively. For application to actual QA/QC of data in the future, these RMSE's can be scaled to confidence intervals of higher probability.

6.3 Relative Accuracy Evaluation of MMS Data

Following the details in section 6.2; the same idea is applied for the case of relative accuracy evaluation. That is, the relative accuracy evaluations are performed dataset-wise, which means for each dataset there will be a set of its own relative accuracy evaluation results as well as the related statistics. As such, the relative accuracy evaluation procedures are described for a single dataset as an example. The same routine is then applied to the case of other datasets. In this section, the same notations are used following the conventions in section 6.2.

In many areas of Geomatics, relative accuracy is better than absolute accuracy. This might arise where a photogrammetric stereo model has good internal geometry, but a poor fit to the control points. Conventionally, when evaluating the relative accuracy of a dataset, one looks at coordinate differences rather than absolute coordinates, and compares data values against reference values. That is the difference in each coordinate component (Easting, Northing, and Elevation) is computed among pairs of validation point: cloud vs. control. The difference between these two groups of differences are compared and reported in terms of the "difference of the difference" (double difference, denoted as ddE, ddN, and ddh for Easting and Northing and Elevation, respectively). It is often to be expected that the distances between pairs of validation points have an effect on the calculated relative accuracy. That is when the distance between a pair of validation points is large; it is likely to produce a large size of ddE, ddN, and ddh, and vice versa. However, this may not be true for the case of evaluating relative accuracy by using a network of validation points distributed over large project area. In particular it may not hold when the data has been registered in an absolute sense, both during collection, and later during post-process. Since the network of the validation points used in this project covers sizable project area, therefore it is desirable to evaluate relative accuracy of the data based on two different approaches. That is, to use the aforementioned method (use the whole network of validation points) and also adopt another approach of evaluating relative accuracy in a very small area of data. In this case the bridge structure passing over the 231Route (see Figure 3.2) is selected to be used for evaluating the relative accuracy (vertical) of the MMS dataset over a small area. The results of bridge clearance determination will reflect the relative accuracy of the MMS dataset over a limited area and in one dimension only (vertical). The detail of these 2 relative accuracy evaluation methods will be discussed separately in section 6.3.1 and 6.3.2, respectively.

6.3.1 Relative Accuracy Evaluations over the Whole Project Area (Use the Whole Network of Validation Points)

The strategy behind the relative accuracy evaluation is to compare the accuracy of the network of validation points detected from point clouds against the reference or control values for the same points. For a network of validation points, those detected from the point cloud (subscripted as "Det") yield values as listed in Equation 6.14 through 6.16. They are computed between a pair of validation point "i" and "j."

$$\begin{bmatrix} dE_{Det} \\ dN_{Det} \\ dh_{Det} \end{bmatrix}_{ij} = \begin{bmatrix} E_{Det} \\ N_{Det} \\ h_{Det} \end{bmatrix}_{i} - \begin{bmatrix} E_{Det} \\ N_{Det} \\ h_{Det} \end{bmatrix}_{j} \tag{6.14}$$

$$dP_{Det_{ij}} = \sqrt{(dE_{Det_{ij}})^2 + (dN_{Det_{ij}})^2} \tag{6.15}$$

$$dQ_{Det_{ij}} = \sqrt{(dE_{Det_{ij}})^2 + (dN_{Det_{ij}})^2 + (dh_{Det_{ij}})^2} \tag{6.16}$$

From all of the possible combinations of pairs of validation points in the underlying network (for all i and j when $i \neq j$) the values as shown in Equation 6.14 through 6.16 are computed.

In a similar way the corresponding reference (or control) coordinates are processed as listed in Equation 6.17 through 6.19. They are similarly computed for all the possible combinations of pairs of validation point point "i" and "j" (when $i \neq j$).

$$\begin{bmatrix} dE_{Ref} \\ dN_{Ref} \\ dh_{Ref} \end{bmatrix}_{ij} = \begin{bmatrix} E_{Ref} \\ N_{Ref} \\ h_{Ref} \end{bmatrix}_{i} - \begin{bmatrix} E_{Ref} \\ N_{Ref} \\ h_{Ref} \end{bmatrix}_{j} \tag{6.17}$$

$$dP_{Ref_{ij}} = \sqrt{(dE_{Ref_{ij}})^2 + (dN_{Ref_{ij}})^2} \tag{6.18}$$

$$dQ_{Ref_{ij}} = \sqrt{(dE_{Ref_{ij}})^2 + (dN_{Ref_{ij}})^2 + (dh_{Ref_{ij}})^2} \tag{6.19}$$

For a pair of validation point "i" and "j" the double difference vectors as expressed in Equation 6.20 and 6.21 are computed.

$$\begin{bmatrix} \mathrm{ddE} \\ \mathrm{ddN} \\ \mathrm{ddh} \\ \mathrm{ddP} \\ \mathrm{ddQ} \end{bmatrix}_{\mathrm{ij}} = \begin{bmatrix} \mathrm{dE_{Det}} \\ \mathrm{dN_{Det}} \\ \mathrm{dh_{Det}} \\ \mathrm{dP_{Det}} \\ \mathrm{dQ_{Det}} \end{bmatrix}_{\mathrm{ij}} - \begin{bmatrix} \mathrm{dE_{Ref}} \\ \mathrm{dN_{Ref}} \\ \mathrm{dh_{Ref}} \\ \mathrm{dP_{Ref}} \\ \mathrm{dQ_{Ref}} \end{bmatrix}_{\mathrm{ij}} \tag{6.20}$$

$$\begin{bmatrix} \mathrm{DDE} \\ \mathrm{DDN} \\ \mathrm{DDh} \\ \mathrm{DDP} \\ \mathrm{DDQ} \end{bmatrix}_{\mathrm{ij}} = \left| \begin{bmatrix} \mathrm{ddE} \\ \mathrm{ddN} \\ \mathrm{ddh} \\ \mathrm{ddP} \\ \mathrm{ddQ} \end{bmatrix}_{\mathrm{ij}} \right| \tag{6.21}$$

The values in Equations 6.20 and 6.21 are computed for all the possible combinations of pairs of validation point "i" and "j" (when i≠j).

The maximum and the minimum of the value of DDE, DDN, DDh, DDP and DDQ when considering from all possible pairs of validation points represent the worst and best case scenario of the relative accuracy from the underlying dataset. A plot of the values of $\mathrm{DDE_{ij}}$, $\mathrm{DDN_{ij}}$, $\mathrm{DDh_{ij}}$, $\mathrm{DDP_{ij}}$, and $\mathrm{DDQ_{ij}}$ against the corresponding distance between points "i" and "j" can also help depict the trend of relative accuracy of the dataset.

The relative accuracy of the MMS data in each coordinate component is expressed in terms of the root mean square errors (RMSE) in Easting (E), Northing (N) and Elevation (h) of the value DDE, DDN, and DDh, respectively. These are shown in Equation 6.22 through 6.24 when n is the total number of combinations of validation point pairs. The relative accuracy of the MMS data in the planimetric position (2D) and the 3D position are expressed as $\mathrm{RMSE_P}$ and $\mathrm{RMSE_Q}$. This is shown in Equations 6.25 and 6.26, respectively.

$$\mathrm{RMSE_E} = \sqrt{\frac{\sum_{\forall ij, i \neq j} \mathrm{DDE}_{ij}^2}{n}} \tag{6.22}$$

$$\mathrm{RMSE_N} = \sqrt{\frac{\sum_{\forall ij, i \neq j} \mathrm{DDN}_{ij}^2}{n}} \tag{6.23}$$

$$\mathrm{RMSE_h} = \sqrt{\frac{\sum_{\forall ij, i \neq j} \mathrm{DDh}_{ij}^2}{n}} \tag{6.24}$$

$$\mathrm{RMSE_P} = \sqrt{\frac{\sum_{\forall ij, i \neq j} (\mathrm{DDP}_{ij})^2}{n}} \tag{6.25}$$

$$\mathrm{RMSE_Q} = \sqrt{\frac{\sum_{\forall ij, i \neq j} (\mathrm{DDQ}_{ij})^2}{n}} \tag{6.26}$$

6.3.2 Relative Accuracy Evaluations over Small Area (Bridge Clearance Determination)

As previously mentioned, a method of evaluating vertical relative accuracy of an MMS dataset over a small area is performed via the bridge clearance determination. In this case the bridge passing over the 231Route, as shown in Figure 3.2, is scanned with the different systems listed inTable 4.4.

For the scanned data from each mobile mapping system, the bridge clearances along the paths which are aligned with seven lane stripes on the road surface were determined (computed) from the scanned point cloud. Therefore, there are total of seven locations (corresponding to seven lane stripes) of the clearance to be computed. The locations, stripe vectors, and their associated reference names are depicted in the perspective view and the top view of the bridge in Figures 6.2 and 6.3, respectively.

The bridge clearances can be measured by using commercial software such as TopoDOT. It is important to note that in the bridge clearance measurement process (as implemented in TopoDOT) there is a required manual positioning or defining of the path line (lane stripe) along which the clearances will be measured. In order to be able to comfortably locate the lane stripes in scanned point clouds, the point clouds must have (a) sufficient point density and (b) good intensity quality. These two qualities are reinforcing each other and make it possible for users to comfortably locate features from the scanned point clouds. Without sufficient point density, features are not well defined and recognition/location of a feature may not be possible. Likewise without good intensity quality the contrast is too low or too high and surface features become difficult to recognize/locate. Good density alone or good intensity alone are not sufficient, we really need both to guarantee reliable identification and location of surface features such as lane stripes.

As mentioned earlier, the bridge clearance measurement process (as implemented in TopoDOT) requires manual positioning or defining of the path line (lane stripe) at which the clearances will be measured, therefore there exist variations in the measurement process performed by different operators (or between repeated measurements done by the same operator).

Even though the bridge clearances can be easily measured from the scanned point clouds using commercial software, the project team has decided not to use it. This is because the software algorithm to arrive at the values of bridge clearances is not fully revealed

and hence the project team has more confidence in our developed algorithm to compute bridge clearance values from the scanned point cloud. However, the team also performed the bridge clearance determination using TopoDOT software and its results are used for double checking the results obtained from the algorithm developed by the team.

In the developed bridge clearance algorithm, the first step is to extract the strip of points along each of the seven lane stripes (as shown in Figure 6.2 and 6.3). This process was manually performed by delineating the polygon enclosing the desired lane stripe on the top view display of the point cloud. Then points are extracted which fall within the drawn polygon. The illustration of this step is shown in Figure 6.4 with lane stripe W3 from data scanned by the Design Grade 2 system as an example. The length of the drawn polygon is not a critical parameter as long as the two main beams of the scanned bridge are well captured. For a lane stripe, the polygon was drawn in such the way that its width is not too wide but just large enough to enclose the width of the stripe. Figure 6.5 illustrates the extracted point cloud of the underlying lane stripe in the side view (the view perpendicular to stripe, looking horizontally).

For a lane stripe, once the points enclosed by the drawn polygon have been extracted (as shown in Figure 6.5), a manual step designates the beams of interest for this profile. For all points in the beams of interest (depicted as point A in exaggerated size in Figure 6.6), the corresponding point on the road surface must be determined (this generally does NOT correspond exactly to a scanned point on the road surface). In order to determine bridge clearance for point A the elevation of the road surface beneath this point must be computed. This is done by using a plane fitting algorithm. The algorithm starts with locating point Ap which is the vertical projection of point A onto the road surface. Point Ap has only X (Easting) and Y (Northing) coordinates which are the same as point A. The scanned ground points, for which (X, Y) coordinates fall within the circle with radius "r" centered at point Ap are retained, the rest are filtered out. These retained ground points (labelled in orange color as shown in Figure 6.7) will be used in a plane fitting algorithm by Least Squares. The radius "r" of the circle is a design parameter and it must be large enough to cover sufficient points to recover the road surface. In our processing, a radius "r" of size 12 cm was adopted for the starting value, the radius "r" may

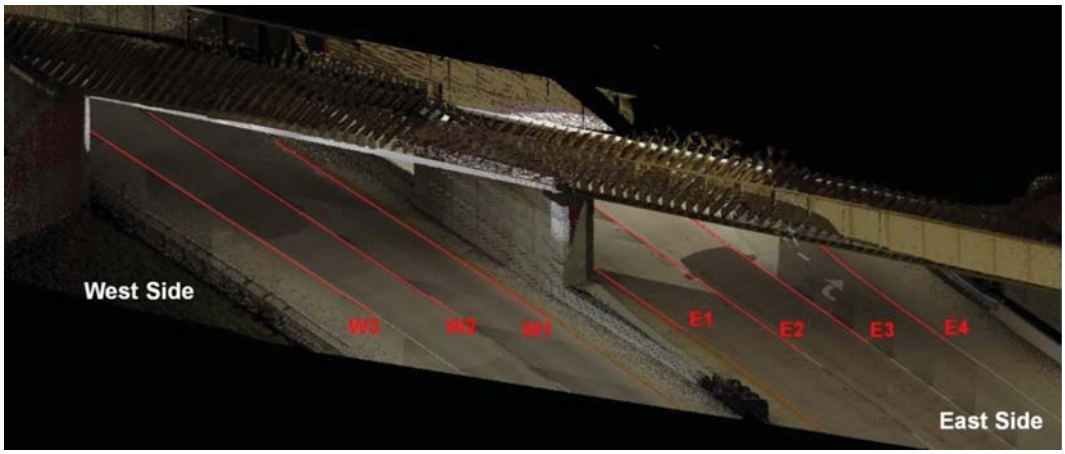

Figure 6.2 Illustration in perspective view of the seven lane stripes for bridge clearance determination.

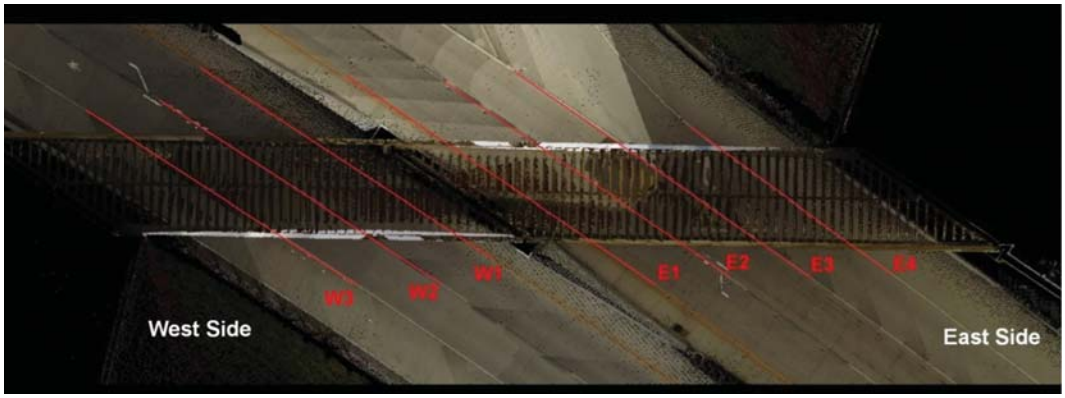

Figure 6.3 Illustration in top view of the seven lane stripes for bridge clearance determination.

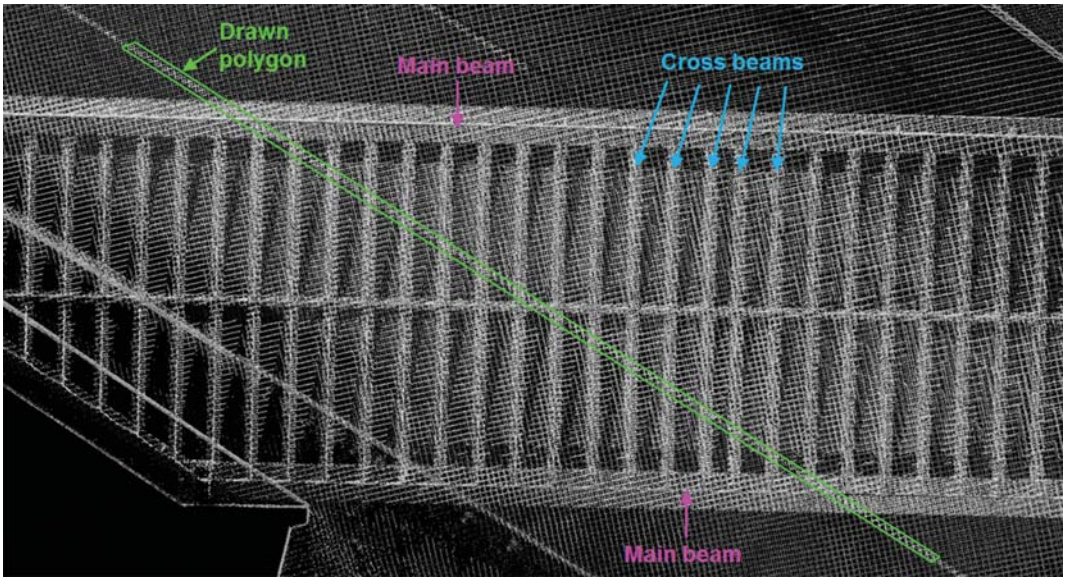

Figure 6.4 Illustration of extracting point cloud strip in top view of lane stripe W3 of Design Grade 2 bridge point cloud for bridge clearance computation.

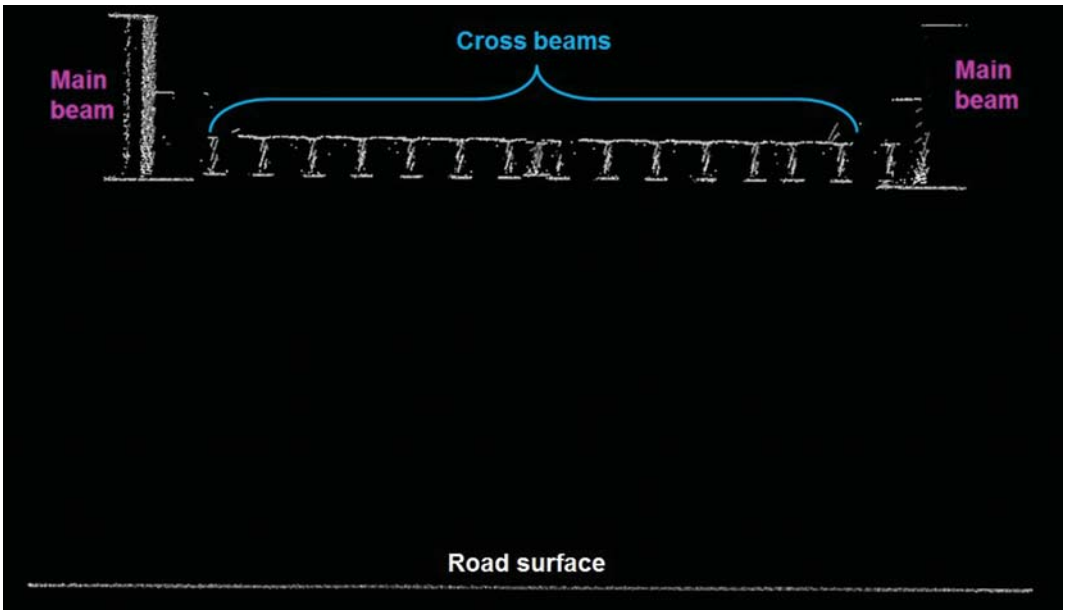

Figure 6.5 Illustration of extracted point cloud by using drawn polygon in the side view (the view perpendicular to the lane stripe, looking horizontally). Note that the stripe crosses the bridge obliquely, leading to the presence of multiple cross beams.

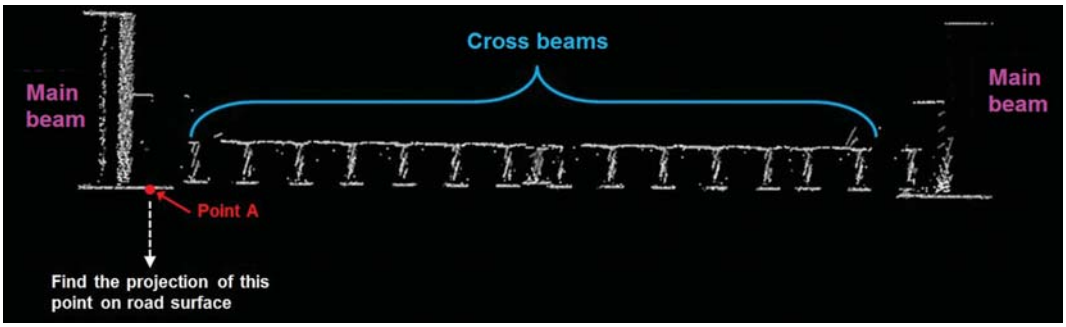

Figure 6.6 Illustration of point A as an example of points on each main beam.

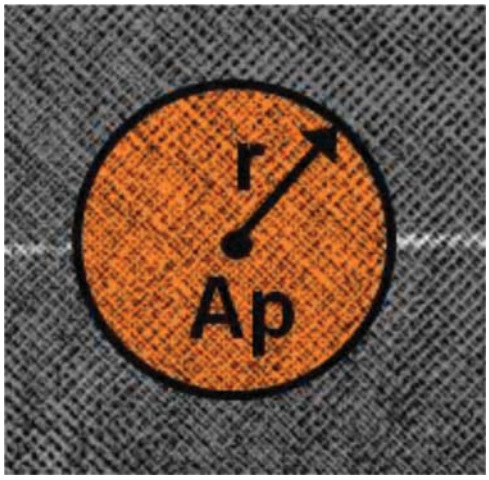

Figure 6.7 Point A projected down to road surface, with circular region enclosing points to be used for plane fit.

be automatically increased when the scanned points are sparse in order to ensure sufficient number of points used for plane fitting.

The bridge clearance at point A is obtained by computing the perpendicular distance from point A to the corresponding fitted ground plane. This process of determining bridge clearance at a single point is applied to all scanned points representing the selected beams of the bridge profile for the currently considered lane stripe. The shortest distance among all computed clearance values is adopted to be the bridge clearance value for the considered stripe.

With our developed procedures the clearances of the bridge are determined from the scanned point clouds obtained from the different systems. The values of bridge clearance determined from scanned MMS point clouds will be compared against the corresponding values determined from the Static Terrestrial Laser Scanning system (see section 4.4 for the detail on how the bridge is scanned by STLS system). The results of bridge clearance computation along the seven lane stripes of the scanned bridge from mobile and static systems are shown in section 7.2.

6.4 Extra Treatment Applied to MMS Data of Asset Grade 1 and Asset Grade 2 to Evaluate Absolute Accuracy

In the next Chapter the results of the absolute and relative accuracy evaluation of each MMS dataset will be presented. That is for each dataset, it has its own absolute and relative accuracy values. The evaluation process and procedures are applied to each delivered dataset n the same manner as described in sections 6.1 through 6.3. However there is an exception for the case of the data obtained from the mobile mapping system Asset Grade 1 and Asset Grade 2. Here the data obtained from these 2 systems have undergone the absolute accuracy evaluation process twice. At first the absolute accuracy evaluation process is applied to the original delivered data obtained from these 2 systems, secondly the same absolute accuracy evaluation process is applied to the refined or trans-formed dataset (we ourselves did the transformation/refinement since it was obviously done poorly by the vendor).

A local transformation through the use of control points (painted targets on asphalt) is applied by the project team to the original delivered data of Asset Grade 1 and 2 to produce the transformed data.

The reason that the original data obtained from the MMS Asset Grade 1 and 2 needs to be transformed is because the results of the absolute accuracy evaluation applied to the original data have shown significant systematic errors (shifts) in the data. The discrepancies between the validation point coordinates obtained from MMS scanned data and the reference ones have shown a systematic pattern (bias). Therefore the results obtained from the absolute accuracy evaluation applied on the original dataset do not well represent the absolute accuracy of the data. The systematic error should be removed through the local transformation process first before evaluating the accuracy of the MMS dataset. In this case it can be inferred that at the point of data delivery the data of Asset Grade 1 and Asset Grade 2 have never undergone any local transformation through the use of control points. This suggests that these vendors could substantially improve their accuracy by a reasonably simple step. In any future contacts between INDOT and asset grade vendors, this issue should come under discussion.

The project team has applied a local transformation to the original dataset of MMS Asset Grade 1 and Asset Grade 2 through the use of the control points (painted targets on asphalt). In the local transformation, the coordinates of the control points detected from the scanned point clouds data are transformed to the reference coordinates of the control points (obtained by GNSS/RTK). In this case the 6-parameter transformation is adopted. The transformation carries rotations and translations in Easting, Northing, and Elevation directions as parameters (scale is fixed at 1.000). To locate the coordinates of the control points in the scanned point clouds is to locate the centers of the painted targets in the cross and square patterns as shown in Figures 3.4 and 3.5. For this the Least Squares matching procedure is applied. The details of the local transformation applied to the original MMS data of Asset Grade 1 and Asset Grade 2 as well as the technique used for locating the centers of the control points (painted targets) in the point clouds dataset can be found in Appendix B.

For a control point, the relationship between the detected coordinates from the scanned point clouds and its associated reference coordinates is expressed in the form of a 6-parameter transformation which involves 3 rotations and 3 translations. The parameters (rotations and translation) of the transformation are solved through a nonlinear Least Squares minimization. Table 6.1 shows the solved parameters of the local transformation which will be applied to the original dataset obtained

TABLE 6.1
Solved parameters of 6-parameters local transformation applied to the original dataset obtained from MMS Asset Grade 1 and Asset Grade 2.

		Rotation			Translation		
		Ω (degree)	Φ (degree)	κ (degree)	$t_{E\ (m)}$	$t_{N\ (m)}$	$t_{h\ (m)}$
Asset Grade 1	231Route	-0.004390 (-15.80″)	0.001025 (3.69″)	0.000338 (1.22″)	1.862	-0.296	0.685
	INDOTLoop	0.000415 (1.49″)	0.001832 (6.60″)	0.000259 (0.93″)	1.879	0.065	0.502
Asset Grade 2	231Route	0.006275 (22.59″)	-0.002956 (-10.64″)	0.000102 (0.37″)	0.489	-0.829	1.139
	INDOTLoop	-0.001563 (-5.63″)	-0.003396 (-12.22″)	-0.000750 (-2.70″)	0.484	-0.840	1.143

from MMS Asset Grade 1 and Asset Grade 2. This will "improve" their absolute accuracy.

As shown in Table 6.1, the data obtained from the Asset Grade 1 and Asset Grade 2 system are transformed by applying rotations Ω, Φ, and κ around East, North and Elevation axes, and translations t_E , t_N, and t_h.

As previously mentioned the reason why the original datasets from these 2 asset grade mobile mapping systems need to be transformed is because the absolute accuracy evaluation results of these 2 systems (see Table 7.7 through Table 7.10) have shown large discrepancies between the validation point coordinates from point cloud and from the control survey. Also a systematic pattern in discrepancies is detected through the fact that the average coordinate discrepancies in all directions (dE_{Avg}, dN_{Avg}, and dh_{Avg}) are not small in size. Rather they are quite large with size comparable to their associated RMSE values ($RMSE_E$, $RMSEN_N$, and $RMSE_h$). This means that the large discrepancies are not arising from only random error but also contain biases or systematic errors.

From the results in Table 6.1, it should be noted that for both datasets (231Route and INDOTLoop) of Asset Grade 1 and 2, the estimated rotation angles are quite small (rotation matrix is almost the identity matrix). This means that the source of the absolute discrepancies is really just a shift or a bias. As such, it is to be expected that the absolute accuracy of the transformed dataset will be much improved compared to the accuracy of the original dataset (untransformed). By contrast, the results of relative accuracy evaluation of the transformed data should not be much improved when compared to the evaluation of the original data. Rather they should be comparable. This is due to the fact that the translations (the shifts) applied to the original data will not change the results in relative accuracy evaluation because all validations points are shifted by the same amount. Even though in this case the transformation carries translations as well as rotations, the very small magnitude of the rotations will not cause a significant change in the results of relative accuracy evaluation.

According to the just mentioned reasons, only the absolute accuracy evaluation results show a difference between original vs. transformed data. The relative accuracy evaluation results are not significantly different between the two. Therefore the relative accuracy will not be investigated for transformed data. Only results for the original dataset will be tabulated (see Table 7.7 through Table 7.10).

6.5 Analysis of the MMS Data Resolution (Point Density)

Another important aspect to be considered when evaluating the quality of the point clouds data is the point spatial resolution or point density. Point density plays an important role in feature extraction from scanned point clouds. The resolution of the MMS dataset is characterized in terms of point density which is the number of points per unit area (points/m^2 or points/ft^2). A point density value itself is not a complete piece of information, it is important that the point density information be accompanied by the location where it was evaluated.

In this case the point densities of the MMS data obtained from different mobile mapping systems are evaluated. A swath of points is cut from each of the datasets at the same location and extent. The location

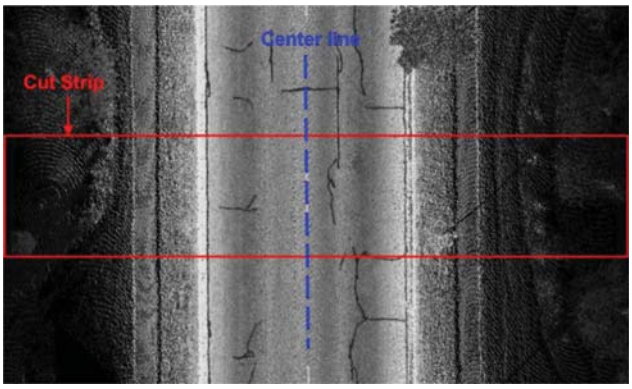

Figure 6.8 The cut strip of point clouds for point density analysis of MMS data.

of the strip of points is at the NE corner of the INDOTLoop. We consider the road centerline as the zero point (offset) of the file (see Figure 6.8). The point density analysis is performed on each side (L&R) of the cut strip. The point density of the MMS data is reported in terms of the number of points per unit area at varies offset distances from the reference center line (the road center). The results of the point density analysis are shown in section 7.6.

7. RESULTS AND DISCUSSIONS

In this section the results of the absolute and relative accuracy evaluation of each dataset will be presented and discussed. First the evaluation results of the absolute accuracy and the relative accuracy (over the whole project area) of each dataset will be presented in section 7.1. In section 7.2, the evaluation results of the relative accuracy (over a small area) obtained from the method of bridge clearance measurements will be presented. The absolute and relative accuracy evaluation results of all datasets will be summarized in sections 7.3 and 7.4. Section 7.5 will cover discussions related to the obtained data accuracy evaluation results. Other important aspects obtained from the analyses of the MMS datasets will also be covered from section 7.6 onwards.

Note that following completion of the tabulation of results and performance of the analysis, we concluded that the concept of relative accuracy over the project area was not a useful concept. MMS are inherently absolute systems, and calling something relative does not make it so. Therefore we present results of the relative analysis here, so the reader can make his own judgement, but we omit them from the final tables.

7.1 Results of the Absolute Accuracy and the Relative Accuracy (over the Whole Project Area), Evaluation of all MMS Datasets

Referring to all 10 MMS datasets of this project and their corresponding names from Table 4.4, each dataset is evaluated for absolute accuracy as described in section 6.2, and for relative accuracy (over whole project area) as described in section 6.3.1. In this section these results are presented in Tables 7.1 through 7.10. The detailed descriptive statistics of the absolute and relative accuracy evaluation for each dataset, starting from the first step of producing Cutlevel 1, through the process of getting Cutlevel 2 and Cutlevel 3, towards the final positions of detected coordinates of validation points, are available in Appendix D.

Refer to and recall the notation discussed in section 6.2 and 6.3. As previously mentioned when considering the relative accuracy, it is often expected that the magnitude of double differences are proportional to distance. However, this may not be the case when evaluating relative accuracy by using a network of validation points distributed over a large project area. Another factor is that MMS data is inherently absolute, and the whole concept of relative accuracy may not be applicable. In order to study the effect of distance between validation point pairs on the computed relative accuracy, the values of computed DDh_{ij}, and DDP_{ij}, (see Equation 6.21) are plotted against their associated sorted distances (between point "i" and point "j" for all possible values of i and j when $i \neq j$).

Figure 7.1 shows the plots of the associated values of DDh and DDP at various sorted distances from all possible validation point pairs for the case of 231Route of Design Grade 1. For the 231Route, there are total of 8 validation points which make the possible number of point pairs 28 (from combinatorics). Associated with each pair are the values of computed DDP and DDh and the distance between the point pair. The distances are sorted and their associated values of DDP and DDh are plotted. From the plot shown in Figure 7.1, we see there is no distance effect on the computed DDP (planimetric) and DDh (vertical). The same idea is applied to other datasets. For each dataset the plots are created. It turns out that all plots show a similar pattern with the values of DDP and DDh being random (up and down) over the range of distances. This confirms the above hypothesis that MMS being inherently absolute, does not exhibit the trend of relative errors being proportional to distance. This prevents one from making statements like "one part in five thousand, or 1:5000" to describe relative accuracy.

If the Asset Grade 2 data had not been "fixed," if the large shifts had been left in, then you would have seen a big improvement in relative accuracy compared to absolute accuracy. It was exactly that difference which led us to "fix" the data by registering to control points. So you can say that if a vendor neglects to properly

TABLE 7.1
Results of the absolute accuracy and the relative accuracy evaluation of 231Route 250KHz of Design Grade 1.

Absolute Accuracy	**$RMSE_E$ (cm)**		**$RMSE_N$ (cm)**		**$RMSE_h$ (cm)**		**$RMSE_P$ (cm)**		**$RMSE_Q$ (cm)**	
	2.6		3.6		0.9		4.5		4.6	
	dE_{Avg} (cm)		**dN_{Avg} (cm)**		**dh_{Avg} (cm)**		**dP_{Avg} (cm)**		**dQ_{Avg} (cm)**	
	0.0		-0.7		-0.2		4.3		4.4	
Relative Accuracy (over whole project area)	**$RMSE_{\|ddE\|}$ (cm)**		**$RMSE_{\|ddN\|}$ (cm)**		**$RMSE_{\|ddh\|}$ (cm)**		**$RMSE_{\|ddP\|}$ (cm)**		**$RMSE_{\|ddQ\|}$ (cm)**	
	4.0		5.4		1.3		3.8		3.8	
	|ddE| (cm)		**|ddN| (cm)**		**|ddh| (cm)**		**|ddP| (cm)**		**|ddQ| (cm)**	
	Min	**Max**	**Min**	**Max**	**Min**	**Max**	**Min**	**Max**	**Min**	**Max**
	0.0	7.3	0.1	10.0	0.0	2.7	0.1	6.7	0.1	6.7

TABLE 7.2
Results of the absolute accuracy and the relative accuracy evaluation of 231Route 500KHz of Design Grade 1.

Absolute Accuracy	**$RMSE_E$ (cm)**	**$RMSE_N$ (cm)**	**$RMSE_h$ (cm)**	**$RMSE_P$ (cm)**	**$RMSE_Q$ (cm)**
	2.4	2.4	1.3	3.4	3.6
	dE_{Avg} (cm)	**dN_{Avg} (cm)**	**dh_{Avg} (cm)**	**dP_{Avg} (cm)**	**dQ_{Avg} (cm)**
	-1.1	0.3	0.0	3.2	3.5
Relative Accuracy (over whole project area)	**$RMSE_{\|ddE\|}$ (cm)**	**$RMSE_{\|ddN\|}$ (cm)**	**$RMSE_{\|ddh\|}$ (cm)**	**$RMSE_{\|ddP\|}$ (cm)**	**$RMSE_{\|ddQ\|}$ (cm)**
	3.2	3.7	1.9	2.2	2.2
	|ddE| (cm)	**|ddN| (cm)**	**|ddh| (cm)**	**|ddP| (cm)**	**|ddQ| (cm)**
	Min **Max**	**Min** **Max**	**Min** **Max**	**Min** **Max**	**Min** **Max**
	0.0 5.0	0.0 7.9	0.0 4.6	0.0 3.9	0.0 4.0

TABLE 7.3
Results of the absolute accuracy and the relative accuracy evaluation of INDOTLoop Acceleration Collection of Design Grade 1.

Absolute Accuracy	**$RMSE_E$ (cm)**	**$RMSE_N$ (cm)**	**$RMSE_h$ (cm)**	**$RMSE_P$ (cm)**	**$RMSE_Q$ (cm)**
	3.4	2.9	2.5	4.5	5.1
	dE_{Avg} (cm)	**dN_{Avg} (cm)**	**dh_{Avg} (cm)**	**dP_{Avg} (cm)**	**dQ_{Avg} (cm)**
	-0.4	-0.1	-1.6	4.3	5.0
Relative Accuracy (over whole project area)	**$RMSE_{\|ddE\|}$ (cm)**	**$RMSE_{\|ddN\|}$ (cm)**	**$RMSE_{\|ddh\|}$ (cm)**	**$RMSE_{\|ddP\|}$ (cm)**	**$RMSE_{\|ddQ\|}$ (cm)**
	5.1	4.3	2.9	5.0	5.0
	|ddE| (cm)	**|ddN| (cm)**	**|ddh| (cm)**	**|ddP| (cm)**	**|ddQ| (cm)**
	Min **Max**	**Min** **Max**	**Min** **Max**	**Min** **Max**	**Min** **Max**
	0.2 10.9	0.0 8.5	0.5 5.9	0.5 10.8	0.5 10.8

TABLE 7.4
Results of the absolute accuracy and the relative accuracy evaluation of INDOTLoop No Acceleration Collection of Design Grade 1.

Absolute Accuracy	**$RMSE_E$ (cm)**	**$RMSE_N$ (cm)**	**$RMSE_h$ (cm)**	**$RMSE_P$ (cm)**	**$RMSE_Q$ (cm)**
	2.9	3.0	2.3	4.2	4.8
	dE_{Avg} (cm)	**dN_{Avg} (cm)**	**dh_{Avg} (cm)**	**dP_{Avg} (cm)**	**dQ_{Avg} (cm)**
	-0.7	-0.9	-1.5	4.0	4.7
Relative Accuracy (over whole project area)	**$RMSE_{\|ddE\|}$ (cm)**	**$RMSE_{\|ddN\|}$ (cm)**	**$RMSE_{\|ddh\|}$ (cm)**	**$RMSE_{\|ddP\|}$ (cm)**	**$RMSE_{\|ddQ\|}$ (cm)**
	4.2	4.4	2.6	4.6	4.6
	|ddE| (cm)	**|ddN| (cm)**	**|ddh| (cm)**	**|ddP| (cm)**	**|ddQ| (cm)**
	Min **Max**	**Min** **Max**	**Min** **Max**	**Min** **Max**	**Min** **Max**
	0.4 8.2	0.0 7.6	0.3 5.0	0.0 8.9	0.0 8.9

TABLE 7.5
Results of the absolute accuracy and the relative accuracy evaluation of 231Route of Design Grade 2.

Absolute Accuracy	**$RMSE_E$ (cm)**	**$RMSE_N$ (cm)**	**$RMSE_h$ (cm)**	**$RMSE_P$ (cm)**	**$RMSE_Q$ (cm)**
	2.5	1.9	0.9	3.2	3.3
	dE_{Avg} (cm)	**dN_{Avg} (cm)**	**dh_{Avg} (cm)**	**dP_{Avg} (cm)**	**dQ_{Avg} (cm)**
	-1.7	0.1	0.5	2.9	3.1
Relative Accuracy (over whole project area)	**$RMSE_{\|ddE\|}$ (cm)**	**$RMSE_{\|ddN\|}$ (cm)**	**$RMSE_{\|ddh\|}$ (cm)**	**$RMSE_{\|ddP\|}$ (cm)**	**$RMSE_{\|ddQ\|}$ (cm)**
	2.8	2.9	1.2	2.6	2.6
	|ddE| (cm)	**|ddN| (cm)**	**|ddh| (cm)**	**|ddP| (cm)**	**|ddQ| (cm)**
	Min **Max**	**Min** **Max**	**Min** **Max**	**Min** **Max**	**Min** **Max**
	0.3 5.9	0.0 5.5	0.2 2.4	0.2 5.4	0.2 5.4

TABLE 7.6
Results of the absolute accuracy and the relative accuracy evaluation of INDOTLoop of Design Grade 2.

Absolute Accuracy	**$RMSE_E$ (cm)**	**$RMSE_N$ (cm)**	**$RMSE_h$ (cm)**	**$RMSE_P$ (cm)**	**$RMSE_Q$ (cm)**	
	1.7	2.4	0.9	3.0	3.1	
	dE_{Avg} (cm)	**dN_{Avg} (cm)**	**dh_{Avg} (cm)**	**dP_{Avg} (cm)**	**dQ_{Avg} (cm)**	
	0.8	-0.1	0.4	2.4	2.6	
Relative Accuracy (over whole project area)	**$RMSE_{\|ddE\|}$ (cm)**	**$RMSE_{\|ddN\|}$ (cm)**	**$RMSE_{\|ddh\|}$ (cm)**	**$RMSE_{\|ddP\|}$ (cm)**	**$RMSE_{\|ddQ\|}$ (cm)**	
	2.3	3.7	1.2	3.3	3.3	
	|ddE| (cm)		**|ddN| (cm)**		**|ddh| (cm)**	
	Min	**Max**	**Min**	**Max**	**Min**	**Max**
	0.0	5.7	0.1	8.2	0.1	2.7
	|ddP| (cm)		**|ddQ| (cm)**			
	Min	**Max**	**Min**	**Max**		
	0.0	7.7	0.0	7.7		

TABLE 7.7
Results of the absolute accuracy and the relative accuracy evaluation of 231Route of Asset Grade 1.

Absolute Accuracy		**$RMSE_E$ (cm)**	**$RMSE_N$ (cm)**	**$RMSE_h$ (cm)**	**$RMSE_P$ (cm)**	**$RMSE_Q$ (cm)**
	Original data	179.2	30.1	78.6	181.7	198.0
	Transformed data	8.2	6.0	11.9	10.2	15.7
		dE_{Avg} (cm)	**dN_{Avg} (cm)**	**dh_{Avg} (cm)**	**dP_{Avg} (cm)**	**dQ_{Avg} (cm)**
	Original data	-179.2	29.5	-78.3	181.7	197.9
	Transformed data	7.0	-0.0	-10.2	9.2	14.9
Relative Accuracy (over whole project area)		**$RMSE_{\|ddE\|}$ (cm)**	**$RMSE_{\|ddN\|}$ (cm)**	**$RMSE_{\|ddh\|}$ (cm)**	**$RMSE_{\|ddP\|}$ (cm)**	**$RMSE_{\|ddQ\|}$ (cm)**
		6.5	9.0	9.0	8.9	8.9
		|ddE| (cm)		**|ddN| (cm)**		**|ddh| (cm)**
		Min	**Max**	**Min**	**Max**	**Min**	**Max**
		0.4	13.9	0.0	20.4	0.1	21.5
		|ddP| (cm)		**|ddQ| (cm)**		
		Min	**Max**	**Min**	**Max**		
		0.2	20.4	0.0	20.4		

register data, then relative accuracy versus absolute accuracy become an issue to consider. However it seems unlikely that vendors can really get by with this kind of neglect.

7.2 Results of the Relative Accuracy (over Small Area) Evaluation of all MMS Datasets

As previously mentioned in section 6.3.2, the evaluation of the relative accuracy of MMS data over small project area may be useful and can be achieved through the idea of bridge clearance determination. These are inherently relative since they involve coordinate differences (in height only). In this section the results of the determined bridge clearances will be presented in Table 7.11. The accuracy of the determined bridge clearances can be evaluated by comparing the determined bridge clearance values from the MMS data against the ones determined from the point cloud obtained by STLS system. Note that the reference static data (STLS) was verified in the field by multiple distance measurements.

The difference in bridge clearance values at lane stripe "i," is denoted as ΔBC^i. This (double) difference

TABLE 7.8
Results of the absolute accuracy and the relative accuracy evaluation of INDOTLoop of Asset Grade 1.

Absolute Accuracy		**$RMSE_E$ (cm)**	**$RMSE_N$ (cm)**	**$RMSE_h$ (cm)**	**$RMSE_P$ (cm)**	**$RMSE_Q$ (cm)**
	Original data	186.0	10.3	61.3	186.3	196.1
	Transformed data	5.0	8.1	12.0	9.6	15.3
		dE_{Avg} (cm)	**dN_{Avg} (cm)**	**dh_{Avg} (cm)**	**dP_{Avg} (cm)**	**dQ_{Avg} (cm)**
	Original data	-185.9	-6.4	-61.1	186.2	196.1
	Transformed data	1.8	0.1	-10.6	8.7	14.1
Relative Accuracy (over whole project area)		**$RMSE_{\|ddE\|}$ (cm)**	**$RMSE_{\|ddN\|}$ (cm)**	**$RMSE_{\|ddh\|}$ (cm)**	**$RMSE_{\|ddP\|}$ (cm)**	**$RMSE_{\|ddQ\|}$ (cm)**
		7.2	12.3	8.2	12.1	12.1
		|ddE| (cm)		**|ddN| (cm)**		**|ddh| (cm)**
		Min	**Max**	**Min**	**Max**	**Min**	**Max**
		0.8	17.1	1.7	23.4	0.2	19.8
		|ddP| (cm)		**|ddQ| (cm)**		
		Min	**Max**	**Min**	**Max**		
		0.2	28.7	0.3	28.7		

TABLE 7.9
Results of the absolute accuracy and the relative accuracy evaluation of 231Route of Asset Grade 2.

Absolute Accuracy		**$RMSE_E$ (cm)**	**$RMSE_N$ (cm)**	**$RMSE_h$ (cm)**	**$RMSE_P$ (cm)**	**$RMSE_Q$ (cm)**
	Original data	48.9	83.5	113.5	96.8	149.1
	Transformed data	2.4	5.2	2.0	5.7	6.1
		dE_{Avg} (cm)	**dN_{Avg} (cm)**	**dh_{Avg} (cm)**	**dP_{Avg} (cm)**	**dQ_{Avg} (cm)**
	Original data	-48.8	83.4	-113.5	96.7	149.1
	Transformed data	0.1	0.5	1.1	5.5	5.9
Relative Accuracy (over whole project area)		**$RMSE_{\|ddE\|}$ (cm)**	**$RMSE_{\|ddN\|}$ (cm)**	**$RMSE_{\|ddh\|}$ (cm)**	**$RMSE_{\|ddP\|}$ (cm)**	**$RMSE_{\|ddQ\|}$ (cm)**
		3.5	7.8	2.5	6.3	6.3
		|ddE| (cm)		**|ddN| (cm)**		**|ddh| (cm)**		**|ddP| (cm)**		**|ddQ| (cm)**	
		Min	**Max**	**Min**	**Max**	**Min**	**Max**	**Min**	**Max**	**Min**	**Max**
		0.0	7.8	0.5	13.0	0.1	5.4	0.1	11.5	0.1	11.5

TABLE 7.10
Results of the absolute accuracy and the relative accuracy evaluation of INDOTLoop of Asset Grade 2.

Absolute Accuracy		**$RMSE_E$ (cm)**	**$RMSE_N$ (cm)**	**$RMSE_h$ (cm)**	**$RMSE_P$ (cm)**	**$RMSE_Q$ (cm)**
	Original data	50.3	84.4	114.7	98.3	151.0
	Transformed data	3.2	4.1	3.9	5.2	6.5
		dE_{Avg} (cm)	**dN_{Avg} (cm)**	**dh_{Avg} (cm)**	**dP_{Avg} (cm)**	**dQ_{Avg} (cm)**
	Original data	-50.2	84.3	-114.7	98.1	151.0
	Transformed data	-1.6	0.4	-1.1	4.4	6.0
Relative Accuracy (over whole project area)		**$RMSE_{\|ddE\|}$ (cm)**	**$RMSE_{\|ddN\|}$ (cm)**	**$RMSE_{\|ddh\|}$ (cm)**	**$RMSE_{\|ddP\|}$ (cm)**	**$RMSE_{\|ddQ\|}$ (cm)**
		4.2	6.0	4.5	6.2	6.2
		|ddE| (cm)		**|ddN| (cm)**		**|ddh| (cm)**		**|ddP| (cm)**		**|ddQ| (cm)**	
		Min	**Max**	**Min**	**Max**	**Min**	**Max**	**Min**	**Max**	**Min**	**Max**
		0.3	9.5	0.2	11.8	0.1	10.2	0.3	14.8	0.3	14.9

is between the MMS clearance (BC^i_{MMS}) and the STLS clearance (BC^i_{STLS}). The same idea is applied to all bridge clearances at other lane stripes (ΔBC^{E1}, ΔBC^{E2} and so on). The results are shown in Table 7.12.

The right hand column of Table 7.12 is a kind of quality metric for the bridge clearance determination (relative vertical accuracy over small area). These results will be discussed more fully in section 7.5.

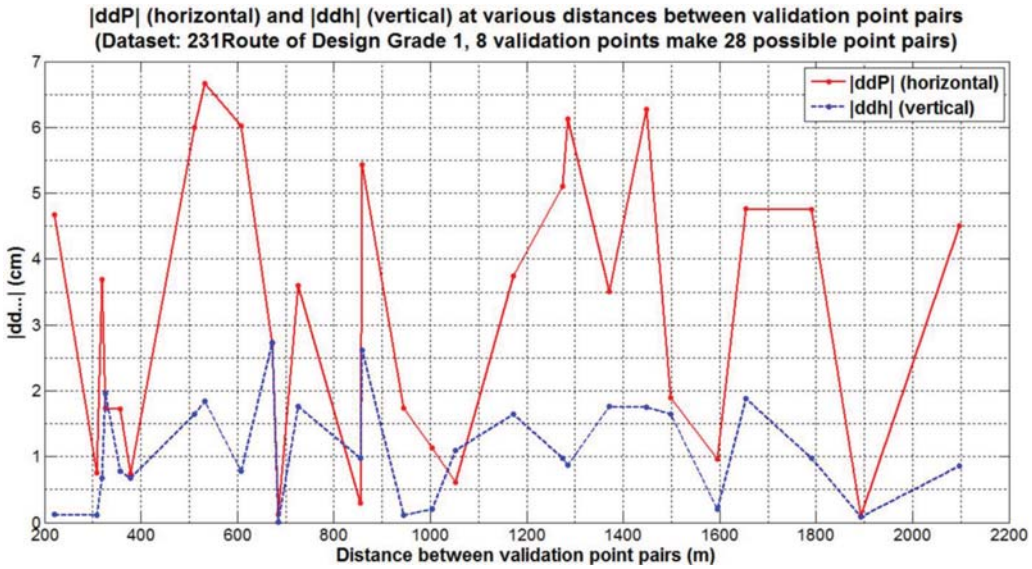

Figure 7.1 Trend of relative accuracy evaluation results when consider the whole network of validation points.

TABLE 7.11
Bridge clearance values obtained from STLS and all MMS used.

System	BC: Bridge clearance at marking (m)						
	E1	E2	E3	E4	W1	W2	W3
STLS (Reference)	5.751	5.541	5.338	5.166	6.034	6.272	6.446
Design Grade 1 250 KHz	5.759	5.567	5.364	5.172	6.040	6.287	6.496
Design Grade 1 500 KHz	5.755	5.556	5.341	5.158	6.034	6.283	6.470
Design Grade 2	5.736	5.518	5.320	5.123	6.025	6.253	6.443
Asset Grade 1	5.731	5.510	5.354	5.109	6.005	6.292	6.459
Asset Grade 2	5.714	5.512	5.313	5.140	6.024	6.233	6.429

TABLE 7.12
The differences in bridge clearances between the ones obtained by MMS and the reference ones from STLS system.

System	ΔBC = BCMMS - BCSTLS Difference of bridge clearances at marking (m)							RMSE of ΔBC (cm)
	ΔBCE1	ΔBCE2	ΔBCE3	ΔBCE4	ΔBCW1	ΔBCW2	ΔBCW3	
Design Grade 1 250 KHz	0.008	0.027	0.026	0.007	0.006	0.015	0.050	**2.5**
Design Grade 1 500 KHz	0.003	0.015	0.003	-0.007	-0.000	0.010	0.023	**1.2**
Design Grade 2	-0.016	-0.023	-0.018	-0.042	-0.010	-0.019	-0.004	**2.2**
Asset Grade 1	-0.021	-0.031	0.016	-0.057	-0.029	0.019	0.013	**3.0**
Asset Grade 2	-0.037	-0.029	-0.025	-0.025	-0.011	-0.039	-0.018	**2.8**

7.3 Summary of the Absolute Accuracy Evaluation Results of all Datasets

See Tables 7.13 and 7.14 for a summary of the absolute accuracy evaluation results of all datasets.

7.4 Summary of the Relative Accuracy Evaluation Results of all MMS Datasets

See Tables 7.15 and 7.16 for a summary of the relative accuracy evaluation results of all MMS datasets.

7.5 Discussions of the Accuracy Evaluation Results

Some discussions about accuracy evaluation have been made along with the presentation of the results in the previous sections. In this section the evaluation and discussion of those results will be consolidated.

From the results of absolute and relative accuracy evaluations as presented in section 7.1 through 7.4, the absolute horizontal accuracy and the absolute vertical accuracy (in term of RMSE of coordinates differences when comparing to the reference ones in horizontal and vertical direction) of each dataset can be summarized in Table 7.17. We have chosen to omit the relative accuracy results, because, as mentioned earlier, they do not appear to be informative. Our opinion is that the concept of relative accuracy for MMS over a large area does not really exist. On the other hand, the concept of relative accuracy within a small area for vertical is a valid concept and is therefore presented. This approach is often used in practice for determination of bridge clearances.

From Table 7.17, we see that the worst case of the absolute horizontal and vertical accuracies for the Design Grade MMS are 4.5 cm and 2.5 cm, respectively. For the case of Asset Grade MMS, the worst case of the absolute horizontal and vertical accuracies are 10.2 cm and 12 cm, respectively.

The relative vertical accuracies within a small area (bridge clearance analysis) are 2.5 cm, 2.2 cm, 3.0 cm

TABLE 7.13
Absolute accuracy evaluation results in terms of RMSE of all datasets.

MMS	Dataset Reference Name	$RMSE_E$ (cm)	$RMSE_N$ (cm)	$RMSE_h$ (cm)	$RMSE_P$ (cm)	$RMSE_Q$ (cm)
Design Grade 1	231Route 250KHz	2.6	3.6	**0.9**	**4.5**	4.6
	231Route 500KHz	2.4	2.4	**1.3**	**3.4**	3.6
	INDOTLoop Acceleration Collection	3.4	2.9	**2.5**	**4.5**	5.1
	INDOTLoop No Acceleration Collection	2.9	3.0	**2.3**	**4.2**	4.8
Design Grade 2	231Route	2.5	1.9	**0.9**	**3.2**	3.3
	INDOTLoop	1.7	2.4	**0.9**	**3.0**	3.1
Asset Grade 1	231Route	8.2	6.0	**11.9**	**10.2**	15.7
	INDOTLoop	5.0	8.1	**12.0**	**9.6**	15.3
Asset Grade 2	231Route	2.4	5.2	**2.0**	**5.7**	6.1
	INDOTLoop	3.2	4.1	**3.9**	**5.2**	6.5

TABLE 7.14
Absolute accuracy evaluation results in terms of average discrepancies of all datasets.

MMS	Dataset Reference Name	dE_{Avg} (cm)	dN_{Avg} (cm)	dh_{Avg} (cm)	dP_{Avg} (cm)	dQ_{Avg} (cm)
Design Grade 1	231Route 250KHz	0.0	-0.7	-0.2	4.3	4.4
	231Route 500KHz	-1.1	0.3	0.0	3.2	3.5
	INDOTLoop Acceleration Collection	-0.4	-0.1	-1.6	4.3	5.0
	INDOTLoop No Acceleration Collection	-0.7	-0.9	-1.5	4.0	4.7
Design Grade 2	231Route	-1.7	0.1	0.5	2.9	3.1
	INDOTLoop	0.8	-0.1	0.4	2.4	2.6
Asset Grade 1	231Route	7.0	-0.0	-10.2	9.2	14.9
	INDOTLoop	1.8	0.1	-10.6	8.7	14.1
Asset Grade 2	231Route	0.1	0.5	1.1	5.5	5.9
	INDOTLoop	-1.6	0.4	-1.1	4.4	6.0

TABLE 7.15
Summary of the relative vertical accuracy evaluation (over small area) results from the method of bridge clearance determination.

MMS	Bridge	RMSE of ΔBC (cm) (reflect relative vertical accuracy over small area)
Design Grade 1	231Route 250KHz	2.5
	231Route 500KHz	1.2
Design Grade 2	231Route	2.2
Asset Grade 1	231Route	3.0
Asset Grade 2	231Route	2.8

and 2.8 cm for the case of Design Grade 1, Design Grade 2, Asset Grade 1 and Asset Grade 2, respectively.

The relative accuracies over the whole project area for both Design and Asset grade MMS showed no particular pattern. This confirms the aforementioned hypothesis (as mentioned in section 7.1) that MMS, being inherently absolute, does not exhibit the trend of relative errors being proportional to distance. Hence evaluating relative accuracy over the large area is not a valid or useful concept. Since relative vertical accuracy within a small area is widely used for bridge clearance determination, it was deemed informative to include this data in the summary table.

The results of relative vertical accuracy evaluation within a small area have shown that the asset grade mobile mapping system can provide quite a good value of 1D relative accuracy (3.0 cm and 2.8 cm for Asset Grade 1 and Asset Grade 2, respectively). This compares favorably with the results for design grade (2.5 cm and 2.2 cm for Design Grade 1 and Design Grade 2, respectively). In this case the 1D relative vertical accuracies produced by asset grade MMS are seen to be slightly inferior but quite close to those of design grade.

Not all of the considered MMS's have better value of 1D relative vertical accuracy within a small area compared to their corresponding absolute accuracy. This illustrates and reinforces an important insight about relative accuracy for MMS data. That is the conventional concept of relative accuracy does not really apply to MMS. This is due to the fact that the MMS is inherently absolute since every single scanned point is individually registered absolutely by a constantly changing transformation (in the post processing). Our recommendation is therefore to deprecate or discourage use of the concept of relative accuracy with MMS (except within a small area, where it is widely used, therefore worthy of study).

TABLE 7.16
Summary of the relative accuracy evaluation (over whole project area) results in terms of RMSE of all datasets.

MMS	Dataset Reference Name	$RMSE_{\|ddE\|}$ (cm)	$RMSE_{\|ddN\|}$ (cm)	$RMSE_{\|ddh\|}$ (cm)	$RMSE_{\|ddP\|}$ (cm)	$RMSE_{\|ddQ\|}$ (cm)
Design Grade 1	231Route 250KHz	4.0	5.4	**1.3**	**3.8**	3.8
	231Route 500KHz	3.2	3.7	**1.9**	**2.2**	2.2
	INDOTLoop Acceleration Collection	5.1	4.3	**2.9**	**5.1**	5.0
	INDOTLoop No Acceleration Collection	4.2	4.4	**2.6**	**4.6**	4.6
Design Grade 2	231Route	2.8	2.9	**1.2**	**2.6**	2.6
	INDOTLoop	2.3	3.7	**1.2**	**3.3**	3.3
Asset Grade 1	231Route	6.5	9.0	**9.0**	**8.9**	8.9
	INDOTLoop	7.2	12.3	**8.2**	**12.1**	12.1
Asset Grade 2	231Route	3.5	7.8	**2.5**	**6.3**	6.3
	INDOTLoop	4.2	6.0	**4.5**	**6.2**	6.2

TABLE 7.17
Complete sets of the absolute and relative accuracies of MMS datasets.

MMS	Dataset Reference Name	Absolute Accuracy (RMSE)		Relative Accuracy (RMSE) (Over Small Area)
		Horizontal (cm)	Vertical (cm)	Vertical (cm)
Design Grade 1	231Route 250KHz	**4.5**	0.9	**2.5**
	231Route 500KHz	3.4	1.3	1.2
	INDOTLoop Acceleration Collection	**4.5**	2.5	
	INDOTLoop No Acceleration Collection	4.2	2.3	
Design Grade 2	231Route	3.2	0.9	**2.2**
	INDOTLoop	3.0	0.9	
Asset Grade 1	231Route	**10.2**	11.9	**3.0**
	INDOTLoop	9.6	**12.0**	
Asset Grade 2	231Route	5.7	2.0	**2.8**
	INDOTLoop	5.2	3.9	

For the case of absolute accuracy in horizontal and vertical, the asset grade systems (Asset Grade 1 and Asset Grade 2) cannot compete with the design grade systems (Design Grade 1 and Design Grade 2). However it was very interesting to see the absolute accuracy of Asset Grade 2 (after being "fixed") improved substantially (unlike Asset Grade 1) when compared to the design grade systems. This emphasizes the importance of high quality post processing, using high quality position and attitude observations and constraints.

In terms of utility, accuracy is not the only factor of importance. Point density, intensity quality, RGB tagging, and registration of RGB (color) to point cloud can be of great importance for visual interpretation of MMS data. We did not quantitatively evaluate these factors, although they were mentioned informally on occasion.

Lastly, one could criticize this project & report for insufficient sampling of vendors and systems. Ideally one would have two or three instances for every available system. This increased sampling would lead to stronger conclusions. In our defense we would say that there were considerable practical challenges dealing with the few vendors and systems that we used. Data anomalies, repeated collection sessions, costs, scheduling, and logistics of preparing the test sites were always a concern. More samples from more vendors would have exacerbated these problems and in fact would not have been possible. We feel that we achieved a good balance of vendor/system diversity and rigorous quality checking, while completing the project in a timely fashion.

7.6 Results and Discussion of Point Density Analysis

Refer to section 6.5 which describes the method of evaluating the resolution or point density of MMS data. The point densities of the point clouds in the cut strip are evaluated at varying offset distance from the reference center line. Figure 7.2 shows the plot of the point densities

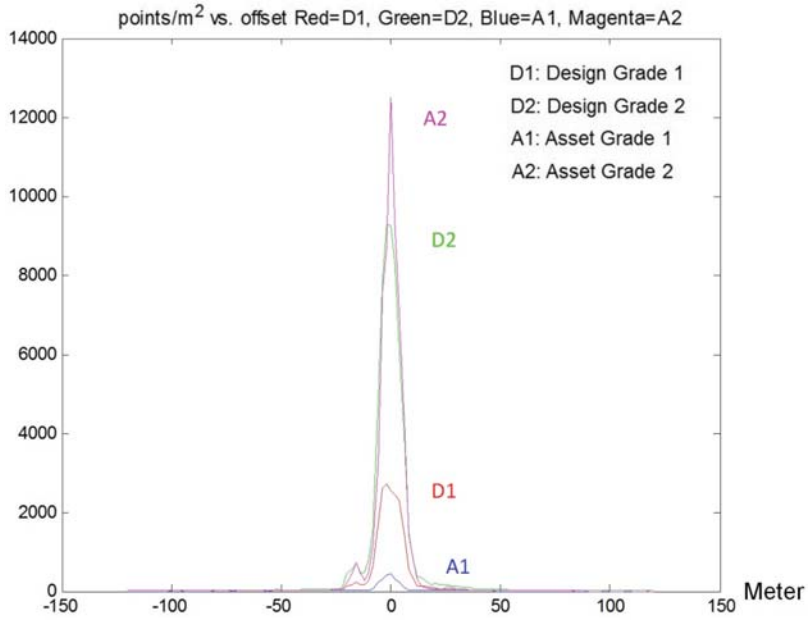

Figure 7.2 Plot point density vs. offset distance from road center line.

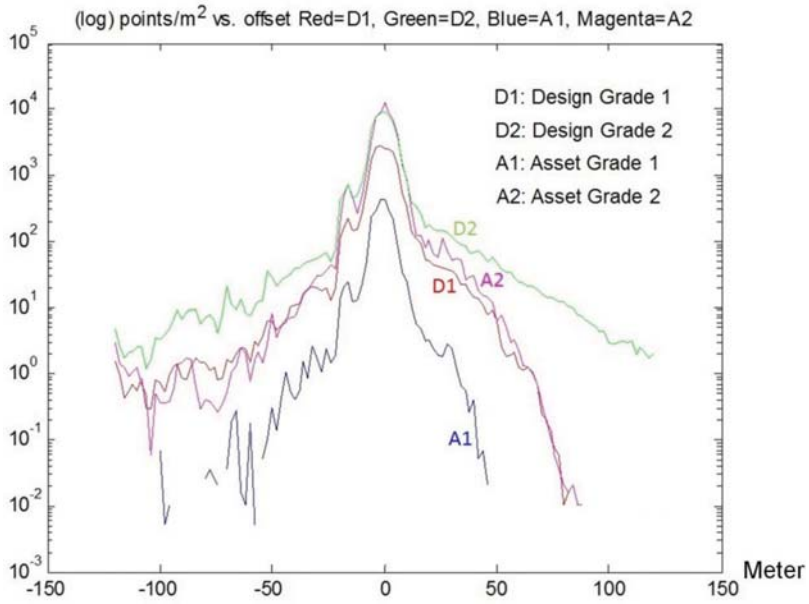

Figure 7.3 Plot in a log scale of point density vs. offset distance from road center line.

at offset distances from the center line for 4 different mobile mapping systems. Similar to Figure 7.2, Figure 7.3 shows the same set of data in a log scale plot.

The results as shown in Figure 7.2 indicate that the MMS Design Grade 2 and Asset Grade 2 have produced higher point density comparing to the ones of Design Grade 1 and Asset Grade 1. The point density values produced by Asset Grade 2 are in the same range as the ones of Design grade 2 with only the difference in the area near the reference centerline (at small offset distances). The point density curve of Asset Grade 2 has peaked over the one of Design Grade 2. The quality of MMS data of Asset Grade 1 in terms of point density seems quite poor as the values of point density even around the center line area are significantly low in comparison to the other systems.

For each dataset itself the variations in point densities over the offset distances from center line is not well observed in the normal plot scale. Figure 7.3 shows the same information in the log scale plot. This plot makes it possible to visualize each dataset as the point densities become small. The point density variation trends of all datasets are similar (the shape of plotted curves are in the similar pattern), that is the point density is high in the vicinity of center line zone and decreasing over the increasing offset distances from the center line, with the possibilities of some small variations (jagged curved or small magnitude of oscillation).

The rate of change in point densities over the offset distances away from the road center line of MMS Design Grade 2 is very slow which means that when the distance is further away its point density gradually decreases. This is obviously not the case for Asset Grade 1 and Asset Grade 2 where the abrupt changes in point densities happened with the increase of offset distances. For the case of Design Grade 1, it somehow possesses both the slow rate of changes in point densities (see left side of the curve) and the abrupt changes in point densities over the course of offset distances (see right side of the curve). We believe that the right side of the curves is the best representation of the density performance. The left side may include some points from an adjacent trajectory. Also the left side had more relief and vegetation than the right side.

Point density plays vital role in further MMS data manipulation processes such feature extraction. The bridge clearance measurements performed in this project has strongly substantiated the above claim. Further discussions about this issue will occur in the next section, with specific comments on each dataset.

7.7 Discussions on Various Properties of each Dataset

In this section many aspects or properties pertaining to the qualities of the MMS dataset will be discussed in the dataset-wise manner. The discussions here are based on the perspectives drawn from the actual data evaluations, analyses, processing, and investigation. The accuracies of the MMS datasets will not be discussed here as they have already been covered in section 7.5.

7.7.1 Discussion on Various Properties of data of MMS Design Grade 1

The overall point density of Design Grade 1 dataset may not be as high as the ones of Design Grade 2 and Asset Grade 2 but it is sufficient for feature extraction tasks such as the automatic sphere target detection. The sphere detection algorithm worked fine with the dataset and produced the robust results of the validation point coordinates from the scanned point clouds. It can be perceived from the visual inspections throughout the scanned point clouds that the point clouds possess fairly good and sufficient point densities.

The inspections throughout the whole point cloud have also given information on the quality of the produced point clouds intensities. It is noticeable that the intensities of the point clouds obtained from Design Grade 1 are of very good quality. The high contrast property of painted targets (control points) on the pavement surface is well captured in the scanned point clouds.

For this Design Grade 1 system, the true color (RGB) information available from the images of the scanned scenes was not well assigned or registered to the point clouds. There are many mismatched patches of RGB color to the point clouds and those are easily noticeable; however, the RGB information are used for only the overall visualization of the point clouds but not in any of the data evaluation processes.

Sufficient point densities and good quality in capturing intensities of the point cloud with this system make bridge clearance determination proceed smoothly. It does not take a huge effort of the project personnel to locate and digitize the lane stripe for extracting the necessary points.

7.7.2 Discussion on Various Properties of data of MMS Design Grade 2

The point densities of Design Grade 2 dataset are noticeably high in comparison to the ones of Design Grade 1 which is same grade of instrument (design grade) and Asset Grade 1, The point densities of Design Grade 2 dataset are in the same range as the ones of Asset Grade 2 with the only difference in the area near the reference center line. The sphere detection algorithm worked fine with the dataset and produced robust results of the validation point coordinates from the scanned point clouds. It can be perceived from the visual inspections throughout the scanned point clouds that this Design Grade 2 system has produced point clouds with very high point densities.

By inspection, it is noticeable that the intensities of the point clouds obtained from Design Grade 2 are of very good quality. The high contrast property of painted targets (control points) on the pavement surface is well captured in the scanned point clouds.

Locating the lane stripes for bridge clearance determination has become much easier because of the high point densities and good intensity quality of the point clouds obtained from this Design Grade 2 system.

Regarding RGB registration, similar to the case of Design Grade 1, even though the true colors (RGB) those got mapped to the point clouds obtained by the Design Grade 2 system, they are not of the best quality but it is sufficient for the overall visualization of the data.

7.7.3 Discussion on Various Properties of data of MMS Asset Grade 1

The quality of MMS data of Asset Grade 1 in term of point density is quite poor as the values of point density even around the center line area are significantly low in comparison to the ones of other systems. The point density values are also decreasing very rapidly with the increase in the offset distance from the reference center line.

The intensity quality of the point clouds can be visually inspected; however, the sparseness of point clouds has made it difficult to perceive or to assess the intensity quality of the point clouds. Further investigation is made especially over the painted targets on the pavement surface in order to better assess the intensity quality of the point clouds. It turns out that the intensity quality of the point clouds are fair enough as the painted square and cross shape targets are still able to be distinguished from the point clouds. It should be mentioned again that the effect of point cloud sparseness has made the intensity quality appear to be worse than it really is. Therefore it is hard to compare the intensity quality of point clouds of Asset Grade 1 against the ones of other systems due to the consequence of its point cloud sparseness that dilutes the actual intensity quality of the point clouds.

Regardless of the fair intensity quality of this Asset Grade 1 dataset, the insufficient point densities of the point cloud has introduced a big challenge in locating the lane stripes for bridge clearance determination. The lane stripes which were not well defined and distinguishable in the scanned points made it difficult for the step of extracting the needed strip of points along the lane stripe. During the process of bridge clearance determination, the ground (road surface) elevation beneath the points above must be determined in order that the bridge clearances at each beam point can be computed. The determination of road surface elevation involves the method of plane fitting to the scanned ground points which falls within the predefined circle centered at the projection of the beam points. The sparseness (low point density) of this dataset requires an increase in the required circle size used for gathering ground points for the plane fitting process. This is because, with the smaller circle size, there were not enough points falling within the circle to robustly perform plane fitting to arrive at the ground elevation. The sparseness (low point density) of this dataset also causes difficulties in obtaining validation point coordinates from the scanned point clouds. The number of scanned points on the sphere targets is not sufficient for the automatic sphere target detection algorithms to robustly extract the sphere points and locate the sphere centers. Since the sparseness of the scanned points on the sphere targets causes failure of the automatic sphere detection algorithms, a manual process is needed to locate the center of the sphere targets in these scanned point clouds.

It is quite interesting that the images of the scan scenes obtained from this Asset Grade 1 system are in a good quality. The RGB information obtained from the images of the scan scenes was also mapped to the point clouds in a good quality. By visually inspection The RGB information of the point clouds are correctly representing the true color of the scanned objects in the scenes. Not so many erroneous patches of colors are

noticed in the RGB mapped point clouds of this Asset Grade 1 system.

7.7.4 Discussion on Various Properties of data of MMS Asset Grade 2

It can be perceived from the visual inspections throughout the scanned point clouds that Asset Grade 2 system has produced point clouds with very high point densities. The point densities are noticeably high in comparison to those of other systems. The point densities of the Asset Grade 2 dataset are in the same range as the ones of Design Grade 2 with only the difference in the area near the reference center line. The sphere detection algorithm worked fine with the dataset and produced robust results of the validation point coordinates from the scanned point clouds.

The intensities of the point clouds obtained from Asset Grade 2 are of good quality even though they are not as good as the ones of the Design Grade 1 and Design Grade 2 (some features such as drainage, manholes, etc. are not as easily noticeable as the ones which appear in dataset of Design Grade 1 and Design Grade 2). The high contrast property of painted targets (control points) on the pavement surface is well captured in the scanned point clouds.

There was no issue in locating lane stripes for bridge clearance determination. This is because the point clouds have high point densities and good intensity quality.

Unfortunately, the delivered point clouds obtained from this Asset Grade 2 system have no information of the RGB color, therefore it is not possible to visualize this point clouds in the true color mode and obviously it is not possible to assess the quality of how well the RGB information was mapped to the point clouds.

7.8 The Effects of the Studied Factors on MMS Data Accuracy and Quality

As previously mentioned some factors that possibly affect the accuracy of MMS data were studied via the MMS data collection plans. In this section the effect of those factors on the accuracy and the quality of the MMS data will be discussed based on the actual results obtained through the MMS data collection process.

7.8.1 The Effect of Different Types of Roadway Neighborhood Environment

It is noticeable that for all the considered mobile mapping systems the points collected on 231Route have sparser density in comparison to the ones of INDOTLoop. This is due to the fact that the 231Route is a highway type of road with higher defined speed limits while the INDOTLoop is in an urban area which requires lower speed limits. In general, for MMS scanning, driving slower produces denser point clouds on the scanned scenes when considering the same set of other scanning factors.

Besides the previously discussed effect, another interesting factor that affects the point density of the object being scanned warrants discussion here is the effect of range (distance) between the objects and the MMS scanner. An object that is further away will have a lesser point density than one which is closer to the MMS scanner, when other factors are the same. Figure 7.4 depicts this effect of range on the scanned point density. It shows the validation point S10 as an example of the target being close to the scanner and point S9 which is further away from scanner. Both target examples are from the INDOTLoop Acceleration Collection of Design Grade 1 dataset. It is easily noticeable that the scanned points on sphere S9 are sparser in compare to one on sphere S10. This is because S9 is located much further away from the road while S10 is placed much closer to the roadway.

7.8.2 The Effect of Different Grades of MMS Used in Data Collection

From the results of the absolute accuracy evaluations, the design grade MMS possesses better absolute accuracy than systems of the asset grade. Of course it is not just a single component which determines asset vs. design grade. The same scanner with different GPS/INS equipment and processing algorithms might have very different absolute accuracy. Absolute accuracy may or may not be important, it depends on the application and intended use of the data. If only relative accuracy in a small area of data is required for a specific type of work, the asset grade MMS may be an appropriate

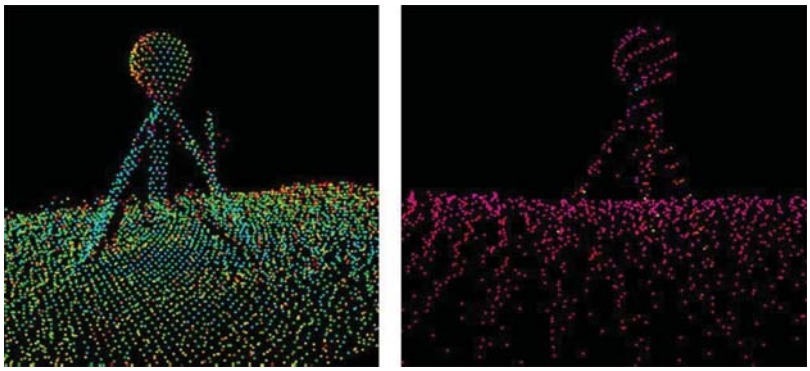

Figure 7.4 Validation point S10 (left) & S9 (right) from the INDOTLoop Acceleration Collection of Design Grade 1 dataset.

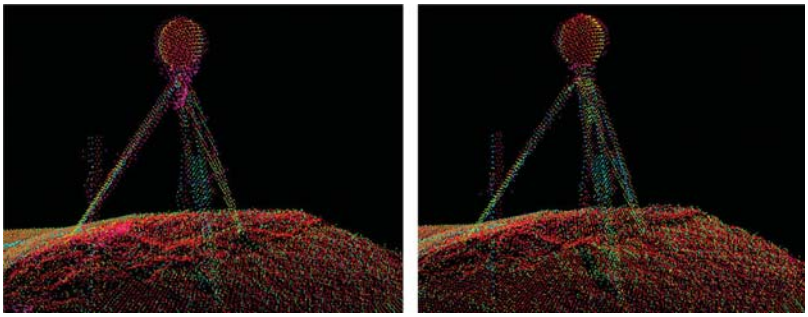

Figure 7.5 Validation point S13 from INDOTLoop Acceleration Collection (left) & No Acceleration Collection (right) of Design Grade 1.

alternative. From the relative accuracy (over the whole project area) evaluation results of each dataset shown in section 7.1, it has given the following insight about the relative accuracy. Following a proper registration to control, there is little benefit in considering the merits of relative accuracy. Absent that registration, relative accuracy can be much higher than absolute accuracy.

7.8.3 The Effect of Different Data Collection Driving Techniques

MMS data collection driving technique does affect the quality of the point clouds in the turning areas. The difference in quality of point clouds in the turning area obtained from Acceleration Collection technique and the ones from No Acceleration Collection technique appear to be significant. The effect of driving technique is studied through the datasets of Design Grade 1 collected over INDOTLoop (INDOTLoop Acceleration Collection and INDOTLoop No Acceleration Collection). These conclusions were not arrived at quantitatively. Rather, just by looking at renderings of the same feature, one can see the effect. The effect of driving technique is well captured in the scanned point clouds around the turning areas. In this case the sphere target S13 which is locating on a traffic island of the turning area on INDOTLoop is used as the example.

The scanned validation point S13 obtained from the scan with Acceleration Collection technique is shown on left side of Figure 7.5, while the one shown on the right side of the figure is the same validation point S13 obtained from the No Acceleration Collection technique. From Figure 7.5, we see that the points clouds obtained from Acceleration Collection technique are much noisier than the one of No Acceleration Collection technique. It is particularly visible in vertical stake in the background, and in the tripod leg on the left.

7.8.4 The Effect of Different Selectable Data Collection Rate (Sampling Rate)

The selectable data collection rate or the sampling rate of MMS does affect the point density of the scanned points if we assume the same driving speed during data collection. In this project, the effect of the selectable data collection rate was studied through the designed data collection strategy mentioned in section 4.3 (see Setting 1a and 1b). In summary the 231Route was scanned twice by MMS Design Grade 1 with the different settings of scan rate at 250 KHz and 500 KHz.

The obvious effect of scanning rate on point density is noticeable in almost all of the scanned sphere targets. The validation points S5, S6 and S8 obtained from different scan rate of MMS Design Grade 1 are presented in Figures 7.6, 7.7, and 7.8, respectively

From Figures 7.6 to 7.8, it is easily noticeable that the point clouds obtained by the higher scanning rate have higher point densities compared to the lower rate. This is exactly what one would expect.

Increasing the scanning rate (sampling rate) in data collection can directly increase the point density of the scanned point clouds when considering that other scanning factors remain unchanged. The increase in the scanning rate which yields the point clouds with higher point densities does not necessarily help improve the accuracy of the scanned point clouds; however, the

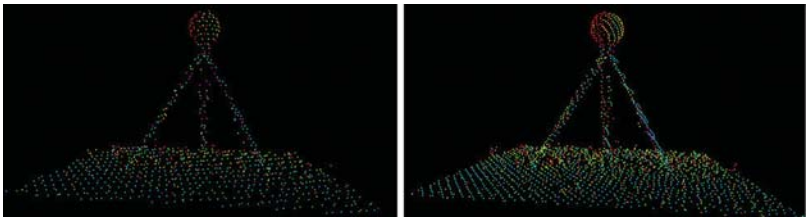

Figure 7.6 Validation point S5 on 231Route got scanned by 250 KHz (left) & 550 KHz (right) scanning rate of MMS Design Grade 1.

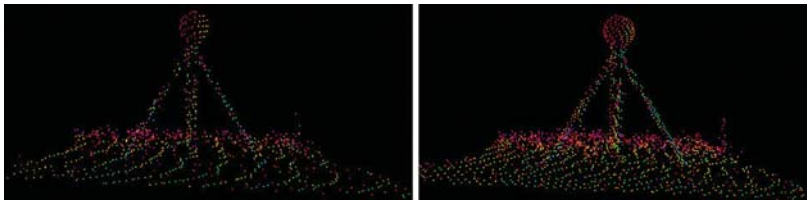

Figure 7.7 Validation point S6 on 231Route got scanned by 250 KHz (left) & 550 KHz (right) scanning rate of MMS Design Grade 1.

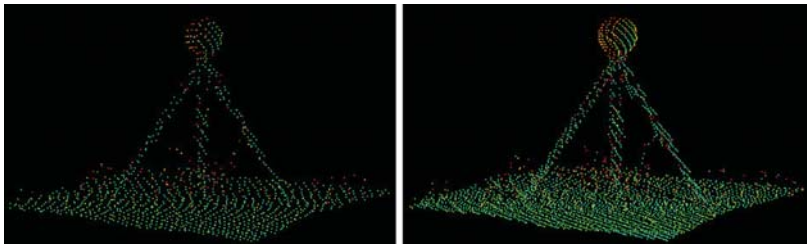

Figure 7.8 Validation point S8 on 231Route got scanned by 250 KHz (left) & 550 KHz (right) scanning rate of MMS Design Grade 1.

point clouds with higher point densities will yield large benefits for feature extraction tasks.

8. CONCLUSIONS

The study undertaken here has provided useful insights in many aspects related to the use of mobile mapping techniques. These include insights about the mechanics of the MMS data collection technique itself, the data post-processing and manipulation, and accuracy attributes of the MMS dataset. A rigorous study about MMS data accuracy has substantiated and justified the contents written in the developed Mobile Terrestrial Laser Scanning (MTLS) Specifications Manual.

For a management oriented manual, it is useful to recast the above statistical results into something that can be tested by INDOT for a given collection. As in other accuracy specifications it is useful to state the requirements as "95% of the tested points shall fall within X of the reference/control value," etc. These figures for MMS data (95% of validation points must fall in the range), considering different system grades, are shown in Table 8.1. "Horizontal" implies a 2D distance comparison, "Vertical" implies a 1D distance comparison.

Be aware of this 95% confidence interval value when comparing our results with others in the literature, which may be in terms of Root Mean Squares Error (RMSE) or standard deviation (68% confidence interval value).

The $RMSE_P$ (horizontal) and $RMSE_h$ (vertical) of both Design and Asset Grade MMS are scaled to arrive at the horizontal and vertical accuracy value at 95% confidence interval as shown in Table 8.1. For 95% confidence interval the relationship between $RMSE_P$ and horizontal accuracy is shown in Equation 8.1 while the one of $RMSE_h$ and vertical accuracy is shown in Equation 8.2 (see pages 10 and 11 in FDGC (1998)). Recall that the stated absolute accuracies refer to validation targets located approximately 4.043 meters (averagely, median value is 2.369 meters) away from the edge of pavement.

TABLE 8.1
95% critical values for testing MMS results.

MMS Grade	Absolute Accuracy		Relative Accuracy (over small area)
	Horizontal (cm)	Vertical (cm)	Vertical (cm)
Design	<8	<5	<5
Asset	<18	<24	<6

TABLE 8.2
Quality in properties of point clouds.

	Design Grade 1	Design Grade 2	Asset Grade 1	Asset Grade 2
Point Densities	Good	Very good	Poor	Very good
Intensities Quality	Very good	Very good	Fair	Good
Mapped RGB Quality	Fair	Fair	Good	N/A

$$\text{Accuracy}_{P-95} = \text{RMSE}_P \times 1.7308 \qquad (8.1)$$

$$\text{Accuracy}_{h-95} = \text{RMSE}_h \times 1.9600 \qquad (8.2)$$

The major properties of point clouds obtained from 4 different mobile mapping systems considered in this project are described in Table 8.2 via an objective but

non quantitative scoring approach, starting with Very Good, Good, Fair and Poor, respectively.

Besides the conclusions about the MMS accuracy and the quality of the MMS point clouds, below are listed some lessons learned from the project.

- Not all the vendors make use of the available control points in the process of applying a coordinate transformation (registration) to the scanned point clouds.
- A client should make a prior agreement with the vendor specifying that the data should meet the defined accuracy requirement and be free from unusable data points such as points in the sky or below the road surface (these can be due to instrument defects or environmental conditions). In the other words, the delivered data should be clean and free from the erroneous points.
- If the delivered data are to be further manipulated by the clients, the TopoDOT software has provided many convenient and easy to access tools to perform specific tasks of interest to INDOT, such as feature extractions, cross sectioning, clearance measurements, etc. The tools are user-friendly and fairly easy to use. However to visualize the whole scanned dataset as an overall view, TopoDOT is not the right choice. This is because TopoDOT has limited the size of file which can be loaded to its viewer. Dividing the whole dataset into tiles and performing analysis tools on these tiles of data is a possible workaround for the case of working with huge dataset with TopoDOT. There exist some other free viewers available in the market that can efficiently serve as a good viewer to visualize the dataset regardless of its size as well as providing more customizable view properties in a fast and intuitive fashion. Bentley Pointools View, and Quick Terrain Reader are just some of the examples. The TerraSolid suite is another more extensive collection of tools which are very good for display and presentation of large point clouds.
- Beware of asset grade data which has not been registered well to control. Either insists that the vendor do it or be prepared to do it yourself.

9. RECOMMENDATIONS

It is recommended that the written Mobile Terrestrial Laser Scanning (MTLS) Specifications Manual are used and referred to when planning and executing a mobile mapping job. We would recommend that INDOT either uses our Test Facility or develops an equivalent one to either (a) prequalify vendors, or (b) qualify them at the time of service delivery. We feel that it is essential that the vendor know the client is prepared to independently evaluate their delivered data, rather than just accept it at face value. Even in our very limited evaluations, there were too many instances of data defects and deficiencies which should never enter a state sponsored archive.

10. DELIVERABLES

The deliverables of this project besides the project report is the developed **Mobile Terrestrial Laser Scanning (MTLS) Specifications Manual** for Indiana Department of Transportation (INDOT), this specifications manual may be included in the Survey Manual of INDOT. The contents of the MTLS Specifications Manual was written based on the rigorous literature reviews and research on the topics of MTLS operations and applications, actual experiences in the field and MMS data processing. The quantitative values related to the accuracy requirements of the MMS data and any technical related numbers or values data presented in the written MTLS Specifications Manual are based on actual data collection and evaluation.

11. EXPECTED BENEFITS

It is to be expected that the developed **Mobile Terrestrial Laser Scanning (MTLS) Specifications Manual** will serve as a valuable reference for the Indiana Department of Transportation (INDOT) agencies in contracting with mobile mapping vendors. It is also to be expected that this written MTLS Specifications Manual will not become obsolete in the very near future even though the technology in mobile mapping technology changes very fast. This is because the developed MTLS Specifications Manual and Standards are performance driven rather than procedure, instrument, or operation driven.

12. IMPLEMENTATIONS

Implementing the recommendations in this report mainly involves developing a facility (or continuing to use ours) to evaluate the accuracy and completeness of vendor supplied data. Building a QA/QC process into everyday workflows will provide benefits of cleaner, higher quality data. This has follow on effects on all of the subsequent design efforts that are built on top of this data. It is a matter of choice for INDOT to decide whether it is easier to manage prequalification or on-the-fly, per-job qualification. Both can work.

13. COST SAVINGS

If dense, high quality data is needed to define both topography and the built infrastructure of the transportation system, and if it is needed quickly, mobile mapping is the only tool which can provide it. Field methods are too labor intensive and slow, photogrammetry will be slower and also will only really define horizontal surfaces, seen from above. Mobile LiDAR, as we have seen defines all visible surfaces, horizontal, vertical, overhangs, even the underside of bridges. If one needs the kind of data provided by mobile LiDAR, any other technology will be prohibitively expensive.

REFERENCES

California Department of Transportation (Caltrans). (2011). Terrestrial laser scanning specifications. In *CALTRANS surveys manual*, Chapter 15. Sacramento, CA: California Department of Transportation. Retrieved from http://www.dot.ca.gov/hq/row/landsurveys/SurveysManual/15_Surveys.pdf

Continental Mapping Consultants, Inc. (2013). *Best practices for planning a mobile LiDAR project*. Sun Prairie, WI: Continental Mapping Consultants, Inc. Retrieved from http://www.continentalmapping.com/whitepapers/Continental%20Mapping%20White%20Paper%20-%20Planning%20a%20Mobile%20Lidar%20Project.pdf

Faber, F. (2014). *Best practice for mobile LiDAR survey requirements: Discussion paper* (Report No. AP-T269-14). Sydney, New South Wales, Australia: Austroads.

Florida Department of Transportation (FDOT). (2012). *Terrestrial mobile LiDAR surveying & mapping guidelines*. Tallahassee, FL: Florida Department of Transportation. Retrieved from http://www.dot.state.fl.us/surveyingandmapping/documentsandpubs/20120823_TML_Guidelines.pdf

Federal Geographic Data Committee (FGDC). (1998). *Geospatial positioning accuracy standards, Part 3: National standard for spatial data accuracy* (Document No. FGDC-STD-007.3-1998). Reston, VA: Federal Geographic Data Committee.

Knaak, T. (2012). *Developing requirements for mobile LiDAR data* (TopoDOT Tech Note No. 1015). Orlando, FL: Certainty 3D. Retrieved from http://www.certainty3d.com/pdf/technotes/MobileLiDARProjectRequirements.pdf

Olsen, M. J., Roe, G. V., Glennie, C., Persi, F., Reedy, M., Hurwitz, D., ... Knodler, M. (2013). *Guidelines for the use of mobile LiDAR in transportation applications* (Project No. NCHRP 15-44). Washington, DC: Transportation Research Board.

Williams, K., Olsen, M. J., Roe, G. V., & Glennie, C. (2013). Synthesis of transportation applications of mobile LiDAR. *Remote Sensing*, *5*(9), 4652–4692. http://dx.doi.org/10.3390/rs5094652

APPENDIX A: SPHERE TARGET CALIBRATION PROCEDURES

The goal in the process of calibrating the sphere targets used in this project is to derive the distance between the sphere center and its mounting aluminum bracket base, and verify the radius, and verify uniformity among our eight spheres. The offset value is referred in this document as the offset distance "D" (see Figure 5.3). The main idea behind this calibration approach is that when a sphere target (with mounting bracket) is placed on the flat surface, the perpendicular distance from the sphere center to the plane surface upon which the sphere is placed, is representing the distance from the sphere center to its base of the mounted aluminum bracket. The steps and procedures in this calibration process are documented as follows.

1. In a testing room, seven spheres (referred to here as Sphere 1–Sphere 7) were places on flat/smooth surfaces (table and floor) and one sphere (referred to here as Sphere 8) is placed on a tripod. The idea of placing one sphere on the tripod is for testing whether it is possible to recover very the small surface area of the tripod upon which the spheres were placed. Figure A.1 depicts the mentioned setup.
2. The spheres were scanned (by a static terrestrial scanner) from two different scanner positions for optimal coverage of each sphere (each sphere remained in the same position, only the scanner was moved).
3. The Cyclone software was used for fitting the 3D scanned point clouds of sphere to a sphere model and fitting the scanned point clouds of the surface where the spheres were placed to a plane model. Through the fitting procedures, the sphere centers were located and the sphere surfaces were formed and plane surfaces were created upon which the spheres were placed. Each surface created had no more than 0.001m variability between observation and model. Figure A.2 depicts typical results of the sphere and plane fitting procedures.
4. Measurements were made from the located sphere centers perpendicular to their associated calculated plane surfaces (at that surface normal). An example of the measurements from a sphere is shown in Figure A.3.
5. An additional piece of information that can be derived from the fitting procedure is the radius of sphere. Once the sphere fitting was realized by the Cyclone software, these points were then extracted and used in a separate (developed by us) sphere fitting algorithm. This sphere fitting algorithm carries the sphere center and radius as parameters; the parameters are solved through the Least Squares adjustment process applied to the extracted point clouds. The radius of each sphere was then obtained from the results of this sphere fitting procedure. Even though the radius of each sphere target is not the goal of this calibration process, the recovered radius values of the spheres provided needed insight about the uniformity of the sphere targets themselves (which are made of the sphere light fixtures) and information about the noise or irregularity of the surface.
6. The final value representing the offset distance D is computed by averaging over the measured offset distances from all spheres. The measurements results and their associated statistics are tabulated in Table A.1.

The following conclusions can be drawn from the results of the sphere calibration process.

1. For the case of Sphere 8 that was placed on the tripod, the surface of tripod upon which the sphere was placed was not recoverable, that means the Cyclone software failed to locate the plane where the Sphere 8 placed on because there were not enough points to robustly

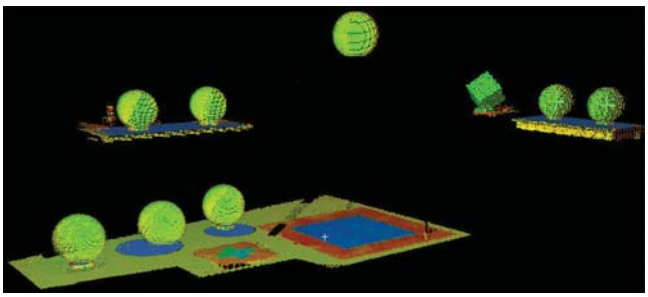

Figure A.1 The setup of eight spheres in sphere calibration process.

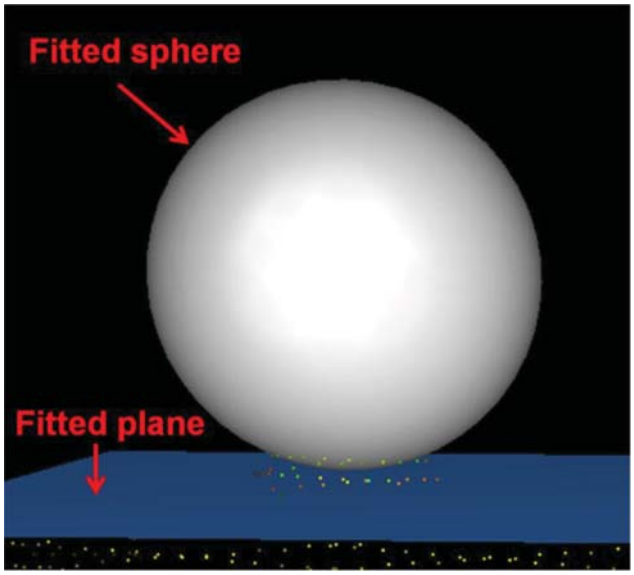

Figure A.2 Typical fitted sphere and plane from fitting procedures.

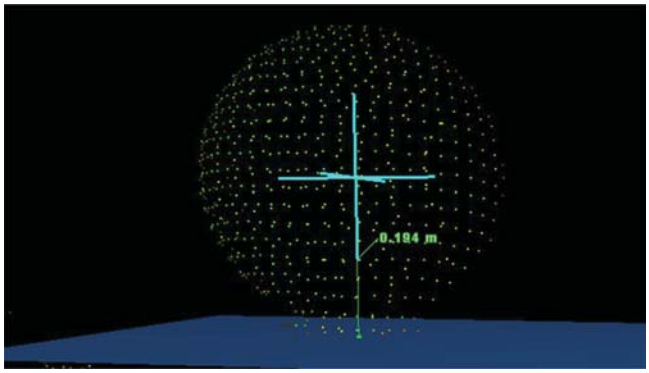

Figure A.3 The measurement along the surface normal from the located sphere center to the located plane surface.

TABLE A.1
Sphere calibration results.

Sphere Target	Setting Environment	Measured Offset Distance (m)	Computed Radius (m)
Sphere 1	Placed on a flat table	0.194	0.177
Sphere 2	Placed on a flat table	0.195	0.177
Sphere 3	Placed on a flat table	0.195	0.177
Sphere 4	Placed on a flat table	0.194	0.177
Sphere 5	Placed on the floor	0.196	0.177
Sphere 6	Placed on the floor	0.193	0.178
Sphere 7	Placed on the floor	0.193	0.178
Sphere 8	Placed on the setup tripod	Unable to recover tripod surface where the sphere was placed on	0.177
		Statistics Computed from 7 Spheres	
Minimum		0.193	0.177
Maximum		0.196	0.178
Average		**0.194**	**0.177**
Standard Deviation		0.001	0.0004

reconstruct the plane surface. When the plane surface was not able to be located, then the offset distance from sphere center to plane could not be computed, therefore the information of offset distance for the case of Sphere 8 is missing. The plane where Sphere 8 was placed could not be defined which made the offset distance not possible to be measured. There was no problem of fitting the sphere to the scanned point clouds of Sphere 8 since fitting the sphere model to the scanned sphere has nothing to do with the ability in recovering the plane surface upon which the sphere was placed. In this case the point cloud representing Sphere 8 was extracted. The aforementioned sphere fitting algorithm using the Least Squares adjustment process was applied to these extracted point clouds resulting the value of the sphere radius as shown in Table A.1.

2. In the case of Sphere 1 to Sphere 7, the Cyclone software has successfully recovered the sphere and located the plane surfaces upon which the spheres are placed. The offset distances were measured and the results are shown in Table A.1 as well as their associated statistics.
3. The average value of the offset distance of 0.194 meter is computed from seven measured offset distances of Sphere 1 to Sphere 7. The standard deviation of 0.001 m (1 mm) of the measured offset distances over seven spheres shows the uniformity of this parameter.
4. The average value of the radius of 0.177 m is computed from eight computed radii of Sphere 1 to Sphere 8. When comparing the computed average radius value of 0.177 m to the reported radius of the spheres from the factory as 0.1778 m (7″), the difference between them is insignificant. It can be implied that all eight sphere light fixtures are accurately produced with the same level of high quality and the standard deviation of 0.0004 m (0.4 mm) of the computed radii over eight spheres simply represents the noise in the surface topography of the plastic or noise from the scanner.
5. The results of radii computations have shown the consistency of all sphere light fixtures from which the sphere targets were made. Therefore there was nothing to be suspected about the quality of the Sphere 8. As such adopting the average value of the offset distance computed from measured offset distances from seven spheres will not cause any issue.
6. The average value of the offset distance (0.194 m) computed from 7 seven spheres are adopted as the representative value of the offset distance D applied to all sphere targets.

APPENDIX B: LOCAL TRANSFORMATION PROCEDURES APPLIED TO SCANNED POINT CLOUDS

The process of adjusting the scanned point clouds to the control point network is often referred to as the process of local transformation. In order to apply the local transformation to scanned point clouds the transformation parameters need to be realized first. In this project, the 6-parameter local transformations were applied to the scanned point clouds obtained from the MMS Asset Grade 1 and Asset Grade 2 only.

To solve for the transformation parameters the coordinates of control points in the scanned point clouds need to be located before the equation for a control point Ti as shown in Equation B.1 can be formed.

$$\begin{bmatrix} E_{Det} \\ N_{Det} \\ h_{Det} \end{bmatrix}_{Ti} = M \begin{bmatrix} E_{Ref} \\ N_{Ref} \\ h_{Ref} \end{bmatrix}_{Ti} + \begin{bmatrix} t_E \\ t_N \\ t_h \end{bmatrix} \quad (B.1)$$

Where $[E_{Det}, N_{Det}, h_{Det}]^T$ are the coordinates in Easting, Northing, and Elevation of the control point Ti detected in the scanned point cloud and the $[E_{Ref}, N_{Ref}, h_{Ref}]^T$ are the reference coordinates of the control point Ti which is the independently obtained by using GNSS with RTK technique (see Table 4.1 for full list of control point coordinates).

M is the rotation matrix which accounts for 3 rotation angles Ω, Φ, and κ around Easting, Northing and Elevation axes, respectively as shown in Equation B.2 and t_E , t_N, and t_h are the translations (shifts) along Easting, Northing, and Elevation axes, respectively.

$$M = R(\kappa) * P(\Phi) * P(\Omega) \quad (B.2)$$

Elementary rotation matrices around Easting, Northing and Elevation axes can be expressed as in Equations B.3 through B.5, respectively.

$$R(\Omega) = \begin{bmatrix} 1 & 0 & 0 \\ 0 & \cos(\Omega) & \sin(\Omega) \\ 0 & -\sin(\Omega) & \cos(\Omega) \end{bmatrix} \quad (B.3)$$

$$R(\Phi) = \begin{bmatrix} \cos(\Phi) & 0 & -\sin(\Phi) \\ 0 & 1 & 0 \\ \sin(\Phi) & 0 & \cos(\Phi) \end{bmatrix} \quad (B.4)$$

$$R(\kappa) = \begin{bmatrix} \cos(\kappa) & \sin(\kappa) & 0 \\ -\sin(\kappa) & \cos(\kappa) & 0 \\ 0 & 0 & 1 \end{bmatrix} \quad (B.5)$$

For a control point Ti the relationship as shown in Equation B.1 is formed, this idea is also applied to all other control points in the data as there are total of seven (T1-T7) and nine control points (T8-T16) in 231Route and INDOTLoop, respectively.

Once the relationship as shown in Equation B.1 is formed for all control points in each site (231Route and INDOTLoop) the six parameters which are rotation angles Ω, Φ, κ and translations t_E , t_N, and t_h (no scale) are solved through the very well-known Least Squares adjustment technique.

To efficiently locate and arrive at the coordinates of the control points from the scanned point clouds the control points must be well captured (scanned) in the scanned scene. For this project the painted targets on the asphalt/concrete in the shape of a cross or square are used as the control points (see Figures 3.4 and 3.5). The scanned painted target of point T8 (cross shape) and T9 (square shape) obtained from the scan of MMS Asset Grade 2 are shown in Figures B.1 and B.2 as examples.

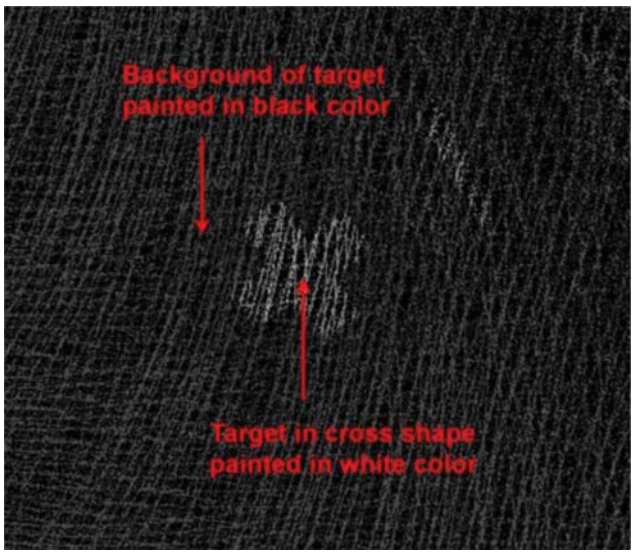

Figure B.1 The scanned target T8 (cross shape) from MMS Asset Grade 2.

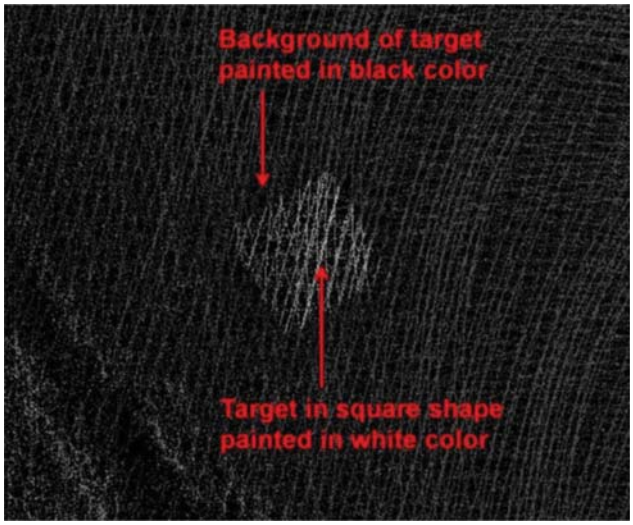

Figure B.2 The scanned target T9 (square shape) from MMS Asset Grade 2.

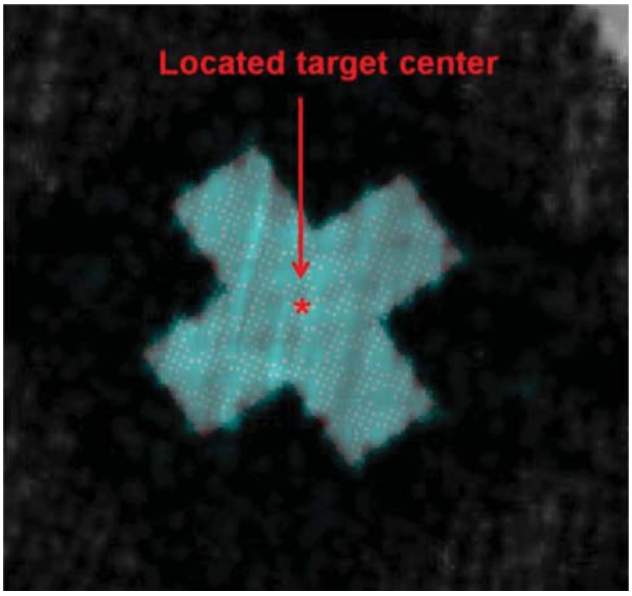

Figure B.3 Located center of target T8 scanned from MMS Asset Grade 2.

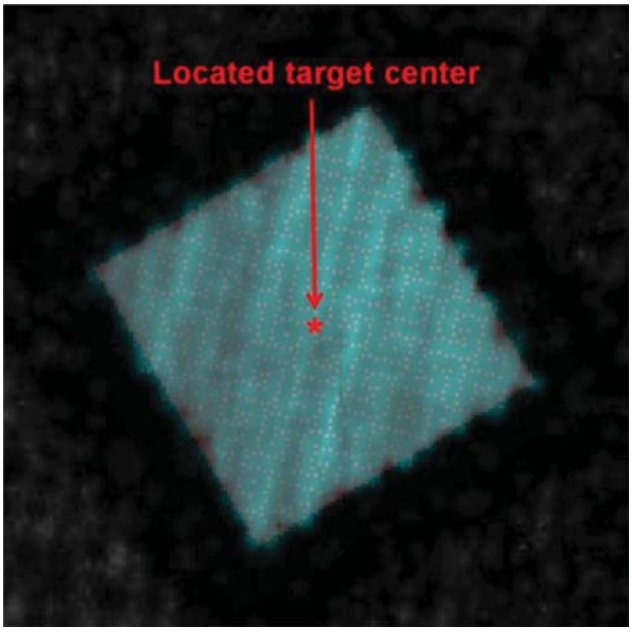

Figure B.4 Located center of target T9 scanned from MMS Asset Grade 2.

The contrast in sensed intensities of the painted targets in the scanned point clouds plays a vital role in the process of locating the center of the targets. In this case the template matching algorithm through the "Least Squares Matching" is applied to all painted targets (T1-T7 in 231Route and T8-T16 in INDOTLoop) in order to locate the center of each target ($[E_{Det}, N_{Det}, h_{Det}]^T$). The templates are created in the form of white color images in the shape of cross and square on a black color background. Once the scanned point clouds of the targets are matched to the template (with acceptable convergence and residuals) the centers of the targets are then located. Figure B.3 and B.4 depict the matching results between the templates and the scanned point clouds for targets T8 and T9, respectively.

When all the centers of painted targets (control points) which are denoted as $[E_{Det}, N_{Det}, h_{Det}]^T$ in Equation B.1 are known, then the transformation parameters can be solved through a Least Squares adjustment. The transformation parameters are then applied to the original scanned point cloud resulting in anew transformed point cloud.

APPENDIX C: EXPERIMENT TO VERIFY SCALE OF THE SCANNED POINT CLOUD FROM STATIC TERRESTRIAL LASER SCANNER

When evaluating the vendor MMS data by determination of bridge clearance (relative accuracy in vertical direction over small area), another point cloud, derived from STLS system was used. To verify that the static terrestrial laser scanned point cloud, itself, was of high quality we compared it with some manually taped distances. This static scanned point cloud was collected in the vicinity of the railroad bridge over US 231. This is the same bridge shown in Figure 3.2, and referenced in the earlier section on relative vertical accuracy and bridge clearance. As shown in Figure C.1, five feature lengths were selected which could be identified in the field and also in the point cloud, so that corresponding measurements could be compared. The five feature lengths were: (1) west pavement width (between stripes), (2) east pavement width (between stripes), (3) main south beam length, (4) vertical distance: pavement stripe to top of main south beam (west), and (5) vertical distance: pavement stripe to top of main south beam (east). These five lengths were taped using a steel tape, and the corresponding lengths were also extracted from the static terrestrial laser scanned point cloud. That data is shown in Table C.1.

Figure C.1 Features selected for distance comparison.

Five condition equations can then be written to estimate the scale factor between the taped lengths and the extracted point cloud lengths. Each equation is of the form as shown in Equation C.1.

$$\frac{T}{P} = SF \tag{C.1}$$

When "T" represents a taped length (corrected for temperature), "P" represents the corresponding, extracted point cloud distance, and "SF" represents the unknown scale factor. The *a priori* standard deviation for the taped distances was 0.005 m; the *a priori* standard deviation of the extracted point cloud lengths was 0.007 m. The scale factor parameter, estimated by least squares, is 1.0000457. This represents a change in the bridge clearance of 0.3 mm. Therefore it was concluded that the static point cloud and the taped distances were consistent. It was further concluded that we were justified to use this point cloud as a reference to evaluate the bridge clearances extracted from the MMS data, since it contains no significant scale errors.

TABLE C.1
Lengths of selected features from taping and from static scanned point cloud.

No.	Feature	Taped Distance (m)	Distance from Point Cloud (m)
1	West pavement width	6.928	6.941
2	East pavement width	10.574	10.586
3	Main south beam length	63.821	63.816
4	Vertical: pavement to beam (west)	9.098	9.094
5	Vertical: pavement to beam (east)	7.821	7.823

APPENDIX D: FULL EVALUATIOIN RESULTS OF ABSOLUTE AND RELATIVE ACCURACY (OVER THE WHOLE PROJECT AREA) OF MMS DATA

In this section the descriptive evaluation results of absolute accuracy and the relative accuracy over the whole project area (the method of using the whole network of validation point) of each dataset will be presented. This includes the results of accuracy evaluation steps started from the very first step of getting scanned point clouds as referred to as Cutlevel 1 through the process of getting Cutlevel 2 and Cutlevel 3 towards the final positions of detected coordinates of validation points from the scanned point clouds and the statistic results of the comparison between the detected validation point (sphere targets) from the MMS point clouds against the corresponding reference ones. For the case of the data from Asset Grade 1, the coordinates of the validation points from the point clouds are obtained by manual detection. The automatic sphere target detection algorithm fail to detect the sphere points in the point clouds obtained from MMS Asset Grade 1 because the scanned spheres do not contain sufficient numbers of points.

Full results of accuracy evaluation of 231Route 250 KHz of Design Grade 1

Absolute accuracy evaluation of MMS data ---- Dataset: 231Route 250KHz of Design Grade 1

Code running and settings summary

Dataset: 231Route 250KHz of Design Grade 1

Radius of sphere from factory (Rf) = 7" = 0.178 m
Fix sphere offset (D) (from sphere center to its aluminium base) = 0.194 m (obtained through sphere calibration process)

Hough transform settings: Cell size = 0.020 m (2.0 cm)
Number of parameter cells in each direction (3D) = 51
Use offset (d) = 3.0 cm from sphere surface to get sphere points (to get Cutlevel2)

	L1	L2
Primary threshold for covergence:	1e-06	1e-06
Iteration max set:	10	10
Secondary threshold:	1e-04	1e-04

Sphere	L1						L2					
	Iter	Reach itermax	Pass second	threshold	abs(delta)		Iter	Reach itermax	Pass second	threshold	abs(delta)	
1	3	N	Y	1.75e-07	5.60e-07	1.96e-07	3	N	Y	1.65e-07	1.05e-07	1.69e-07
2	6	N	Y	1.27e-07	8.55e-08	6.91e-08	4	N	Y	1.20e-08	4.73e-09	1.57e-08
3	4	N	Y	2.13e-11	6.80e-12	4.57e-12	3	N	Y	1.56e-07	2.11e-07	2.90e-07
4	4	N	Y	4.33e-11	1.06e-10	0.00e+00	3	N	Y	1.56e-07	3.48e-07	1.18e-07
5	3	N	Y	2.70e-08	4.05e-08	5.53e-08	4	N	Y	1.44e-08	1.98e-08	6.26e-09
6	4	N	Y	0.00e+00	4.16e-09	2.82e-09	3	N	Y	1.32e-07	1.00e-07	6.63e-07
7	4	N	Y	3.76e-11	5.01e-11	1.26e-12	3	N	Y	5.52e-07	4.38e-08	4.06e-08
8	3	N	Y	1.50e-07	6.46e-08	1.44e-07	4	N	Y	3.45e-09	5.64e-08	4.37e-08

Absolute accuracy evaluation of MMS data (continued) ---- Dataset: 231Route 250KHz of Design Grade 1

Overall results of fitting Cutlevel 2 to sphere model through estimation by L1-norm minimization

Total surface area of sphere = 0.397 sqaure meter (coverage area of 100%)

After L1 fitting, filter the points with magnitude of fitting residual (||V||) > 1.0 cm (the outliers)

	Sphere 1	Sphere 2	Sphere 3	Sphere 4	Sphere 5	Sphere 6	Sphere 7	Sphere 8
# points in Cutlevel 1	280	137	120	144	96	92	123	108
# points in Cutlevel 2 (Cutlevel 2 obtained from Hough transform)	195	96	76	96	65	59	83	70
% CovArea BEFORE (percentage of area on sphere covered by point clouds before removing the points those are outliers)	73.68	68.07	55.23	59.98	55.90	61.76	64.79	58.09

Fit by L1: (V is residual vector, ||V|| is the magnitude of residual vector)

RMSE ||V||	0.010	0.010	0.011	0.012	0.008	0.009	0.010	0.009
Smallest ||V|| (m)	0.000	0.000	0.000	0.000	0.000	0.000	0.000	0.000
Largest ||V|| (m)	0.039	0.024	0.028	0.036	0.026	0.023	0.034	0.021
# outliers removed	39	27	21	28	15	13	21	17
# points remain (Cutlevel 3)	156	69	55	68	50	46	62	53
% CovArea AFTER (percentage of area on sphere covered by point clouds after removing the points those are outliers)	62.91	46.73	36.49	42.18	44.62	53.12	53.09	36.63
% CovArea Removed (% CovArea BEFORE - % CovArea AFTER)	10.77	21.34	18.74	17.80	11.28	8.65	11.70	21.46

Absolute accuracy evaluation of MMS data (continued) ---- Dataset: 231Route 250KHz of Design Grade 1

Detail results of fitting Cutlevel 3 to sphere model through estimation by Least Squares minimization

	Sphere 1	Sphere 2	Sphere 3	Sphere 4	Sphere 5	Sphere 6	Sphere 7	Sphere 8
# points in Cutlevel 3	156	69	55	68	50	46	62	53
Smallest ||V|| (m) in								
Easting (E)	0.000	0.000	0.000	0.000	0.000	0.000	0.000	0.000
Northing (N)	0.000	0.000	0.000	0.000	0.000	0.000	0.000	0.000
Elevation (h)	0.000	0.000	0.000	0.000	0.000	0.000	0.000	0.000
Largest ||V|| (m) in								
Easting (E)	0.008	0.009	0.009	0.005	0.005	0.008	0.010	0.008
Northing (N)	0.009	0.007	0.004	0.003	0.006	0.007	0.007	0.005
Elevation (h)	0.008	0.005	0.005	0.007	0.005	0.005	0.006	0.005
RMSE ||V|| (m)	0.003	0.003	0.003	0.003	0.003	0.004	0.003	0.004
Smallest ||V|| (m)	0.000	0.000	0.000	0.000	0.000	0.000	0.000	0.000
Largest ||V|| (m)	0.009	0.009	0.009	0.008	0.007	0.009	0.010	0.009

Statistics of V's computed from all 8 sphere targets

Average RMSE ||V|| = 0.003 m (0.3 cm)
Min RMSE ||V|| = 0.003 m (0.3 cm), of Sphere 4
Max RMSE ||V|| = 0.004 m (0.4 cm), of Sphere 6

Smallest ||V|| = 0.000 m (0.0 cm), of Sphere 3
Largest ||V|| = 0.010 m (1.0 cm), of Sphere 7

Absolute accuracy evaluation of MMS data (continued) ---- Dataset: 231Route 250KHz of Design Grade 1

Detail results of fitting Cutlevel 3 to sphere model with L2 estimation (Least Squares) (continued)

	Sphere 1	Sphere 2	Sphere 3	Sphere 4	Sphere 5	Sphere 6	Sphere 7	Sphere 8
Detected								
E_Det (m)	913898.526	913897.073	913784.326	913622.264	913167.777	912790.592	912484.227	912261.273
N_Det (m)	572908.245	573264.531	573571.455	573720.301	573953.100	573917.456	574004.672	574217.225
h_Det (m)	166.359	171.894	174.556	174.648	186.067	186.589	185.115	187.412
Reference								
E_Ref (m)	913898.492	913897.112	913784.294	913622.253	913167.782	912790.581	912484.231	912261.312
N_Ref (m)	572908.244	573264.548	573571.427	573720.365	573953.064	573917.508	574004.643	574217.243
h_Ref (m)	166.374	171.901	174.543	174.637	186.072	186.587	185.120	187.418
Dif (Detected-Reference)								
dE (m)	0.034	-0.039	0.032	0.011	-0.005	0.011	-0.004	-0.039
dN (m)	0.001	-0.017	0.028	-0.064	0.036	-0.052	0.029	-0.018
dh (m)	-0.015	-0.007	0.013	0.011	-0.005	0.002	-0.005	-0.006
|Dif| (absolute value of Dif)								
|dE| (m)	0.034	0.039	0.032	0.011	0.005	0.011	0.004	0.039
|dN| (m)	0.001	0.017	0.028	0.064	0.036	0.052	0.029	0.018
|dh| (m)	0.015	0.007	0.013	0.011	0.005	0.002	0.005	0.006
dP (planimetric) (m)	0.034	0.042	0.043	0.065	0.036	0.054	0.030	0.043
dQ (3Q) (m)	0.037	0.043	0.045	0.066	0.037	0.054	0.030	0.043

Statistics computed from all 8 sphere targets

Average dE = 0.000 m (0.0 cm), Worst dE = 0.039 m (3.9 cm)
Average dN = -0.007 m (-0.7 cm), Worst dN = 0.064 m (6.4 cm)
Average dh = -0.002 m (-0.2 cm), Worst dh = 0.015 m (1.5 cm)
Average dP (planimetric) = 0.043 m (4.3 cm), Worst dP = 0.065 m (6.5 cm)
Average dQ (3D) = 0.044 m (4.4 cm), Worst dQ = 0.066 m (6.6 cm)

RMSE E = 0.026 m (2.6 cm)
RMSE N = 0.036 m (3.6 cm)
RMSE h = 0.009 m (0.9 cm)
RMSE P (planimetric) = 0.045 m (4.5 cm)
RMSE Q (3D) = 0.046 m (4.6 cm)

Relative accuracy evaluation of MMS data (use the whole network of validation points)
Dataset: 231Route 250KHz of Design Grade 1

	Min	Between		Max	Between		
Distance (m)	220.044	S3	S4	2096.299	S1	S8	
	Min	Between	Distance (m)	Max	Between		Distance (m)
|ddE| (cm)	0.0	S 4	S 6	854.805	7.3	S1	S2	356.332
|ddN| (cm)	0.1	S 3	S 7	1370.419	10.0	S4	S5	510.768
|ddh| (cm)	0.0	S 5	S 7	685.494	2.7	S1	S3	673.021
|ddP| (cm)	0.1	S 2	S 8	1893.068	6.7	S2	S4	532.215
|ddQ| (cm)	0.1	S 2	S 8	1893.068	6.7	S2	S4	532.215

RMSE |ddE| = 0.040 m (4.0 cm)
RMSE |ddN| = 0.054 m (5.4 cm)
RMSE |ddh| = 0.013 m (1.3 cm)
RMSE |ddP| (planimetric) = 0.038 m (3.8 cm)
RMSE |ddQ| (3D) = 0.038 m (3.8 cm)

Sorted distance (Ascending) (m)	Between		|ddE| (cm)	|ddN| (cm)	|ddh| (cm)	|ddP| (cm)	|ddQ| (cm)
220.044	S 3	S 4	2.1	9.2	0.1	4.7	4.7
308.046	S 7	S 8	3.5	4.7	0.1	0.8	0.8
318.541	S 6	S 7	1.5	8.2	0.7	3.7	3.7
326.988	S 2	S 3	7.2	4.5	2.0	1.7	1.8
356.332	S 1	S 2	7.3	1.8	0.8	1.7	1.7
378.866	S 5	S 6	1.6	8.9	0.7	0.7	0.7
510.768	S 4	S 5	1.6	10.0	1.6	6.0	6.0
532.215	S 2	S 4	5.0	4.8	1.8	6.7	6.7
608.310	S 6	S 8	5.0	3.5	0.8	6.0	6.0
673.021	S 1	S 3	0.1	2.7	2.7	2.7	2.8
685.494	S 5	S 7	0.1	0.7	0.0	0.1	0.1
725.202	S 3	S 5	3.7	0.8	1.8	3.6	3.6
854.805	S 4	S 6	0.0	1.2	1.0	0.3	0.3
857.802	S 1	S 4	2.3	6.5	2.6	5.4	5.4
944.200	S 5	S 8	3.4	5.4	0.1	1.7	1.7
1003.095	S 2	S 5	3.4	5.3	0.2	1.1	1.1
1052.316	S 3	S 6	2.2	8.1	1.1	0.6	0.6
1173.075	S 4	S 7	1.5	9.4	1.6	3.7	3.7
1275.188	S 1	S 5	3.9	3.5	1.0	5.1	5.1
1284.845	S 2	S 6	5.0	3.6	0.9	6.1	6.1
1370.419	S 3	S 7	3.7	0.1	1.8	3.5	3.5
1448.928	S 4	S 8	5.0	4.6	1.8	6.3	6.3
1498.811	S 1	S 6	2.3	5.3	1.6	1.9	1.9
1595.029	S 2	S 7	3.5	4.6	0.2	1.0	1.0
1654.350	S 3	S 8	7.1	4.6	1.9	4.8	4.7
1789.622	S 1	S 7	3.8	2.8	1.0	4.8	4.8
1893.068	S 2	S 8	0.0	0.1	0.1	0.1	0.1
2096.299	S 1	S 8	7.3	1.9	0.9	4.5	4.5

Full results of accuracy evaluation of 231Route 500 KHz of Design Grade 1

Absolute accuracy evaluation of MMS data ---- Dataset: 231Route 500KHz of Design Grade 1

Code running and settings summary

Dataset: 231Route 500KHz of Design Grade 1

Radius of sphere from factory (Rf) = 7" = 0.178 m
Fix sphere offset (D)(from sphere center to its aluminium base) = 0.194 m (obtained through sphere calibration process)

Hough transform settings: Cell size = 0.020 m (2.0 cm)
Number of parameter cells in each direction (3D) = 51
Use offset (d) = 3.0 cm from sphere surface to get sphere points (to get Cutlevel2)

	L1	L2
Primary threshold for covergence:	1e-06	1e-06
Iteration max set:	10	10
Secondary threshold:	1e-04	1e-04

Sphere	L1						L2					
	Iter	Reach itermax	Pass second	threshold	abs(delta)		Iter	Reach itermax	Pass second	threshold	abs(delta)	
1	3	N	Y	4.61e-08	2.14e-08	4.68e-08	3	N	Y	7.48e-07	2.11e-08	3.08e-07
2	4	N	Y	1.17e-11	4.48e-11	3.17e-12	4	N	Y	7.98e-08	2.76e-08	3.25e-08
3	3	N	Y	6.16e-08	2.59e-07	2.66e-07	4	N	Y	5.43e-08	5.82e-08	6.86e-08
4	4	N	Y	1.75e-09	2.06e-09	2.08e-09	4	N	Y	3.76e-08	6.56e-08	2.62e-08
5	10	Y	N	3.62e-04	1.09e-03	4.08e-04	3	N	Y	2.34e-07	9.63e-07	2.46e-07
6	3	N	Y	5.49e-07	2.56e-07	8.75e-07	3	N	Y	9.45e-08	3.93e-07	1.03e-07
7	4	N	Y	0.00e+00	3.06e-11	4.14e-13	3	N	Y	6.66e-07	3.49e-07	4.44e-07
8	4	N	Y	4.11e-09	1.17e-09	5.57e-10	4	N	Y	1.09e-07	2.60e-08	2.96e-08

Absolute accuracy evaluation of MMS data (continued) ---- Dataset: 231Route 500KHz of Design Grade 1

Overall results of fitting Cutlevel 2 to sphere model through estimation by L1-norm minimization

Total surface area of sphere = 0.397 sqaure meter (coverage area of 100%)

After L1 fitting, filter the points with magnitude of fitting residual (||V||) > 1.0 cm (the outliers)

	Sphere 1	Sphere 2	Sphere 3	Sphere 4	Sphere 5	Sphere 6	Sphere 7	Sphere 8
# points in Cutlevel 1	406	276	271	276	192	164	266	254
# points in Cutlevel 2 (Cutlevel 2 obtained from Hough transform)	279	187	182	193	137	80	177	161
% CovArea BEFORE (percentage of area on sphere covered by point clouds before removing the points those are outliers)	69.98	68.23	63.03	71.16	62.28	57.83	69.12	63.66

Fit by L1: (V is residual vector, ||V|| is the magnitude of residual vector)

RMSE ||V||	0.007	0.009	0.008	0.012	0.008	0.007	0.007	0.008
Smallest ||V|| (m)	0.000	0.000	0.000	0.000	0.000	0.000	0.000	0.000
Largest ||V|| (m)	0.033	0.028	0.036	0.041	0.030	0.027	0.029	0.037
# outliers removed	19	40	14	59	20	14	11	28
# points remain (Cutlevel 3)	260	147	168	134	117	66	166	133
% CovArea AFTER (percentage of area on sphere covered by point clouds after removing the points those are outliers)	63.13	60.66	60.57	58.83	58.91	53.45	69.02	63.27

Absolute accuracy evaluation of MMS data (continued) ---- Dataset: 231Route 500KHz of Design Grade 1

Detail results of fitting Cutlevel 3 to sphere model through estimation by Least Squares minimization

	Sphere 1	Sphere 2	Sphere 3	Sphere 4	Sphere 5	Sphere 6	Sphere 7	Sphere 8
# points in Cutlevel 3	260	147	168	134	117	66	166	133
Smallest ||V|| (m) in								
Easting (E)	0.000	0.000	0.000	0.000	0.000	0.000	0.000	0.000
Northing (N)	0.000	0.000	0.000	0.000	0.000	0.000	0.000	0.000
Elevation (h)	0.000	0.000	0.000	0.000	0.000	0.000	0.000	0.000
Largest ||V|| (m) in								
Easting (E)	0.006	0.010	0.010	0.009	0.008	0.008	0.008	0.010
Northing (N)	0.007	0.010	0.007	0.005	0.009	0.005	0.008	0.006
Elevation (h)	0.007	0.009	0.009	0.008	0.008	0.006	0.006	0.005
RMSE ||V|| (m)	0.003	0.004	0.004	0.003	0.004	0.003	0.004	0.004
Smallest ||V|| (m)	0.000	0.000	0.000	0.000	0.000	0.000	0.000	0.000
Largest ||V|| (m)	0.008	0.011	0.010	0.009	0.009	0.008	0.009	0.011

Statistics of V's computed from all 8 sphere targets

Average RMSE ||V|| = 0.004 m (0.4 cm)
Min RMSE ||V|| = 0.003 m (0.3 cm), of Sphere 6
Max RMSE ||V|| = 0.004 m (0.4 cm), of Sphere 5

Smallest ||V|| = 0.000 m (0.0 cm), of Sphere 4
Largest ||V|| = 0.011 m (1.1 cm), of Sphere 2

Absolute accuracy evaluation of MMS data (continued) ---- Dataset: 231Route 500KHz of Design Grade 1

Detail results of fitting Cutlevel 3 to sphere model with L2 estimation (Least Squares) (continued)

	Sphere 1	Sphere 2	Sphere 3	Sphere 4	Sphere 5	Sphere 6	Sphere 7	Sphere 8
Detected								
E_Det (m)	913898.507	913897.079	913784.309	913622.227	913167.766	912790.547	912484.247	912261.287
N_Det (m)	572908.247	573264.551	573571.445	573720.348	573953.093	573917.457	574004.665	574217.259
h_Det (m)	166.355	171.896	174.571	174.646	186.065	186.584	185.115	187.421
Reference								
E_Ref (m)	913898.492	913897.112	913784.294	913622.253	913167.782	912790.581	912484.231	912261.312
N_Ref (m)	572908.244	573264.548	573571.427	573720.365	573953.064	573917.508	574004.643	574217.243
h_Ref (m)	166.374	171.901	174.543	174.637	186.072	186.587	185.120	187.418
Dif (Detected-Reference)								
dE (m)	0.015	-0.033	0.015	-0.026	-0.016	-0.034	0.016	-0.025
dN (m)	0.003	0.003	0.018	-0.017	0.029	-0.051	0.022	0.016
dh (m)	-0.019	-0.005	0.028	0.009	-0.007	-0.003	-0.005	0.003
|Dif| (absolute value of Dif)								
|dE| (m)	0.015	0.033	0.015	0.026	0.016	0.034	0.016	0.025
|dN| (m)	0.003	0.003	0.018	0.017	0.029	0.051	0.022	0.016
|dh| (m)	0.019	0.005	0.028	0.009	0.007	0.003	0.005	0.003
dP (planimetric) (m)	0.015	0.033	0.023	0.031	0.033	0.061	0.027	0.030
dQ (3Q) (m)	0.024	0.033	0.036	0.033	0.033	0.061	0.028	0.030

Statistics computed from all 8 sphere targets

Average dE = -0.011 m (-1.1 cm), Worst dE = 0.034 m (3.4 cm)
Average dN = 0.003 m (0.3 cm), Worst dN = 0.051 m (5.1 cm)
Average dh = 0.000 m (0.0 cm), Worst dh = 0.028 m (2.8 cm)
Average dP (planimetric) = 0.032 m (3.2 cm), Worst dP = 0.061 m (6.1 cm)
Average dQ (3D) = 0.035 m (3.5 cm), Worst dQ = 0.061 m (6.1 cm)

RMSE E = 0.024 m (2.4 cm)
RMSE N = 0.024 m (2.4 cm)
RMSE h = 0.013 m (1.3 cm)
RMSE P (planimetric) = 0.034 m (3.4 cm)
RMSE Q (3D) = 0.036 m (3.6 cm)

Relative accuracy evaluation of MMS data (use the whole network of validation points)
Dataset: 231Route 500KHz of Design Grade 1

	Min	Between		Max	Between	
Distance (m)	220.097	S3	S4	2096.293	S1	S8

	Min	Between		Distance (m)	Max	Between		Distance (m)
|ddE| (cm)	0.0	S 1	S 3	673.008	5.0	S6	S7	318.476
|ddN| (cm)	0.0	S 1	S 2	356.350	7.9	S5	S6	378.900
|ddh| (cm)	0.0	S 2	S 7	1595.005	4.6	S1	S3	673.008
|ddP| (cm)	0.0	S 2	S 8	1893.069	3.9	S1	S8	2096.293
|ddQ| (cm)	0.0	S 2	S 8	1893.069	4.0	S1	S8	2096.293

RMSE |ddE| = 0.032 m (3.2 cm)
RMSE |ddN| = 0.037 m (3.7 cm)
RMSE |ddh| = 0.019 m (1.9 cm)
RMSE |ddP| (planimetric) = 0.022 m (2.2 cm)
RMSE |ddQ| (3D) = 0.022 m (2.2 cm)

Sorted distance (Ascending) (m)	Between		|ddE| (cm)	|ddN| (cm)	|ddh| (cm)	|ddP| (cm)	|ddQ| (cm)
220.097	S 3	S 4	4.1	3.5	1.9	0.7	0.7
308.079	S 7	S 8	4.1	0.6	0.8	2.5	2.5
318.476	S 6	S 7	5.0	7.3	0.2	2.8	2.8
326.968	S 2	S 3	4.8	1.5	3.3	0.3	0.3
356.350	S 1	S 2	4.8	0.0	1.3	0.0	0.0
378.900	S 5	S 6	1.9	7.9	0.4	2.6	2.6
510.720	S 4	S 5	1.1	4.6	1.6	1.2	1.1
532.261	S 2	S 4	0.7	2.0	1.4	2.1	2.1
608.274	S 6	S 8	0.9	6.7	0.5	2.5	2.5
673.008	S 1	S 3	0.0	1.5	4.6	1.4	1.5
685.463	S 5	S 7	3.1	0.6	0.2	3.2	3.2
725.198	S 3	S 5	3.1	1.1	3.5	3.2	3.1
854.802	S 4	S 6	0.8	3.3	1.2	0.0	0.0
857.850	S 1	S 4	4.1	2.0	2.8	0.6	0.6
944.188	S 5	S 8	1.0	1.3	0.9	0.6	0.6
1003.089	S 2	S 5	1.7	2.6	0.2	0.5	0.5
1052.346	S 3	S 6	4.9	6.8	3.0	2.4	2.4
1173.007	S 4	S 7	4.2	4.0	1.4	3.1	3.1
1275.175	S 1	S 5	3.1	2.6	1.2	3.8	3.9
1284.880	S 2	S 6	0.1	5.4	0.3	2.6	2.6
1370.385	S 3	S 7	0.1	0.5	3.3	0.1	0.1
1448.876	S 4	S 8	0.1	3.3	0.7	1.1	1.0
1498.830	S 1	S 6	4.9	5.4	1.6	0.0	0.0
1595.005	S 2	S 7	4.8	1.9	0.0	3.4	3.4
1654.339	S 3	S 8	4.0	0.2	2.5	3.6	3.6
1789.586	S 1	S 7	0.1	1.9	1.4	1.1	1.1
1893.069	S 2	S 8	0.8	1.3	0.8	0.0	0.0
2096.293	S 1	S 8	4.0	1.3	2.1	3.9	4.0

Full results of accuracy evaluation of INDOTLoop Acceleration Collection of Design Grade 1

Absolute accuracy evaluation of MMS data ---- **Dataset: INDOTLoop Acceleration Collection of Design Grade 1**

Code running and settings summary

Dataset: INDOTLoop Continuous Driving of Design Grade 1

Radius of sphere from factory (Rf) = 7" = 0.178 m
Fix sphere offset (D) (from sphere center to its aluminium base) = 0.194 m (obtained through sphere calibration process)

Hough transform settings: Cell size = 0.020 m (2.0 cm)
Number of parameter cells in each direction (3D) = 51
Use offset (d) = 3.0 cm from sphere surface to get sphere points (to get Cutlevel2)

	L1	L2
Primary threshold for covergence:	1e-06	1e-06
Iteration max set:	10	10
Secondary threshold:	1e-04	1e-04

Sphere	L1						L2					
	Iter	Reach itermax	Pass second	threshold	abs(delta)		Iter	Reach itermax	Pass second	threshold	abs(delta)	
9	4	N	Y	3.34e-10	2.16e-08	1.90e-08	4	N	Y	2.03e-07	1.71e-07	3.04e-07
10	3	N	Y	9.19e-07	3.34e-07	4.33e-07	3	N	Y	3.88e-07	4.04e-07	9.24e-08
11	4	N	Y	3.89e-11	3.11e-11	4.38e-13	3	N	Y	3.18e-07	5.08e-07	2.17e-07
12	10	Y	Y	5.87e-05	5.08e-05	5.61e-05	3	N	Y	1.52e-07	3.01e-07	5.07e-07
13	8	N	Y	4.67e-07	1.51e-07	2.14e-07	4	N	Y	5.42e-08	1.16e-07	4.72e-08
14	5	N	Y	1.28e-10	1.50e-10	9.00e-11	4	N	Y	4.64e-08	4.90e-08	1.62e-07
15	4	N	Y	2.38e-07	1.07e-07	0.00e+00	4	N	Y	4.30e-09	1.57e-08	1.85e-08
16	4	N	Y	3.27e-10	4.79e-11	3.87e-10	3	N	Y	2.82e-07	7.57e-07	2.76e-07

Absolute accuracy evaluation of MMS data (continued) ---- Dataset: INDOTLoop Acceleration Collection of Design Grade 1

Overall results of fitting Cutlevel 2 to sphere model through estimation by L1-norm minimization

Total surface area of sphere = 0.397 sqaure meter (coverage area of 100%)

After L1 fitting, filter the points with magnitude of fitting residual (||V||) > 1.0 cm (the outliers)

	Sphere 9	Sphere10	Sphere11	Sphere12	Sphere13	Sphere14	Sphere15	Sphere16
# points in Cutlevel 1	88	229	181	452	1273	95	135	139
# points in Cutlevel 2 (Cutlevel 2 obtained from Hough transform)	60	152	117	312	804	65	94	85
% CovArea BEFORE (percentage of area on sphere covered by point clouds before removing the points those are outliers)	56.10	65.79	60.75	94.91	100.00	68.24	63.49	65.82

Fit by L1: (V is residual vector, ||V|| is the magnitude of residual vector)

RMSE ||V||	0.012	0.012	0.014	0.027	0.028	0.016	0.017	0.014
Smallest ||V|| (m)	0.000	0.000	0.000	0.000	0.000	0.000	0.000	0.000
Largest ||V|| (m)	0.060	0.034	0.043	0.080	0.114	0.051	0.052	0.044
# outliers removed	19	40	38	144	538	30	31	26
# points remain (Cutlevel 3)	41	112	79	168	266	35	63	59
% CovArea AFTER (percentage of area on sphere covered by point clouds after removing the points those are outliers)	39.85	45.35	50.39	57.25	79.47	30.20	52.48	44.50
% CovArea Removed (% CovArea BEFORE - % CovArea AFTER)	16.26	20.44	10.36	37.66	20.53	38.04	11.01	21.32

Absolute accuracy evaluation of MMS data (continued) ---- **Dataset: INDOTLoop Acceleration Collection of Design Grade 1**

Detail results of fitting Cutlevel 3 to sphere model through estimation by Least Squares minimization

	Sphere 9	Sphere10	Sphere11	Sphere12	Sphere13	Sphere14	Sphere15	Sphere16
# points in Cutlevel 3	41	112	79	168	266	35	63	59
Smallest ||V|| (m) in								
Easting (E)	0.000	0.000	0.000	0.000	0.000	0.000	0.000	0.000
Northing (N)	0.000	0.000	0.000	0.000	0.000	0.000	0.000	0.000
Elevation (h)	0.000	0.000	0.000	0.000	0.000	0.000	0.000	0.000
Largest ||V|| (m) in								
Easting (E)	0.008	0.009	0.008	0.008	0.008	0.007	0.007	0.009
Northing (N)	0.010	0.005	0.006	0.005	0.010	0.006	0.004	0.005
Elevation (h)	0.008	0.009	0.007	0.008	0.008	0.007	0.007	0.007
RMSE ||V|| (m)	0.005	0.003	0.003	0.003	0.005	0.004	0.003	0.003
Smallest ||V|| (m)	0.000	0.000	0.000	0.000	0.000	0.000	0.000	0.000
Largest ||V|| (m)	0.010	0.009	0.008	0.009	0.011	0.009	0.007	0.009

Statistics of V's computed from all 8 sphere targets

Average RMSE ||V|| = 0.004 m (0.4 cm)
Min RMSE ||V|| = 0.003 m (0.3 cm), of Sphere 15
Max RMSE ||V|| = 0.005 m (0.5 cm), of Sphere 9

Smallest ||V|| = 0.000 m (0.0 cm), of Sphere 13
Largest ||V|| = 0.011 m (1.1 cm), of Sphere 13

Absolute accuracy evaluation of MMS data (continued) ---- **Dataset: INDOTLoop Acceleration Collection of Design Grade 1**

Detail results of fitting Cutlevel 3 to sphere model with L2 estimation (Least Squares) (continued)

	Sphere 9	Sphere10	Sphere11	Sphere12	Sphere13	Sphere14	Sphere15	Sphere16
Detected								
E_Det (m)	913372.872	913229.545	913110.035	912977.140	912917.386	913392.242	913484.378	913457.523
N_Det (m)	578087.285	578263.057	578463.261	578703.684	579162.553	579134.417	578741.389	578387.303
h_Det (m)	217.473	215.965	214.269	213.195	211.632	211.959	214.313	215.720
Reference								
E_Ref (m)	913372.904	913229.567	913109.996	912977.117	912917.393	913392.229	913484.352	913457.593
N_Ref (m)	578087.309	578263.011	578463.251	578703.722	579162.528	579134.455	578741.393	578387.289
h_Ref (m)	217.476	215.964	214.261	213.204	211.646	212.011	214.355	215.740
Dif (Detected-Reference)								
dE (m)	-0.032	-0.022	0.039	0.023	-0.007	0.013	0.026	-0.070
dN (m)	-0.024	0.046	0.010	-0.038	0.025	-0.038	-0.004	0.014
dh (m)	-0.003	0.001	0.008	-0.009	-0.014	-0.052	-0.042	-0.020
|Dif| (absolute value of Dif)								
|dE| (m)	0.032	0.022	0.039	0.023	0.007	0.013	0.026	0.070
|dN| (m)	0.024	0.046	0.010	0.038	0.025	0.038	0.004	0.014
|dh| (m)	0.003	0.001	0.008	0.009	0.014	0.052	0.042	0.020
dP (planimetric) (m)	0.040	0.051	0.040	0.045	0.026	0.040	0.026	0.071
dQ (3Q) (m)	0.040	0.051	0.041	0.046	0.030	0.065	0.049	0.074

Statistics computed from all 8 sphere targets

Average dE = -0.004 m (-0.4 cm), Worst dE = 0.070 m (7.0 cm)
Average dN = -0.001 m (-0.1 cm), Worst dN = 0.046 m (4.6 cm)
Average dh = -0.016 m (-1.6 cm), Worst dh = 0.052 m (5.2 cm)
Average dP (planimetric) = 0.043 m (4.3 cm), Worst dP = 0.071 m (7.1 cm)
Average dQ (3D) = 0.050 m (5.0 cm), Worst dQ = 0.074 m (7.4 cm)

RMSE E = 0.034 m (3.4 cm)
RMSE N = 0.029 m (2.9 cm)
RMSE h = 0.025 m (2.5 cm)
RMSE P (planimetric) = 0.045 m (4.5 cm)
RMSE Q (3D) = 0.051 m (5.1 cm)

Relative accuracy evaluation of MMS data (use the whole network of validation points)
Dataset: INDOTLoop Acceleration Collection of Design Grade 1

	Min	Between		Max	Between	
Distance (m)	226.806	S9	S10	1167.778	S9	S13

	Min	Between		Distance (m)	Max	Between		Distance (m)
|ddE| (cm)	0.2	S12	S15	508.638	10.9	S11	S16	355.696
|ddN| (cm)	0.0	S12	S14	598.199	8.5	S10	S12	507.806
|ddh| (cm)	0.5	S 9	S10	226.806	5.9	S11	S14	728.077
|ddP| (cm)	0.5	S12	S15	508.638	10.8	S11	S16	355.696
|ddQ| (cm)	0.5	S12	S15	508.638	10.8	S11	S16	355.696

RMSE |ddE| = 0.051 m (5.1 cm)
RMSE |ddN| = 0.043 m (4.3 cm)
RMSE |ddh| = 0.029 m (2.9 cm)
RMSE |ddP| (planimetric) = 0.050 m (5.0 cm)
RMSE |ddQ| (3D) = 0.050 m (5.0 cm)

Sorted distance (Ascending) (m)	Between		|ddE| (cm)	|ddN| (cm)	|ddh| (cm)	|ddP| (cm)	|ddQ| (cm)
226.806	S 9	S10	1.0	7.1	0.5	4.9	4.9
233.167	S10	S11	6.1	3.6	0.7	6.3	6.3
259.636	S10	S16	4.8	3.2	2.2	5.8	5.8
274.709	S11	S12	1.6	4.8	1.7	3.5	3.5
311.737	S 9	S16	3.8	3.9	1.7	2.7	2.7
355.106	S15	S16	9.6	1.8	2.1	1.1	1.0
355.696	S11	S16	10.9	0.4	2.8	10.8	10.8
403.689	S14	S15	1.3	3.5	1.0	3.1	3.1
458.750	S 9	S11	7.1	3.4	1.1	1.2	1.3
462.747	S12	S13	3.1	6.4	0.5	6.7	6.7
466.356	S11	S15	1.3	1.3	5.0	1.9	1.9
475.689	S13	S14	2.0	6.4	3.7	2.4	2.4
507.806	S10	S12	4.5	8.5	1.0	9.6	9.6
508.638	S12	S15	0.2	3.5	3.3	0.5	0.5
541.982	S10	S15	4.8	5.0	4.3	2.2	2.1
575.213	S12	S16	9.3	5.3	1.1	10.7	10.7
598.199	S12	S14	1.0	0.0	4.2	0.7	0.7
663.548	S 9	S15	5.7	2.1	3.8	3.0	3.0
706.305	S13	S15	3.3	2.9	2.7	4.4	4.4
725.349	S11	S13	4.6	1.6	2.2	2.7	2.7
728.077	S11	S14	2.6	4.8	5.9	5.4	5.4
732.509	S 9	S12	5.5	1.4	0.6	4.2	4.1
749.970	S14	S16	8.3	5.2	3.1	6.0	5.9
886.428	S10	S14	3.5	8.4	5.3	7.7	7.6
944.869	S13	S16	6.3	1.1	0.6	2.7	2.7
952.132	S10	S13	1.5	2.1	1.6	2.5	2.4
1047.326	S 9	S14	4.4	1.4	4.8	1.3	1.3
1167.778	S 9	S13	2.4	5.0	1.1	3.6	3.6

Full results of accuracy evaluation of INDOTLoop No Acceleration Collection of Design Grade 1

Absolute accuracy evaluation of MMS data ---- **Dataset: INDOTLoop No Acceleration Collection of Design Grade 1**

Code running and settings summary

Dataset: INDOTLoop No Turn Driving of Design Grade 1

Radius of sphere from factory (Rf) = 7" = 0.178 m
Fix sphere offset (D)(from sphere center to its aluminium base) = 0.194 m (obtained through sphere calibration process)

Hough transform settings: Cell size = 0.020 m (2.0 cm)
Number of parameter cells in each direction (3D) = 51
Use offset (d) = 3.0 cm from sphere surface to get sphere points (to get Cutlevel2)

	L1	L2
Primary threshold for covergence:	1e-06	1e-06
Iteration max set:	10	10
Secondary threshold:	1e-04	1e-04

Sphere	L1						L2					
	Iter	Reach itermax	Pass second	threshold	abs(delta)		Iter	Reach itermax	Pass second	threshold	abs(delta)	
9	10	Y	N	1.69e-04	1.40e-03	3.31e-04	4	N	Y	3.37e-08	2.31e-07	1.47e-07
10	4	N	Y	0.00e+00	8.15e-10	3.16e-12	4	N	Y	7.27e-10	3.41e-09	7.92e-09
11	10	Y	N	7.29e-06	2.93e-04	3.23e-05	3	N	Y	8.32e-07	8.14e-07	4.56e-07
12	4	N	Y	1.24e-11	5.16e-11	0.00e+00	4	N	Y	6.53e-08	7.55e-08	2.20e-08
13	8	N	Y	3.70e-09	2.87e-09	1.31e-09	4	N	Y	3.99e-08	1.03e-08	5.37e-08
14	4	N	Y	8.13e-08	5.93e-07	1.31e-07	4	N	Y	3.81e-07	4.99e-08	4.69e-07
15	3	N	Y	2.54e-07	8.12e-08	2.22e-08	4	N	Y	5.77e-07	5.91e-07	5.76e-07
16	3	N	Y	1.62e-07	7.22e-09	2.77e-08	4	N	Y	1.72e-08	2.50e-08	8.89e-09

Absolute accuracy evaluation of MMS data (continued) ---- Dataset: INDOTLoop No Acceleration Collection of Design Grade 1

Overall results of fitting Cutlevel 2 to sphere model through estimation by L1-norm minimization

Total surface area of sphere = 0.397 sqaure meter (coverage area of 100%)

After L1 fitting, filter the points with magnitude of fitting residual (||V||) > 1.0 cm (the outliers)

	Sphere 9	Sphere10	Sphere11	Sphere12	Sphere13	Sphere14	Sphere15	Sphere16
# points in Cutlevel 1	87	219	171	455	1089	98	132	113
# points in Cutlevel 2 (Cutlevel 2 obtained from Hough transform)	60	142	113	308	726	63	86	78
% CovArea BEFORE (percentage of area on sphere covered by point clouds before removing the points those are outliers)	52.77	68.84	59.45	92.35	100.00	52.10	58.09	52.85
Fit by L1: (V is residual vector, ||V|| is the magnitude of residual vector)								
RMSE ||V||	0.020	0.011	0.011	0.025	0.023	0.012	0.013	0.011
Smallest ||V|| (m)	0.000	0.000	0.000	0.000	0.000	0.000	0.000	0.000
Largest ||V|| (m)	0.074	0.037	0.030	0.076	0.076	0.030	0.032	0.034
# outliers removed	30	40	31	136	311	25	39	23
# points remain (Cutlevel 3)	30	102	82	172	415	38	47	55
% CovArea AFTER (percentage of area on sphere covered by point clouds after removing the points those are outliers)	39.34	48.34	46.73	75.56	76.94	36.25	36.67	40.82
% CovArea Removed (% CovArea BEFORE - % CovArea AFTER)	13.43	20.51	12.72	16.79	23.06	15.85	21.42	12.03

Absolute accuracy evaluation of MMS data (continued) ---- **Dataset: INDOTLoop No Acceleration Collection of Design Grade 1**

Detail results of fitting Cutlevel 3 to sphere model through estimation by Least Squares minimization

	Sphere 9	Sphere10	Sphere11	Sphere12	Sphere13	Sphere14	Sphere15	Sphere16
# points in Cutlevel 3	30	102	82	172	415	38	47	55
Smallest ||V|| (m) in								
Easting (E)	0.000	0.000	0.000	0.000	0.000	0.000	0.000	0.000
Northing (N)	0.000	0.000	0.000	0.000	0.000	0.000	0.000	0.000
Elevation (h)	0.000	0.000	0.000	0.000	0.000	0.000	0.000	0.000
Largest ||V|| (m) in								
Easting (E)	0.006	0.009	0.007	0.008	0.009	0.004	0.007	0.006
Northing (N)	0.008	0.005	0.004	0.008	0.010	0.007	0.008	0.005
Elevation (h)	0.004	0.007	0.006	0.008	0.011	0.009	0.008	0.007
RMSE ||V|| (m)	0.004	0.003	0.003	0.004	0.004	0.004	0.004	0.003
Smallest ||V|| (m)	0.000	0.000	0.000	0.000	0.000	0.000	0.000	0.000
Largest ||V|| (m)	0.009	0.010	0.008	0.009	0.011	0.010	0.009	0.008

Statistics of V's computed from all 8 sphere targets

Average RMSE ||V|| = 0.004 m (0.4 cm)
Min RMSE ||V|| = 0.003 m (0.3 cm), of Sphere 11
Max RMSE ||V|| = 0.004 m (0.4 cm), of Sphere 15

Smallest ||V|| = 0.000 m (0.0 cm), of Sphere 12
Largest ||V|| = 0.011 m (1.1 cm), of Sphere 13

Absolute accuracy evaluation of MMS data (continued) ---- **Dataset: INDOTLoop No Acceleration Collection of Design Grade 1**

Detail results of fitting Cutlevel 3 to sphere model with L2 estimation (Least Squares) (continued)

	Sphere 9	Sphere10	Sphere11	Sphere12	Sphere13	Sphere14	Sphere15	Sphere16
Detected								
E_Det (m)	913372.897	913229.555	913110.021	912977.137	912917.350	913392.229	913484.368	913457.537
N_Det (m)	578087.264	578263.042	578463.282	578703.680	579162.523	579134.415	578741.390	578387.292
h_Det (m)	217.457	215.969	214.226	213.201	211.654	211.984	214.313	215.732
Reference								
E_Ref (m)	913372.904	913229.567	913109.996	912977.117	912917.393	913392.229	913484.352	913457.593
N_Ref (m)	578087.309	578263.011	578463.251	578703.722	579162.528	579134.455	578741.393	578387.289
h_Ref (m)	217.476	215.964	214.261	213.204	211.646	212.011	214.355	215.740
Dif (Detected-Reference)								
dE (m)	-0.007	-0.012	0.025	0.020	-0.043	-0.000	0.016	-0.056
dN (m)	-0.045	0.031	0.031	-0.042	-0.005	-0.040	-0.003	0.003
dh (m)	-0.019	0.005	-0.035	-0.003	0.008	-0.027	-0.042	-0.008
|Dif| (absolute value of Dif)								
|dE| (m)	0.007	0.012	0.025	0.020	0.043	0.000	0.016	0.056
|dN| (m)	0.045	0.031	0.031	0.042	0.005	0.040	0.003	0.003
|dh| (m)	0.019	0.005	0.035	0.003	0.008	0.027	0.042	0.008
dP (planimetric) (m)	0.046	0.033	0.040	0.047	0.043	0.040	0.017	0.056
dQ (3Q) (m)	0.049	0.034	0.054	0.047	0.044	0.048	0.045	0.057

Statistics computed from all 8 sphere targets

Average dE = -0.007 m (-0.7 cm), Worst dE = 0.056 m (5.6 cm)
Average dN = -0.009 m (-0.9 cm), Worst dN = 0.045 m (4.5 cm)
Average dh = -0.015 m (-1.5 cm), Worst dh = 0.042 m (4.2 cm)
Average dP (planimetric) = 0.040 m (4.0 cm), Worst dP = 0.056 m (5.6 cm)
Average dQ (3D) = 0.047 m (4.7 cm), Worst dQ = 0.057 m (5.7 cm)

RMSE E = 0.029 m (2.9 cm)
RMSE N = 0.030 m (3.0 cm)
RMSE h = 0.023 m (2.3 cm)
RMSE P (planimetric) = 0.042 m (4.2 cm)
RMSE Q (3D) = 0.048 m (4.8 cm)

Relative accuracy evaluation of MMS data (use the whole network of validation points)

Dataset: INDOTLoop No Acceleration Collection of Design Grade 1

	Min	Between		Max	Between		
Distance (m)	226.819	S9	S10	1167.792	S9	S13	
	Min	**Between**		**Distance (m)**	**Max**	**Between**	**Distance (m)**
|ddE| (cm)	0.4	S12	S15	508.632	8.2	S11 S16	355.730
|ddN| (cm)	0.0	S10	S11	233.212	7.6	S9 S11	458.807
|ddh| (cm)	0.3	S10	S13	952.132	5.0	S13 S15	706.307
|ddP| (cm)	0.0	S15	S16	355.116	8.9	S12 S16	575.232
|ddQ| (cm)	0.0	S15	S16	355.116	8.9	S12 S16	575.232

RMSE |ddE| = 0.042 m (4.2 cm)
RMSE |ddN| = 0.044 m (4.4 cm)
RMSE |ddh| = 0.026 m (2.6 cm)
RMSE |ddP| (planimetric) = 0.046 m (4.6 cm)
RMSE |ddQ| (3D) = 0.046 m (4.6 cm)

Sorted distance (Ascending) (m)	Between		|ddE| (cm)	|ddN| (cm)	|ddh| (cm)	|ddP| (cm)	|ddQ| (cm)
226.819	S 9	S10	0.5	7.6	2.4	6.2	6.2
233.212	S10	S11	3.7	0.0	4.1	1.9	1.8
259.641	S10	S16	4.4	2.8	1.3	5.2	5.2
274.682	S11	S12	0.5	7.3	3.2	6.2	6.2
311.743	S 9	S16	4.9	4.8	1.1	3.3	3.3
355.116	S15	S16	7.3	0.6	3.4	0.0	0.0
355.730	S11	S16	8.2	2.9	2.8	7.4	7.3
403.688	S14	S15	1.7	3.7	1.5	3.2	3.2
458.807	S 9	S11	3.2	7.6	1.7	4.4	4.4
462.724	S12	S13	6.3	3.6	1.1	4.4	4.4
466.347	S11	S15	0.9	3.4	0.7	2.7	2.7
475.710	S13	S14	4.3	3.4	3.5	4.4	4.4
507.823	S10	S12	3.2	7.3	0.8	7.9	7.9
508.632	S12	S15	0.4	3.9	3.9	0.1	0.1
541.987	S10	S15	2.8	3.4	4.7	1.7	1.6
575.232	S12	S16	7.7	4.5	0.5	8.9	8.9
598.193	S12	S14	2.1	0.2	2.4	1.3	1.3
663.564	S 9	S15	2.4	4.2	2.3	4.5	4.6
706.307	S13	S15	5.9	0.2	5.0	4.6	4.6
725.304	S11	S13	6.8	3.7	4.4	1.7	1.8
728.056	S11	S14	2.5	7.1	0.9	7.5	7.5
732.538	S 9	S12	2.8	0.3	1.6	1.2	1.2
749.982	S14	S16	5.6	4.3	1.9	4.7	4.7
886.437	S10	S14	1.2	7.1	3.2	6.7	6.7
944.881	S13	S16	1.4	0.8	1.6	1.5	1.5
952.132	S10	S13	3.1	3.6	0.3	2.4	2.4
1047.344	S 9	S14	0.7	0.5	0.8	0.5	0.5
1167.792	S 9	S13	3.6	4.0	2.7	5.0	5.0

Full results of accuracy evaluation of 231Route of Design Grade 2

Absolute accuracy evaluation of MMS data ---- Dataset: 231Route of Design Grade 2

Code running and settings summary

Dataset: 231Route of Design Grade 2

Radius of sphere from factory (Rf) = 7" = 0.178 m
Fix sphere offset (D)(from sphere center to its aluminium base) = 0.194 m (obtained through sphere calibration process)

Hough transform settings: Cell size = 0.020 m (2.0 cm)
Number of parameter cells in each direction (3D) = 51
Use offset (d) = 3.0 cm from sphere surface to get sphere points (to get Cutlevel2)

	L1	L2
Primary threshold for covergence:	1e-06	1e-06
Iteration max set:	10	10
Secondary threshold:	1e-04	1e-04

Sphere	L1						L2					
	Iter	Reach itermax	Pass second threshold	abs(delta)			Iter	Reach itermax	Pass second threshold	abs(delta)		
1	10	Y	N	9.94e-05	5.07e-04	5.54e-05	4	N	Y	5.73e-08	2.72e-08	1.82e-08
2	3	N	Y	7.47e-07	7.67e-07	7.54e-07	4	N	Y	3.55e-08	1.06e-07	2.88e-08
3	3	N	Y	6.89e-07	9.33e-07	7.27e-07	3	N	Y	7.15e-07	8.89e-07	5.34e-07
4	4	N	Y	6.78e-21	7.74e-09	1.30e-08	4	N	Y	1.50e-08	9.24e-08	1.58e-08
5	4	N	Y	0.00e+00	1.36e-10	0.00e+00	4	N	Y	5.56e-08	7.14e-08	1.87e-08
6	4	N	Y	0.00e+00	0.00e+00	0.00e+00	4	N	Y	5.62e-09	8.96e-08	6.42e-08
7	4	N	Y	5.70e-11	1.09e-11	8.20e-12	3	N	Y	6.51e-07	7.14e-07	4.80e-07
8	7	N	Y	2.29e-07	5.36e-07	7.26e-07	3	N	Y	1.48e-07	7.73e-07	3.73e-07

Absolute accuracy evaluation of MMS data (continued) ---- Dataset: 231Route of Design Grade 2

Overall results of fitting Cutlevel 2 to sphere model through estimation by L1-norm minimization

Total surface area of sphere = 0.397 sqaure meter (coverage area of 100%)

After L1 fitting, filter the points with magnitude of fitting residual (||V||) > 1.0 cm (the outliers)

	Sphere 1	Sphere 2	Sphere 3	Sphere 4	Sphere 5	Sphere 6	Sphere 7	Sphere 8
# points in Cutlevel 1	668	667	575	610	531	476	596	767
# points in Cutlevel 2 (Cutlevel 2 obtained from Hough transform)	456	479	387	415	355	310	428	515

% CovArea BEFORE (percentage of area on sphere covered by point clouds before removing the points those are outliers)

	73.01	69.73	71.39	72.82	67.79	70.81	75.25	71.87

Fit by L1: (V is residual vector, ||V|| is the magnitude of residual vector)

RMSE ||V||	0.018	0.014	0.014	0.015	0.013	0.014	0.015	0.017
Smallest ||V|| (m)	0.000	0.000	0.000	0.000	0.000	0.000	0.000	0.000
Largest ||V|| (m)	0.088	0.069	0.047	0.083	0.048	0.052	0.048	0.058
# outliers removed	219	181	148	200	135	123	158	229
# points remain (Cutlevel 3)	237	298	239	215	220	187	270	286

% CovArea AFTER (percentage of area on sphere covered by point clouds after removing the points those are outliers)

	69.48	63.13	71.39	68.65	62.43	64.63	64.67	60.52

% CovArea Removed (% CovArea BEFORE - % CovArea AFTER)

	3.53	6.60	0.00	4.16	5.36	6.18	10.58	11.35

Absolute accuracy evaluation of MMS data (continued) ---- Dataset: 231Route of Design Grade 2

Detail results of fitting Cutlevel 3 to sphere model through estimation by Least Squares minimization

	Sphere 1	Sphere 2	Sphere 3	Sphere 4	Sphere 5	Sphere 6	Sphere 7	Sphere 8
# points in Cutlevel 3	237	298	239	215	220	187	270	286
Smallest ||V|| (m) in								
Easting (E)	0.000	0.000	0.000	0.000	0.000	0.000	0.000	0.000
Northing (N)	0.000	0.000	0.000	0.000	0.000	0.000	0.000	0.000
Elevation (h)	0.000	0.000	0.000	0.000	0.000	0.000	0.000	0.000
Largest ||V|| (m) in								
Easting (E)	0.010	0.008	0.007	0.009	0.009	0.011	0.008	0.010
Northing (N)	0.008	0.010	0.010	0.008	0.008	0.009	0.009	0.008
Elevation (h)	0.008	0.008	0.007	0.008	0.009	0.009	0.008	0.008
RMSE ||V|| (m)	0.004	0.005	0.004	0.005	0.004	0.005	0.004	0.003
Smallest ||V|| (m)	0.000	0.000	0.000	0.000	0.000	0.000	0.000	0.000
Largest ||V|| (m)	0.011	0.011	0.010	0.010	0.009	0.011	0.010	0.010

Statistics of V's computed from all 8 sphere targets

Average RMSE ||V|| = 0.004 m (0.4 cm)
Min RMSE ||V|| = 0.003 m (0.3 cm), of Sphere 8
Max RMSE ||V|| = 0.005 m (0.5 cm), of Sphere 4

Smallest ||V|| = 0.000 m (0.0 cm), of Sphere 7
Largest ||V|| = 0.011 m (1.1 cm), of Sphere 6

Absolute accuracy evaluation of MMS data (continued) ---- Dataset: 231Route of Design Grade 2

Detail results of fitting Cutlevel 3 to sphere model with L2 estimation (Least Squares) (continued)

	Sphere 1	Sphere 2	Sphere 3	Sphere 4	Sphere 5	Sphere 6	Sphere 7	Sphere 8
Detected								
E_Det (m)	913898.501	913897.070	913784.291	913622.237	913167.763	912790.575	912484.218	912261.262
N_Det (m)	572908.262	573264.537	573571.444	573720.330	573953.071	573917.490	574004.663	574217.256
h_Det (m)	166.371	171.902	174.549	174.654	186.065	186.602	185.125	187.427
Reference								
E_Ref (m)	913898.492	913897.112	913784.294	913622.253	913167.782	912790.581	912484.231	912261.312
N_Ref (m)	572908.244	573264.548	573571.427	573720.365	573953.064	573917.508	574004.643	574217.243
h_Ref (m)	166.374	171.901	174.543	174.637	186.072	186.587	185.120	187.418
Dif (Detected-Reference)								
dE (m)	0.009	-0.042	-0.003	-0.016	-0.019	-0.006	-0.013	-0.050
dN (m)	0.018	-0.011	0.017	-0.035	0.007	-0.018	0.020	0.013
dh (m)	-0.003	0.001	0.006	0.017	-0.007	0.015	0.005	0.009
|Dif| (absolute value of Dif)								
|dE| (m)	0.009	0.042	0.003	0.016	0.019	0.006	0.013	0.050
|dN| (m)	0.018	0.011	0.017	0.035	0.007	0.018	0.020	0.013
|dh| (m)	0.003	0.001	0.006	0.017	0.007	0.015	0.005	0.009
dP (planimetric) (m)	0.020	0.044	0.018	0.038	0.021	0.019	0.024	0.051
dQ (3Q) (m)	0.020	0.044	0.019	0.042	0.022	0.024	0.024	0.052

Statistics computed from all 8 sphere targets

Average dE = -0.017 m (-1.7 cm), Worst dE = 0.050 m (5.0 cm)
Average dN = 0.001 m (0.1 cm), Worst dN = 0.035 m (3.5 cm)
Average dh = 0.005 m (0.5 cm), Worst dh = 0.017 m (1.7 cm)
Average dP (planimetric) = 0.029 m (2.9 cm), Worst dP = 0.051 m (5.1 cm)
Average dQ (3D) = 0.031 m (3.1 cm), Worst dQ = 0.052 m (5.2 cm)

RMSE E = 0.025 m (2.5 cm)
RMSE N = 0.019 m (1.9 cm)
RMSE h = 0.009 m (0.9 cm)
RMSE P (planimetric) = 0.032 m (3.2 cm)
RMSE Q (3D) = 0.033 m (3.3 cm)

Relative accuracy evaluation of MMS data (use the whole network of validation points)
Dataset: 231Route of Design Grade 2

	Min	Between		Max	Between		
Distance (m)	220.064	S3	S4	2096.297	S1	S8	
	Min	Between		Distance (m)	Max	Between	Distance (m)
|ddE| (cm)	0.3	S 3	S 6	1052.313	5.9	S1 S8	2096.297
|ddN| (cm)	0.0	S 1	S 3	672.995	5.5	S4 S7	1173.048
|ddh| (cm)	0.2	S 3	S 7	1370.394	2.4	S4 S5	510.731
|ddP| (cm)	0.2	S 1	S 3	672.995	5.4	S6 S8	608.303
|ddQ| (cm)	0.2	S 1	S 3	672.995	5.4	S6 S8	608.303

RMSE |ddE| = 0.028 m (2.8 cm)
RMSE |ddN| = 0.029 m (2.9 cm)
RMSE |ddh| = 0.012 m (1.2 cm)
RMSE |ddP| (planimetric) = 0.026 m (2.6 cm)
RMSE |ddQ| (3D) = 0.026 m (2.6 cm)

Sorted distance (Ascending) (m)	Between		|ddE| (cm)	|ddN| (cm)	|ddh| (cm)	|ddP| (cm)	|ddQ| (cm)
220.064	S 3	S 4	1.3	5.2	1.0	2.6	2.6
308.075	S 7	S 8	3.7	0.7	0.4	2.2	2.2
318.522	S 6	S 7	0.7	3.8	1.0	1.7	1.7
326.984	S 2	S 3	3.9	2.9	0.5	1.4	1.4
356.320	S 1	S 2	5.1	2.9	0.4	2.9	2.9
378.863	S 5	S 6	1.3	2.5	2.2	1.1	1.1
510.731	S 4	S 5	0.3	4.2	2.4	2.2	2.2
532.248	S 2	S 4	2.6	2.3	1.6	3.4	3.4
608.303	S 6	S 8	4.4	3.2	0.6	5.4	5.4
672.995	S 1	S 3	1.2	0.0	0.9	0.2	0.2
685.490	S 5	S 7	0.6	1.3	1.2	0.5	0.5
725.175	S 3	S 5	1.6	1.0	1.4	0.8	0.8
854.796	S 4	S 6	1.0	1.7	0.2	0.6	0.6
857.814	S 1	S 4	2.5	5.3	2.0	4.2	4.2
944.213	S 5	S 8	3.0	0.6	1.6	3.1	3.1
1003.080	S 2	S 5	2.3	1.9	0.8	0.4	0.4
1052.313	S 3	S 6	0.3	3.6	0.9	0.9	0.9
1173.048	S 4	S 7	0.3	5.5	1.2	1.1	1.0
1275.144	S 1	S 5	2.8	1.1	0.4	0.8	0.7
1284.871	S 2	S 6	3.6	0.7	1.4	3.5	3.5
1370.394	S 3	S 7	1.0	0.3	0.2	1.0	1.0
1448.914	S 4	S 8	3.4	4.8	0.8	4.8	4.8
1498.816	S 1	S 6	1.5	3.6	1.8	1.3	1.3
1595.027	S 2	S 7	2.9	3.1	0.4	1.1	1.1
1654.344	S 3	S 8	4.6	0.4	0.2	4.1	4.1
1789.593	S 1	S 7	2.2	0.2	0.8	1.9	1.9
1893.088	S 2	S 8	0.7	2.5	0.8	1.9	1.9
2096.297	S 1	S 8	5.9	0.4	1.2	4.3	4.3

Full results of accuracy evaluation of INDOTLoop of Design Grade 2

Absolute accuracy evaluation of MMS data ---- Dataset: INDOTLoop of Design Grade 2

Code running and settings summary

Dataset: INDOTLoop of Design Grade 2

Radius of sphere from factory (Rf) = 7" = 0.178 m
Fix sphere offset (D)(from sphere center to its aluminium base) = 0.194 m (obtained through sphere calibration process)

Hough transform settings: Cell size = 0.020 m (2.0 cm)
Number of parameter cells in each direction (3D) = 51
Use offset (d) = 3.0 cm from sphere surface to get sphere points (to get Cutlevel2)

	L1	L2
Primary threshold for covergence:	1e-06	1e-06
Iteration max set:	10	10
Secondary threshold:	1e-04	1e-04

Sphere	L1						L2					
	Iter	Reach itermax	Pass second	threshold	abs(delta)		Iter	Reach itermax	Pass second	threshold	abs(delta)	
9	6	N	Y	1.82e-08	2.77e-07	5.02e-07	4	N	Y	7.40e-08	1.14e-07	6.71e-09
10	10	Y	N	4.43e-04	2.63e-03	1.17e-03	4	N	Y	4.26e-09	9.18e-08	8.20e-09
11	10	Y	Y	4.22e-05	7.84e-05	4.00e-05	4	N	Y	5.69e-08	3.35e-08	4.82e-08
12	4	N	Y	6.47e-08	3.16e-09	4.36e-07	4	N	Y	3.87e-08	1.96e-07	4.80e-08
13	10	Y	N	5.66e-02	0.00e+00	1.07e-01	10	Y	Y	5.08e-06	6.15e-06	7.28e-06
14	4	N	Y	3.70e-09	7.37e-09	0.00e+00	4	N	Y	2.58e-08	7.54e-08	1.07e-08
15	4	N	Y	6.59e-11	0.00e+00	5.99e-11	4	N	Y	4.62e-08	1.07e-08	4.87e-09
16	4	N	Y	7.57e-07	3.21e-07	4.48e-07	4	N	Y	7.77e-08	1.09e-07	7.71e-09

Absolute accuracy evaluation of MMS data (continued) ---- Dataset: INDOTLoop of Design Grade 2

Overall results of fitting Cutlevel 2 to sphere model through estimation by L1-norm minimization

Total surface area of sphere = 0.397 sqaure meter (coverage area of 100%)

After L1 fitting, filter the points with magnitude of fitting residual (||V||) > 1.0 cm (the outliers)

	Sphere 9	Sphere10	Sphere11	Sphere12	Sphere13	Sphere14	Sphere15	Sphere16
# points in Cutlevel 1	321	773	549	1421	2421	360	234	208
# points in Cutlevel 2 (Cutlevel 2 obtained from Hough transform)	209	511	355	948	1707	187	159	140
% CovArea BEFORE (percentage of area on sphere covered by point clouds before removing the points those are outliers)	66.66	65.13	64.39	100.00	100.00	65.52	61.56	66.09

Fit by L1: (V is residual vector, ||V|| is the magnitude of residual vector)

RMSE ||V||	0.022	0.016	0.020	0.021	0.080	0.034	0.024	0.017
Smallest ||V|| (m)	0.000	0.000	0.000	0.000	0.000	0.000	0.000	0.000
Largest ||V|| (m)	0.100	0.054	0.068	0.134	0.347	0.118	0.071	0.047
# outliers removed	130	230	201	563	1442	116	95	67
# points remain (Cutlevel 3)	79	281	154	385	265	71	64	73
% CovArea AFTER (percentage of area on sphere covered by point clouds after removing the points those are outliers)	51.94	63.63	60.47	90.81	68.99	48.28	50.99	52.94
% CovArea Removed (% CovArea BEFORE - % CovArea AFTER)	14.72	1.50	3.92	9.19	31.01	17.24	10.57	13.15

Absolute accuracy evaluation of MMS data (continued) ---- Dataset: INDOTLoop of Design Grade 2

Detail results of fitting Cutlevel 3 to sphere model through estimation by Least Squares minimization

	Sphere 9	Sphere10	Sphere11	Sphere12	Sphere13	Sphere14	Sphere15	Sphere16
# points in Cutlevel 3	79	281	154	385	265	71	64	73
Smallest ||V|| (m) in								
Easting (E)	0.000	0.000	0.000	0.000	0.000	0.000	0.000	0.000
Northing (N)	0.000	0.000	0.000	0.000	0.000	0.000	0.000	0.000
Elevation (h)	0.000	0.000	0.000	0.000	0.000	0.000	0.000	0.000
Largest ||V|| (m) in								
Easting (E)	0.009	0.010	0.009	0.010	0.041	0.009	0.011	0.008
Northing (N)	0.008	0.010	0.010	0.009	0.027	0.009	0.007	0.005
Elevation (h)	0.009	0.009	0.008	0.009	0.049	0.008	0.008	0.008
RMSE ||V|| (m)	0.004	0.004	0.005	0.005	0.013	0.004	0.005	0.003
Smallest ||V|| (m)	0.000	0.000	0.000	0.000	0.000	0.000	0.000	0.000
Largest ||V|| (m)	0.009	0.010	0.010	0.010	0.065	0.010	0.011	0.009

Statistics of V's computed from all 8 sphere targets

Average RMSE ||V|| = 0.005 m (0.5 cm)
Min RMSE ||V|| = 0.003 m (0.3 cm), of Sphere 16
Max RMSE ||V|| = 0.013 m (1.3 cm), of Sphere 13

Smallest ||V|| = 0.000 m (0.0 cm), of Sphere 12
Largest ||V|| = 0.065 m (6.5 cm), of Sphere 13

Absolute accuracy evaluation of MMS data (continued) ---- Dataset: INDOTLoop of Design Grade 2

Detail results of fitting Cutlevel 3 to sphere model with L2 estimation (Least Squares) (continued)

	Sphere 9	Sphere10	Sphere11	Sphere12	Sphere13	Sphere14	Sphere15	Sphere16
Detected								
E_Det (m)	913372.908	913229.574	913110.011	912977.102	912917.397	913392.226	913484.394	913457.602
N_Det (m)	578087.309	578263.026	578463.252	578703.707	579162.535	579134.419	578741.439	578387.261
h_Det (m)	217.471	215.981	214.264	213.212	211.635	212.018	214.360	215.749
Reference								
E_Ref (m)	913372.904	913229.567	913109.996	912977.117	912917.393	913392.229	913484.352	913457.593
N_Ref (m)	578087.309	578263.011	578463.251	578703.722	579162.528	579134.455	578741.393	578387.289
h_Ref (m)	217.476	215.964	214.261	213.204	211.646	212.011	214.355	215.740
Dif (Detected-Reference)								
dE (m)	0.004	0.007	0.015	-0.015	0.004	-0.003	0.042	0.009
dN (m)	-0.000	0.015	0.001	-0.015	0.007	-0.036	0.046	-0.028
dh (m)	-0.005	0.017	0.003	0.008	-0.011	0.007	0.005	0.009
|Dif| (absolute value of Dif)								
|dE| (m)	0.004	0.007	0.015	0.015	0.004	0.003	0.042	0.009
|dN| (m)	0.000	0.015	0.001	0.015	0.007	0.036	0.046	0.028
|dh| (m)	0.005	0.017	0.003	0.008	0.011	0.007	0.005	0.009
dP (planimetric) (m)	0.004	0.017	0.015	0.021	0.008	0.036	0.062	0.030
dQ (3Q) (m)	0.006	0.024	0.016	0.022	0.013	0.036	0.063	0.031

Statistics computed from all 8 sphere targets

Average dE = 0.008 m (0.8 cm), Worst dE = 0.042 m (4.2 cm)
Average dN = -0.001 m (-0.1 cm), Worst dN = 0.046 m (4.6 cm)
Average dh = 0.004 m (0.4 cm), Worst dh = 0.017 m (1.7 cm)
Average dP (planimetric) = 0.024 m (2.4 cm), Worst dP = 0.062 m (6.2 cm)
Average dQ (3D) = 0.026 m (2.6 cm), Worst dQ = 0.063 m (6.3 cm)

RMSE E = 0.017 m (1.7 cm)
RMSE N = 0.024 m (2.4 cm)
RMSE h = 0.009 m (0.9 cm)
RMSE P (planimetric) = 0.030 m (3.0 cm)
RMSE Q (3D) = 0.031 m (3.1 cm)

Relative accuracy evaluation of MMS data (use the whole network of validation points)
Dataset: INDOTLoop of Design Grade 2

	Min	Between		Max	Between	
Distance (m)	226.767	S9	S10	1167.748	S9	S13

	Min	Between		Distance (m)	Max	Between		Distance (m)
|ddE| (cm)	0.0	S 9	S13	1167.748	5.7	S12	S15	508.694
|ddN| (cm)	0.1	S 9	S11	458.757	8.2	S14	S15	403.651
|ddh| (cm)	0.1	S12	S16	575.348	2.7	S10	S13	952.150
|ddP| (cm)	0.0	S11	S16	355.804	7.7	S15	S16	355.193
|ddQ| (cm)	0.0	S11	S16	355.804	7.7	S15	S16	355.193

RMSE |ddE| = 0.023 m (2.3 cm)
RMSE |ddN| = 0.037 m (3.7 cm)
RMSE |ddh| = 0.012 m (1.2 cm)
RMSE |ddP| (planimetric) = 0.033 m (3.3 cm)
RMSE |ddQ| (3D) = 0.033 m (3.3 cm)

Sorted distance (Ascending) (m)	Between		|ddE| (cm)	|ddN| (cm)	|ddh| (cm)	|ddP| (cm)	|ddQ| (cm)
226.767	S 9	S10	0.3	1.5	2.2	1.0	1.0
233.214	S10	S11	0.8	1.4	1.3	1.6	1.6
259.675	S10	S16	0.2	4.3	0.8	1.9	1.9
274.745	S11	S12	3.0	1.6	0.5	0.1	0.1
311.685	S 9	S16	0.6	2.8	1.4	2.5	2.5
355.193	S15	S16	3.2	7.4	0.4	7.7	7.7
355.804	S11	S16	0.6	2.9	0.6	0.0	0.0
403.651	S14	S15	4.5	8.2	0.2	6.9	6.9
458.757	S 9	S11	1.2	0.1	0.8	0.6	0.6
462.699	S12	S13	1.9	2.2	1.9	1.9	1.9
466.423	S11	S15	2.6	4.5	0.2	4.8	4.8
475.661	S13	S14	0.7	4.2	1.7	0.4	0.4
507.887	S10	S12	2.2	3.0	0.9	1.5	1.5
508.694	S12	S15	5.7	6.1	0.3	6.1	6.1
542.047	S10	S15	3.5	3.1	1.2	4.4	4.4
575.348	S12	S16	2.4	1.3	0.1	2.8	2.8
598.199	S12	S14	1.2	2.1	0.1	0.7	0.7
663.570	S 9	S15	3.8	4.7	1.0	5.2	5.2
706.268	S13	S15	3.8	3.9	1.5	0.7	0.7
725.330	S11	S13	1.2	0.6	1.4	0.9	0.9
728.090	S11	S14	1.9	3.7	0.3	4.1	4.1
732.549	S 9	S12	1.9	1.4	1.3	0.2	0.2
750.023	S14	S16	1.3	0.7	0.2	0.6	0.6
886.452	S10	S14	1.0	5.1	1.0	5.2	5.2
944.928	S13	S16	0.6	3.5	2.0	3.2	3.2
952.150	S10	S13	0.3	0.8	2.7	0.7	0.7
1047.303	S 9	S14	0.7	3.5	1.2	3.5	3.5
1167.748	S 9	S13	0.0	0.7	0.6	0.6	0.7

Full results of accuracy evaluation of 231Route of Asset Grade 1

Absolute accuracy evaluation of MMS data
Dataset: 231Route of Asset Grade 1 (original data (WITHOUT Transformation))

Note: For this case, the detected coordinates of validation points were obtained from manual detection.

	Sphere 1	Sphere 2	Sphere 3	Sphere 4	Sphere 5	Sphere 6	Sphere 7	Sphere 8
Detected								
E_Det (m)	913896.673	913895.334	913782.564	913620.442	913165.975	912788.797	912482.362	912259.577
N_Det (m)	572908.605	573264.705	573571.742	573720.683	573953.386	573917.756	574004.961	574217.566
h_Det (m)	165.609	171.159	173.736	173.851	185.376	185.676	184.312	186.665
Reference								
E_Ref (m)	913898.492	913897.112	913784.294	913622.253	913167.782	912790.581	912484.231	912261.312
N_Ref (m)	572908.244	573264.548	573571.427	573720.365	573953.064	573917.508	574004.643	574217.243
h_Ref (m)	166.374	171.901	174.543	174.637	186.072	186.587	185.120	187.418
Dif (Detected-Reference)								
dE (m)	-1.819	-1.778	-1.730	-1.811	-1.807	-1.784	-1.869	-1.735
dN (m)	0.361	0.157	0.315	0.318	0.322	0.248	0.318	0.323
dh (m)	-0.765	-0.742	-0.807	-0.786	-0.696	-0.911	-0.808	-0.753
|Dif| (absolute value of Dif)								
|dE| (m)	1.819	1.778	1.730	1.811	1.807	1.784	1.869	1.735
|dN| (m)	0.361	0.157	0.315	0.318	0.322	0.248	0.318	0.323
|dh| (m)	0.765	0.742	0.807	0.786	0.696	0.911	0.808	0.753
dP (planimetric) (m)	1.854	1.785	1.758	1.839	1.835	1.801	1.896	1.765
dQ (3D) (m)	2.006	1.933	1.935	2.000	1.963	2.018	2.061	1.919

Statistics computed from all 8 sphere targets

Average dE = -1.792 m (-179.2 cm), Worst dE = 1.869 m (186.9 cm)
Average dN = 0.295 m (29.5 cm), Worst dN = 0.361 m (36.1 cm)
Average dh = -0.783 m (-78.3 cm), Worst dh = 0.911 m (91.1 cm)
Average dP (planimetric) = 1.817 m (181.7 cm), Worst dP = 1.896 m (189.6 cm)
Average dQ (3D) = 1.979 m (197.9 cm), Worst dQ = 2.061 m (206.1 cm)

RMSE E = 1.792 m (179.2 cm)
RMSE N = 0.301 m (30.1 cm)
RMSE h = 0.786 m (78.6 cm)
RMSE P (planimetric) = 1.817 m (181.7 cm)
RMSE Q (3D) = 1.980 m (198.0 cm)

Absolute accuracy evaluation of MMS data (continued)
Dataset: 231Route of Asset Grade 1 (transformed data)

	Sphere 1	Sphere 2	Sphere 3	Sphere 4	Sphere 5	Sphere 6	Sphere 7	Sphere 8
Detected								
E_Det (m)	913898.530	913897.193	913784.425	913622.304	913167.838	912790.660	912484.226	912261.442
N_Det (m)	572908.307	573264.406	573571.444	573720.386	573953.090	573917.463	574004.670	574217.276
h_Det (m)	166.242	171.819	174.417	174.541	186.076	186.366	185.003	187.369
Reference								
E_Ref (m)	913898.492	913897.112	913784.294	913622.253	913167.782	912790.581	912484.231	912261.312
N_Ref (m)	572908.244	573264.548	573571.427	573720.365	573953.064	573917.508	574004.643	574217.243
h_Ref (m)	166.374	171.901	174.543	174.637	186.072	186.587	185.120	187.418
Dif (Detected-Reference)								
dE (m)	0.038	0.081	0.131	0.051	0.056	0.079	-0.005	0.130
dN (m)	0.063	-0.142	0.017	0.021	0.026	-0.045	0.027	0.033
dh (m)	-0.132	-0.082	-0.126	-0.096	0.004	-0.221	-0.117	-0.049
|Dif| (absolute value of Dif)								
|dE| (m)	0.038	0.081	0.131	0.051	0.056	0.079	0.005	0.130
|dN| (m)	0.063	0.142	0.017	0.021	0.026	0.045	0.027	0.033
|dh| (m)	0.132	0.082	0.126	0.096	0.004	0.221	0.117	0.049
dP (planimetric) (m)	0.073	0.163	0.132	0.055	0.062	0.091	0.027	0.134
dQ (3D) (m)	0.151	0.183	0.182	0.111	0.062	0.239	0.120	0.143

Statistics computed from all 8 sphere targets

Average dE = 0.070 m (7.0 cm), Worst dE = 0.131 m (13.1 cm)
Average dN = -0.000 m (-0.0 cm), Worst dN = 0.142 m (14.2 cm)
Average dh = -0.102 m (-10.2 cm), Worst dh = 0.221 m (22.1 cm)
Average dP (planimetric) = 0.092 m (9.2 cm), Worst dP = 0.163 m (16.3 cm)
Average dQ (3D) = 0.149 m (14.9 cm), Worst dQ = 0.239 m (23.9 cm)

RMSE E = 0.082 m (8.2 cm)
RMSE N = 0.060 m (6.0 cm)
RMSE h = 0.119 m (11.9 cm)
RMSE P (planimetric) = 0.102 m (10.2 cm)
RMSE Q (3D) = 0.157 m (15.7 cm)

Absolute accuracy evaluation of MMS data (continued): BEFORE transformation vs. AFTER transformation
Dataset: 231Route of Asset Grade 1

	Sphere 1	Sphere 2	Sphere 3	Sphere 4	Sphere 5	Sphere 6	Sphere 7	Sphere 8
Dif BEFORE (Detected-Reference) (from originally data)								
dE (m)	-1.819	-1.778	-1.730	-1.811	-1.807	-1.784	-1.869	-1.735
dN (m)	0.361	0.157	0.315	0.318	0.322	0.248	0.318	0.323
dh (m)	-0.765	-0.742	-0.807	-0.786	-0.696	-0.911	-0.808	-0.753
Dif AFTER (Detected-Reference) (from originally data)								
dE (m)	0.038	0.081	0.131	0.051	0.056	0.079	-0.005	0.130
dN (m)	0.063	-0.142	0.017	0.021	0.026	-0.045	0.027	0.033
dh (m)	-0.132	-0.082	-0.126	-0.096	0.004	-0.221	-0.117	-0.049

Transformation parameters

3 Rotations				Translation (shift)	
		Degree	Min	Second	
Omega =	-0.004390250 degree =	-0.00000	-0.00000	-15.80490	TE (m) = 1.862
Phi =	0.001024550 degree =	0.00000	0.00000	3.68838	TN (m) = -0.296
Kappa =	0.000337708 degree =	0.00000	0.00000	1.21575	Th (m) = 0.684

Statistics computed from all 8 sphere targets : BEFORE transformation (origianl) vs. AFTER transformation

BEFORE transformation (original data)		AFTER transformation	
Average dE = -179.2 cm,	Worst dE = 186.9 cm	Average dE = 7.0 cm,	Worst dE = 13.1 cm
Average dN = 29.5 cm,	Worst dN = 36.1 cm	Average dN = -0.0 cm,	Worst dN = 14.2 cm
Average dh = -78.3 cm,	Worst dh = 91.1 cm	Average dh = -10.2 cm,	Worst dh = 22.1 cm
Average dP = 181.7 cm,	Worst dP = 189.6 cm	Average dP = 9.2 cm,	Worst dP = 16.3 cm
Average dQ = 197.9 cm,	Worst dQ = 206.1 cm	Average dQ = 14.9 cm,	Worst dQ = 23.9 cm
RMSE E = 1.792 m (179.2 cm)		RMSE E = 0.082 m (8.2 cm)	
RMSE N = 0.301 m (30.1 cm)		RMSE N = 0.060 m (6.0 cm)	
RMSE h = 0.786 m (78.6 cm)		RMSE h = 0.119 m (11.9 cm)	
RMSE P (planimetric) = 1.817 m (181.7 cm)		RMSE P (planimetric) = 0.102 m (10.2 cm)	
RMSE Q (3D) = 1.980 m (198.0 cm)		RMSE Q (3D) = 0.157 m (15.7 cm)	

Relative accuracy evaluation of MMS data (use the whole network of validation points)
Dataset: 231Route of Asset Grade 1

	Min	Between		Max	Between		
Distance (m)	220.152	S3	S4	2096.164	S1	S8	
	Min	Between		Dist (m)	Max	Between	Dist (m)
|ddE| (cm)	0.4	S 4	S 5	510.709	13.9	S3 S7	1370.517
|ddN| (cm)	0.0	S 4	S 7	1173.094	20.4	S1 S2	356.146
|ddh| (cm)	0.1	S 3	S 7	1370.517	21.5	S5 S6	378.857
|ddP| (cm)	0.2	S 4	S 5	510.709	20.4	S1 S2	356.146
|ddQ| (cm)	0.0	S 4	S 5	510.709	20.4	S1 S2	356.146

RMSE |ddE| = 0.065 m (6.5 cm)
RMSE |ddN| = 0.090 m (9.0 cm)
RMSE |ddh| = 0.090 m (9.0 cm)
RMSE |ddP| (planimetric) = 0.089 m (8.9 cm)
RMSE |ddQ| (3D) = 0.089 m (8.9 cm)

Sorted distance (Ascending) (m)	Between		|ddE| (cm)	|ddN| (cm)	|ddh| (cm)	|ddP| (cm)	|ddQ| (cm)
220.152	S 3	S 4	8.1	0.3	2.1	6.2	6.2
307.960	S 7	S 8	13.4	0.5	5.5	9.4	9.3
318.605	S 6	S 7	8.5	7.0	10.3	10.1	10.0
327.102	S 2	S 3	4.8	15.8	6.5	13.2	13.1
356.146	S 1	S 2	4.1	20.4	2.3	20.4	20.4
378.857	S 5	S 6	2.3	7.4	21.5	1.6	1.6
510.709	S 4	S 5	0.4	0.4	9.0	0.2	0.0
532.437	S 2	S 4	3.3	16.1	4.4	15.5	15.5
608.244	S 6	S 8	4.9	7.5	15.8	0.6	0.5
672.932	S 1	S 3	8.9	4.6	4.2	6.0	6.1
685.557	S 5	S 7	6.2	0.4	11.2	6.2	6.2
725.238	S 3	S 5	7.7	0.7	11.1	6.9	7.1
854.758	S 4	S 6	2.7	7.0	12.5	4.2	4.4
857.812	S 1	S 4	0.8	4.3	2.1	4.3	4.3
944.113	S 5	S 8	7.2	0.1	5.7	6.9	6.9
1003.219	S 2	S 5	2.9	16.5	4.6	13.4	13.5
1052.350	S 3	S 6	5.4	6.7	10.4	2.9	2.8
1173.094	S 4	S 7	5.8	0.0	2.2	5.6	5.6
1275.099	S 1	S 5	1.2	3.9	6.9	3.9	3.8
1284.955	S 2	S 6	0.6	9.1	16.9	5.1	4.9
1370.517	S 3	S 7	13.9	0.3	0.1	13.3	13.3
1448.796	S 4	S 8	7.6	0.5	3.3	7.0	6.9
1498.725	S 1	S 6	3.5	11.3	14.6	10.2	10.4
1595.193	S 2	S 7	9.1	16.1	6.6	15.5	15.5
1654.311	S 3	S 8	0.5	0.8	5.4	0.8	0.8
1789.587	S 1	S 7	5.0	4.3	4.3	1.3	1.3
1893.115	S 2	S 8	4.3	16.6	1.1	4.6	4.6
2096.164	S 1	S 8	8.4	3.8	1.2	8.9	8.9

Full results of accuracy evaluation of INDOTLoop of Asset Grade 1

```
Absolute accuracy evaluation of MMS data
Dataset: INDOTLoop of Asset Grade 1 (original data (WITHOUT Transformation))

Note: For this case, the detected coordinates of validation points were obtained from manual detection.

                    Sphere 9     Sphere10     Sphere11     Sphere12     Sphere13     Sphere14     Sphere15     Sphere16
  Detected
    E_Det (m)     913371.019   913227.785   913108.178   912975.278   912915.540   913390.352   913482.399   913455.726
    N_Det (m)     578087.319   578263.063   578463.279   578703.672   579162.386   579134.350   578741.211   578387.167
    h_Det (m)        216.907      215.263      213.632      212.589      211.041      211.508      213.707      215.123
  Reference
    E_Ref (m)     913372.904   913229.567   913109.996   912977.117   912917.393   913392.229   913484.352   913457.593
    N_Ref (m)     578087.309   578263.011   578463.251   578703.722   579162.528   579134.455   578741.393   578387.289
    h_Ref (m)        217.476      215.964      214.261      213.204      211.646      212.011      214.355      215.740

Dif (Detected-Reference)
    dE (m)           -1.885       -1.782       -1.818       -1.839       -1.853       -1.877       -1.953       -1.867
    dN (m)            0.010        0.052        0.028       -0.050       -0.142       -0.105       -0.182       -0.122
    dh (m)           -0.569       -0.701       -0.629       -0.615       -0.605       -0.503       -0.648       -0.617
|Dif| (absolute value of Dif)
   |dE| (m)           1.885        1.782        1.818        1.839        1.853        1.877        1.953        1.867
   |dN| (m)           0.010        0.052        0.028        0.050        0.142        0.105        0.182        0.122
   |dh| (m)           0.569        0.701        0.629        0.615        0.605        0.503        0.648        0.617

dP (planimetric) (m)  1.885        1.783        1.818        1.840        1.858        1.880        1.961        1.871
dQ (3D) (m)           1.969        1.916        1.924        1.940        1.954        1.946        2.066        1.970

                                        Statistics computed from all 8 sphere targets

Average dE                = -1.859 m (-185.9 cm),   Worst dE =   1.953 m (195.3 cm)
Average dN                = -0.064 m (  -6.4 cm),   Worst dN =   0.182 m (18.2 cm)
Average dh                = -0.611 m ( -61.1 cm),   Worst dh =   0.701 m (70.1 cm)
Average dP (planimetric)  =  1.862 m ( 186.2 cm),   Worst dP =   1.961 m (196.1 cm)
Average dQ (3D)           =  1.961 m ( 196.1 cm),   Worst dQ =   2.066 m (206.6 cm)

RMSE E                =  1.860 m (186.0 cm)
RMSE N                =  0.103 m (10.3 cm)
RMSE h                =  0.613 m (61.3 cm)
RMSE P (planimetric)  =  1.863 m (186.3 cm)
RMSE Q (3D)           =  1.961 m (196.1 cm)

Absolute accuracy evaluation of MMS data (continued)
Dataset: INDOTLoop of Asset Grade 1 (transformed data)

                    Sphere 9     Sphere10     Sphere11     Sphere12     Sphere13     Sphere14     Sphere15     Sphere16
  Detected
    E_Det (m)     913372.894   913229.661   913110.055   912977.156   912917.420   913392.232   913484.277   913457.602
    N_Det (m)     578087.383   578263.128   578463.344   578703.738   579162.452   579134.414   578741.274   578387.231
    h_Det (m)        217.419      215.770      214.133      213.084      211.531      212.014      214.218      215.636
  Reference
    E_Ref (m)     913372.904   913229.567   913109.996   912977.117   912917.393   913392.229   913484.352   913457.593
    N_Ref (m)     578087.309   578263.011   578463.251   578703.722   579162.528   579134.455   578741.393   578387.289
    h_Ref (m)        217.476      215.964      214.261      213.204      211.646      212.011      214.355      215.740

Dif (Detected-Reference)
    dE (m)           -0.010        0.094        0.059        0.039        0.027        0.003       -0.075        0.009
    dN (m)            0.074        0.117        0.093        0.016       -0.076       -0.041       -0.119       -0.058
    dh (m)           -0.057       -0.194       -0.128       -0.120       -0.115        0.003       -0.137       -0.104

|Dif| (absolute value of Dif)
   |dE| (m)           0.010        0.094        0.059        0.039        0.027        0.003        0.075        0.009
   |dN| (m)           0.074        0.117        0.093        0.016        0.076        0.041        0.119        0.058
   |dh| (m)           0.057        0.194        0.128        0.120        0.115        0.003        0.137        0.104

dP (planimetric) (m)  0.075        0.150        0.110        0.042        0.081        0.041        0.140        0.059
dQ (3D) (m)           0.094        0.245        0.169        0.127        0.140        0.041        0.196        0.120

                                        Statistics computed from all 8 sphere targets

Average dE                =  0.018 m (   1.8 cm),   Worst dE =   0.094 m (9.4 cm)
Average dN                =  0.001 m (   0.1 cm),   Worst dN =   0.119 m (11.9 cm)
Average dh                = -0.106 m ( -10.6 cm),   Worst dh =   0.194 m (19.4 cm)
Average dP (planimetric)  =  0.087 m (   8.7 cm),   Worst dP =   0.150 m (15.0 cm)
Average dQ (3D)           =  0.141 m (  14.1 cm),   Worst dQ =   0.245 m (24.5 cm)

RMSE E                =  0.050 m (5.0 cm)
RMSE N                =  0.081 m (8.1 cm)
RMSE h                =  0.120 m (12.0 cm)
RMSE P (planimetric)  =  0.096 m (9.6 cm)
RMSE Q (3D)           =  0.153 m (15.3 cm)
```

Absolute accuracy evaluation of MMS data (continued): BEFORE transformation vs. AFTER transformation
Dataset: INDOTLoop of Asset Grade 1

	Sphere 9	Sphere10	Sphere11	Sphere12	Sphere13	Sphere14	Sphere15	Sphere16
Dif BEFORE (Detected-Reference) (from originally data)								
dE (m)	-1.885	-1.782	-1.818	-1.839	-1.853	-1.877	-1.953	-1.867
dN (m)	0.010	0.052	0.028	-0.050	-0.142	-0.105	-0.182	-0.122
dh (m)	-0.569	-0.701	-0.629	-0.615	-0.605	-0.503	-0.648	-0.617
Dif AFTER (Detected-Reference) (from originally data)								
dE (m)	-0.010	0.094	0.059	0.039	0.027	0.003	-0.075	0.009
dN (m)	0.074	0.117	0.093	0.016	-0.076	-0.041	-0.119	-0.058
dh (m)	-0.057	-0.194	-0.128	-0.120	-0.115	0.003	-0.137	-0.104

Transformation parameters

3 Rotations				Translation (shift)	
	Degree	Min	Second		
Omega = 0.000414864 degree =	0.00000	0.00000	1.49351	TE (m) =	1.878
Phi = 0.001832193 degree =	0.00000	0.00000	6.59589	TN (m) =	0.065
Kappa = 0.000258569 degree =	0.00000	0.00000	0.93085	Th (m) =	0.502

Statistics computed from all 8 sphere targets : BEFORE transformation (origianl) vs. AFTER transformation

BEFORE transformation (original data)	AFTER transformation
Average dE = -185.9 cm, Worst dE = 195.3 cm	Average dE = 1.8 cm, Worst dE = 9.4 cm
Average dN = -6.4 cm, Worst dN = 18.2 cm	Average dN = 0.1 cm, Worst dN = 11.9 cm
Average dh = -61.1 cm, Worst dh = 70.1 cm	Average dh = -10.6 cm, Worst dh = 19.4 cm
Average dP = 186.2 cm, Worst dP = 196.1 cm	Average dP = 8.7 cm, Worst dP = 15.0 cm
Average dQ = 196.1 cm, Worst dQ = 206.6 cm	Average dQ = 14.1 cm, Worst dQ = 24.5 cm
RMSE E = 1.860 m (186.0 cm)	RMSE E = 0.050 m (5.0 cm)
RMSE N = 0.103 m (10.3 cm)	RMSE N = 0.081 m (8.1 cm)
RMSE h = 0.613 m (61.3 cm)	RMSE h = 0.120 m (12.0 cm)
RMSE P (planimetric) = 1.863 m (186.3 cm)	RMSE P (planimetric) = 0.096 m (9.6 cm)
RMSE Q (3D) = 1.961 m (196.1 cm)	RMSE Q (3D) = 0.153 m (15.3 cm)

Relative accuracy evaluation of MMS data (use the whole network of validation points)
Dataset: INDOTLoop of Asset Grade 1

	Min	Between		Max	Between		
Distance (m)	226.726	S9	S10	1167.589	S9	S13	
	Min	Between		Dist (m)	Max	Between	Dist (m)
|ddE| (cm)	0.8	S 9	S14	1047.223	17.1	S10 S15	541.716
|ddN| (cm)	1.7	S14	S16	750.046	23.4	S10 S15	541.716
|ddh| (cm)	0.2	S12	S16	575.337	19.8	S10 S14	886.331
|ddP| (cm)	0.2	S10	S11	233.227	28.7	S10 S15	541.716
|ddQ| (cm)	0.3	S10	S11	233.227	28.7	S10 S15	541.716

RMSE |ddE| = 0.072 m (7.2 cm)
RMSE |ddN| = 0.123 m (12.3 cm)
RMSE |ddh| = 0.082 m (8.2 cm)
RMSE |ddP| (planimetric) = 0.121 m (12.1 cm)
RMSE |ddQ| (3D) = 0.121 m (12.1 cm)

Sorted distance (Ascending) (m)	Between		|ddE| (cm)	|ddN| (cm)	|ddh| (cm)	|ddP| (cm)	|ddQ| (cm)
226.726	S 9	S10	10.3	4.2	13.2	3.3	3.2
233.227	S10	S11	3.6	2.4	7.2	0.2	0.3
259.536	S10	S16	8.5	17.4	8.4	15.8	15.8
274.686	S11	S12	2.1	7.8	1.4	5.8	5.8
311.588	S 9	S16	1.8	13.2	4.8	12.2	12.2
355.050	S15	S16	8.6	6.0	3.1	6.6	6.6
355.788	S11	S16	4.9	15.0	1.2	1.6	1.6
403.777	S14	S15	7.6	7.7	14.5	5.8	5.7
458.740	S 9	S11	6.7	1.8	6.0	2.4	2.3
462.590	S12	S13	1.4	9.2	1.0	8.9	8.9
466.141	S11	S15	13.5	21.0	1.9	23.4	23.4
475.639	S13	S14	2.4	3.7	10.2	2.6	2.6
507.842	S10	S12	5.7	10.2	8.6	6.0	6.1
508.510	S12	S15	11.4	13.2	3.3	12.3	12.4
541.716	S10	S15	17.1	23.4	5.3	28.7	28.7
575.337	S12	S16	2.8	7.2	0.2	1.6	1.6
598.140	S12	S14	3.8	5.5	11.2	6.6	6.6
663.318	S 9	S15	6.8	19.2	7.9	20.1	20.0
706.204	S13	S15	10.0	4.0	4.3	5.6	5.7
725.167	S11	S13	3.5	17.0	2.4	15.5	15.5
727.986	S11	S14	5.9	13.3	12.6	14.5	14.6
732.476	S 9	S12	4.6	6.0	4.6	7.5	7.5
750.046	S14	S16	1.0	1.7	11.4	1.8	1.7
886.331	S10	S14	9.5	15.7	19.8	17.2	17.3
944.871	S13	S16	1.4	2.0	1.2	2.4	2.4
951.996	S10	S13	7.1	19.4	9.6	16.0	16.0
1047.223	S 9	S14	0.8	11.5	6.6	11.5	11.5
1167.589	S 9	S13	3.2	15.2	3.6	15.2	15.2

Full results of accuracy evaluation of 231Route of Asset Grade 2

```
================================================================================
Absolute accuracy evaluation of MMS data ---- Dataset: 231Route of Asset Grade 2
================================================================================

                                Code running and settings summary
--------------------------------------------------------------------------------
Dataset: 231Route of Asset Grade 2

Radius of sphere from factory (Rf) = 7" = 0.178 m
Fix sphere offset (D)(from sphere center to its aluminium base) = 0.194 m (obtained through sphere calibration process)

Hough transform settings: Cell size = 0.020 m  (2.0 cm)
                          Number of parameter cells in each direction (3D) = 101
                          Use offset (d) = 3.0 cm from sphere surface to get sphere points (to get Cutlevel2)

-------------------------------------------------------------------------
                                        L1     |      L2
---------------------------------------------------|----------------------
Primary threshold for covergence:          1e-06   |    1e-06
Iteration max set:                          10     |      10
Secondary threshold:                       1e-04   |    1e-04

-------------------------------------------------------------------------------------------------------------------------
Sphere |                          L1                                    |                              L2
-------|----------------------------------------------------------------|-------------------------------------------------
       | Iter   Reach     Pass                abs(delta)                | Iter   Reach     Pass                abs(delta)
       |      itermax  second threshold                                 |     itermax  second threshold
       |
  1    | 10       Y       N        2.35e-04   2.13e-04  5.50e-04   |  4       N       Y        3.26e-07   2.89e-08  1.09e-07
  2    |  4       N       Y        1.65e-08   4.39e-09  8.47e-09   |  4       N       Y        2.78e-07   2.57e-07  2.64e-07
  3    | 10       Y       N        2.60e-05   3.72e-04  1.99e-04   |  3       N       Y        2.37e-07   8.04e-08  8.86e-07
  4    |  3       N       Y        4.03e-08   1.60e-08  8.14e-08   |  4       N       Y        1.66e-07   9.87e-08  6.23e-08
  5    |  5       N       Y        4.73e-10   1.05e-09  1.18e-09   |  3       N       Y        1.41e-07   4.82e-08  4.86e-07
  6    |  7       N       Y        4.37e-11   3.40e-11  5.72e-12   |  4       N       Y        2.88e-08   1.08e-07  1.60e-08
  7    | 10       Y       N        7.67e-05   6.15e-05  1.80e-04   |  3       N       Y        3.33e-07   9.84e-07  3.44e-07
  8    | 10       Y       N        8.03e-04   5.66e-04  1.24e-03   |  4       N       Y        1.46e-07   1.69e-07  9.74e-08
================================================================================
Absolute accuracy evaluation of MMS data (continued) ---- Dataset: 231Route of Asset Grade 2
================================================================================

            Overall results of fitting Cutlevel 2 to sphere model through estimation by L1-norm minimization
--------------------------------------------------------------------------------

Total surface area of sphere  = 0.397 sqaure meter (coverage area of 100%)

After L1 fitting, filter the points with magnitude of fitting residual (||V||) > 1.0 cm (the outliers)


                        Sphere 1    Sphere 2     Sphere 3     Sphere 4      Sphere 5     Sphere 6     Sphere 7     Sphere 8

# points in Cutlevel 1  2154         1634         1514         1805          775          834          1574         1240
# points in Cutlevel 2   164          136          189          177          127          129          181          104
 (Cutlevel 2 obtained from Hough transform)

% CovArea BEFORE  (percentage of area on sphere covered by point clouds before removing the points those are outliers)
                       64.92        55.95        64.08        64.02        68.10        77.66        61.75        59.26


Fit by L1: (V is residual vector, ||V|| is the magnitude of residual vector)

RMSE ||V||             0.024        0.026        0.024        0.020        0.031        0.038        0.020        0.021
Smallest ||V|| (m)     0.000        0.000        0.000        0.000        0.000        0.000        0.000        0.000
Largest  ||V|| (m)     0.068        0.075        0.067        0.062        0.127        0.120        0.083        0.099

# outliers removed      115          102          115          108           82           93          113           52
# points remain          49           34           74           69           45           36           68           52
 (Cutlevel 3)

% CovArea AFTER (percentage of area on sphere covered by point clouds after removing the points those are outliers)
                       57.37        43.30        49.14        50.77        49.62        47.26        49.59        48.29

% CovArea Removed (% CovArea BEFORE - % CovArea AFTER)
                        7.54        12.66        14.94        13.25        18.48        30.41        12.15        10.97
```

Absolute accuracy evaluation of MMS data (continued) ---- Dataset: 231Route of Asset Grade 2

Detail results of fitting Cutlevel 3 to sphere model through estimation by Least Squares minimization

	Sphere 1	Sphere 2	Sphere 3	Sphere 4	Sphere 5	Sphere 6	Sphere 7	Sphere 8
# points in Cutlevel 3	49	34	74	69	45	36	68	52
Smallest ||V|| (m) in								
Easting (E)	0.000	0.000	0.000	0.000	0.000	0.000	0.000	0.000
Northing (N)	0.000	0.000	0.000	0.000	0.000	0.000	0.000	0.000
Elevation (h)	0.000	0.000	0.000	0.000	0.000	0.000	0.000	0.000
Largest ||V|| (m) in								
Easting (E)	0.011	0.009	0.009	0.007	0.008	0.006	0.007	0.010
Northing (N)	0.007	0.008	0.008	0.010	0.008	0.007	0.007	0.006
Elevation (h)	0.010	0.006	0.007	0.008	0.007	0.008	0.008	0.008
RMSE ||V|| (m)	0.005	0.004	0.005	0.005	0.005	0.004	0.004	0.005
Smallest ||V|| (m)	0.000	0.000	0.000	0.000	0.000	0.000	0.000	0.000
Largest ||V|| (m)	0.012	0.009	0.009	0.010	0.009	0.009	0.008	0.011

Statistics of V's computed from all 8 sphere targets

Average RMSE ||V|| = 0.005 m (0.5 cm)
Min RMSE ||V|| = 0.004 m (0.4 cm), of Sphere 2
Max RMSE ||V|| = 0.005 m (0.5 cm), of Sphere 3

Smallest ||V|| = 0.000 m (0.0 cm), of Sphere 4
Largest ||V|| = 0.012 m (1.2 cm), of Sphere 1

Absolute accuracy evaluation of MMS data (continued)
Dataset: 231Route of Asset Grade 2 (original data (WITHOUT Transformation))

	Sphere 1	Sphere 2	Sphere 3	Sphere 4	Sphere 5	Sphere 6	Sphere 7	Sphere 8
Detected								
E_Det (m)	913897.990	913896.631	913783.807	913621.751	913167.332	912790.053	912483.771	912260.813
N_Det (m)	572909.058	573265.408	573572.194	573721.250	573953.851	573918.398	574005.414	574218.140
h_Det (m)	165.220	170.746	173.412	173.536	184.934	185.462	183.977	186.288
Reference								
E_Ref (m)	913898.492	913897.112	913784.294	913622.253	913167.782	912790.581	912484.231	912261.312
N_Ref (m)	572908.244	573264.548	573571.427	573720.365	573953.064	573917.508	574004.643	574217.243
h_Ref (m)	166.374	171.901	174.543	174.637	186.072	186.587	185.120	187.418
Dif (Detected-Reference)								
dE (m)	-0.502	-0.481	-0.487	-0.502	-0.450	-0.528	-0.460	-0.499
dN (m)	0.814	0.860	0.767	0.885	0.787	0.890	0.771	0.897
dh (m)	-1.154	-1.155	-1.131	-1.101	-1.138	-1.125	-1.143	-1.130
|Dif| (absolute value of Dif)								
|dE| (m)	0.502	0.481	0.487	0.502	0.450	0.528	0.460	0.499
|dN| (m)	0.814	0.860	0.767	0.885	0.787	0.890	0.771	0.897
|dh| (m)	1.154	1.155	1.131	1.101	1.138	1.125	1.143	1.130
dP (planimetric) (m)	0.956	0.985	0.908	1.017	0.907	1.035	0.898	1.026
dQ (3D) (m)	1.499	1.518	1.451	1.499	1.455	1.528	1.454	1.527

Statistics computed from all 8 sphere targets

Average dE = -0.488 m (-48.8 cm), Worst dE = 0.528 m (52.8 cm)
Average dN = 0.834 m (83.4 cm), Worst dN = 0.897 m (89.7 cm)
Average dh = -1.135 m (-113.5 cm), Worst dh = 1.155 m (115.5 cm)
Average dP (planimetric) = 0.967 m (96.7 cm), Worst dP = 1.035 m (103.5 cm)
Average dQ (3D) = 1.491 m (149.1 cm), Worst dQ = 1.528 m (152.8 cm)

RMSE E = 0.489 m (48.9 cm)
RMSE N = 0.835 m (83.5 cm)
RMSE h = 1.135 m (113.5 cm)
RMSE P (planimetric) = 0.968 m (96.8 cm)
RMSE Q (3D) = 1.491 m (149.1 cm)

Absolute accuracy evaluation of MMS data (continued)
Dataset: 231Route of Asset Grade 2 (transformed data)

	Sphere 1	Sphere 2	Sphere 3	Sphere 4	Sphere 5	Sphere 6	Sphere 7	Sphere 8
Detected								
E_Det (m)	913898.478	913897.119	913784.296	913622.241	913167.822	912790.543	912484.261	912261.304
N_Det (m)	572908.227	573264.577	573571.363	573720.420	573953.024	573917.571	574004.588	574217.314
h_Det (m)	166.418	171.905	174.542	174.659	186.054	186.606	185.127	187.426
Reference								
E_Ref (m)	913898.492	913897.112	913784.294	913622.253	913167.782	912790.581	912484.231	912261.312
N_Ref (m)	572908.244	573264.548	573571.427	573720.365	573953.064	573917.508	574004.643	574217.243
h_Ref (m)	166.374	171.901	174.543	174.637	186.072	186.587	185.120	187.418
Dif (Detected-Reference)								
dE (m)	-0.014	0.007	0.002	-0.012	0.040	-0.038	0.030	-0.008
dN (m)	-0.017	0.029	-0.064	0.055	-0.040	0.063	-0.055	0.071
dh (m)	0.044	0.004	-0.001	0.022	-0.018	0.019	0.007	0.008
|Dif| (absolute value of Dif)								
|dE| (m)	0.014	0.007	0.002	0.012	0.040	0.038	0.030	0.008
|dN| (m)	0.017	0.029	0.064	0.055	0.040	0.063	0.055	0.071
|dh| (m)	0.044	0.004	0.001	0.022	0.018	0.019	0.007	0.008
dP (planimetric) (m)	0.022	0.030	0.064	0.057	0.057	0.073	0.063	0.071
dQ (3D) (m)	0.049	0.030	0.064	0.061	0.060	0.076	0.064	0.072

Statistics computed from all 8 sphere targets

Average dE = 0.001 m (0.1 cm), Worst dE = 0.040 m (4.0 cm)
Average dN = 0.005 m (0.5 cm), Worst dN = 0.071 m (7.1 cm)
Average dh = 0.011 m (1.1 cm), Worst dh = 0.044 m (4.4 cm)
Average dP (planimetric) = 0.055 m (5.5 cm), Worst dP = 0.073 m (7.3 cm)
Average dQ (3D) = 0.059 m (5.9 cm), Worst dQ = 0.076 m (7.6 cm)

RMSE E = 0.024 m (2.4 cm)
RMSE N = 0.052 m (5.2 cm)
RMSE h = 0.020 m (2.0 cm)
RMSE P (planimetric) = 0.057 m (5.7 cm)
RMSE Q (3D) = 0.061 m (6.1 cm)

Absolute accuracy evaluation of MMS data (continued): BEFORE transformation vs. AFTER transformation
Dataset: 231Route of Asset Grade 2

	Sphere 1	Sphere 2	Sphere 3	Sphere 4	Sphere 5	Sphere 6	Sphere 7	Sphere 8
Dif BEFORE (Detected-Reference) (from originally data)								
dE (m)	-0.502	-0.481	-0.487	-0.502	-0.450	-0.528	-0.460	-0.499
dN (m)	0.814	0.860	0.767	0.885	0.787	0.890	0.771	0.897
dh (m)	-1.154	-1.155	-1.131	-1.101	-1.138	-1.125	-1.143	-1.130
Dif AFTER (Detected-Reference) (from originally data)								
dE (m)	-0.014	0.007	0.002	-0.012	0.040	-0.038	0.030	-0.008
dN (m)	-0.017	0.029	-0.064	0.055	-0.040	0.063	-0.055	0.071
dh (m)	0.044	0.004	-0.001	0.022	-0.018	0.019	0.007	0.008

Transformation parameters

3 Rotations				Translation (shift)	
	Degree	Min	Second		
Omega = 0.006275208 degree =	0.00000	0.00000	22.59075	TE (m) =	0.489
Phi = -0.002955822 degree =	-0.00000	-0.00000	-10.64096	TN (m) =	-0.829
Kappa = 0.000102004 degree =	0.00000	0.00000	0.36722	Th (m) =	1.139

Statistics computed from all 8 sphere targets : BEFORE transformation (origianl) vs. AFTER transformation

BEFORE transformation (original data)	AFTER transformation
Average dE = -48.8 cm, Worst dE = 52.8 cm	Average dE = 0.1 cm, Worst dE = 4.0 cm
Average dN = 83.4 cm, Worst dN = 89.7 cm	Average dN = 0.5 cm, Worst dN = 7.1 cm
Average dh = -113.5 cm, Worst dh = 115.5 cm	Average dh = 1.1 cm, Worst dh = 4.4 cm
Average dP = 96.7 cm, Worst dP = 103.5 cm	Average dP = 5.5 cm, Worst dP = 7.3 cm
Average dQ = 149.1 cm, Worst dQ = 152.8 cm	Average dQ = 5.9 cm, Worst dQ = 7.6 cm
RMSE E = 0.489 m (48.9 cm)	RMSE E = 0.024 m (2.4 cm)
RMSE N = 0.835 m (83.5 cm)	RMSE N = 0.052 m (5.2 cm)
RMSE h = 1.135 m (113.5 cm)	RMSE h = 0.020 m (2.0 cm)
RMSE P (planimetric) = 0.968 m (96.8 cm)	RMSE P (planimetric) = 0.057 m (5.7 cm)
RMSE Q (3D) = 1.491 m (149.1 cm)	RMSE Q (3D) = 0.061 m (6.1 cm)

Relative accuracy evaluation of MMS data (use the whole network of validation points)
Dataset: 231Route of Asset Grade 2

	Min	Between		Max	Between	
Distance (m)	220.181	S3	S4	2096.303	S1	S8

	Min	Between		Dist (m)	Max	Between		Dist (m)
|ddE| (cm)	0.0	S 1	S 4	857.923	7.8	S5	S6	378.942
|ddN| (cm)	0.5	S 3	S 7	1370.359	13.0	S3	S8	1654.365
|ddh| (cm)	0.1	S 3	S 8	1654.365	5.4	S2	S4	532.314
|ddP| (cm)	0.1	S 4	S 8	1448.867	11.5	S7	S8	308.168
|ddQ| (cm)	0.1	S 4	S 8	1448.867	11.5	S7	S8	308.168

RMSE |ddE| = 0.035 m (3.5 cm)
RMSE |ddN| = 0.078 m (7.8 cm)
RMSE |ddh| = 0.025 m (2.5 cm)
RMSE |ddP| (planimetric) = 0.063 m (6.3 cm)
RMSE |ddQ| (3D) = 0.063 m (6.3 cm)

Sorted distance (Ascending) (m)	Between		|ddE| (cm)	|ddN| (cm)	|ddh| (cm)	|ddP| (cm)	|ddQ| (cm)
220.181	S 3	S 4	1.5	11.8	3.0	9.1	9.1
308.168	S 7	S 8	3.9	12.6	1.3	11.5	11.5
318.406	S 6	S 7	6.8	11.8	1.8	9.8	9.8
326.885	S 2	S 3	0.6	9.3	2.3	8.5	8.5
356.395	S 1	S 2	2.1	4.6	0.1	4.5	4.5
378.942	S 5	S 6	7.8	10.2	1.3	6.8	6.8
510.617	S 4	S 5	5.2	9.8	3.7	9.1	9.1
532.314	S 2	S 4	2.1	2.5	5.4	3.2	3.3
608.228	S 6	S 8	2.9	0.7	0.6	2.2	2.2
672.944	S 1	S 3	1.5	4.8	2.3	4.9	4.9
685.504	S 5	S 7	1.0	1.6	0.5	0.9	0.9
725.146	S 3	S 5	3.7	2.1	0.7	2.1	2.1
854.828	S 4	S 6	2.6	0.5	2.4	2.7	2.6
857.923	S 1	S 4	0.0	7.1	5.3	6.7	6.7
944.260	S 5	S 8	4.9	11.0	0.8	7.8	7.8
1003.012	S 2	S 5	3.1	7.2	1.7	7.2	7.2
1052.402	S 3	S 6	4.1	12.3	0.6	7.9	7.9
1172.969	S 4	S 7	4.2	11.4	4.2	6.8	6.8
1275.085	S 1	S 5	5.2	2.7	1.6	5.2	5.1
1284.962	S 2	S 6	4.7	3.0	3.0	5.6	5.6
1370.359	S 3	S 7	2.7	0.5	1.2	2.4	2.4
1448.867	S 4	S 8	0.3	1.2	2.9	0.1	0.1
1498.900	S 1	S 6	2.6	7.6	2.9	7.0	7.1
1594.979	S 2	S 7	2.1	8.8	1.1	6.0	6.0
1654.365	S 3	S 8	1.2	13.0	0.1	6.2	6.2
1789.515	S 1	S 7	4.2	4.3	1.1	5.9	5.9
1893.103	S 2	S 8	1.8	3.7	2.4	3.4	3.4
2096.303	S 1	S 8	0.3	8.3	2.3	4.9	5.0

Full results of accuracy evaluation of INDOTLoop of Asset Grade 2

```
Absolute accuracy evaluation of MMS data ---- Dataset: INDOTLoop of Asset Grade 2

                                        Code running and settings summary

Dataset: INDOTLoop of Asset Grade 2

Radius of sphere from factory (Rf) = 7" = 0.178 m
Fix sphere offset (D)(from sphere center to its aluminium base) = 0.194 m (obtained through sphere calibration process)

Hough transform settings: Cell size = 0.020 m  (2.0 cm)
                          Number of parameter cells in each direction (3D) = 101
                          Use offset (d) = 3.0 cm from sphere surface to get sphere points (to get Cutlevel2)

                                                  L1      |      L2
--------------------------------------------------------|--------------------------
Primary threshold for covergence:                1e-06    |    1e-06
Iteration max set:                                10      |      10
Secondary threshold:                             1e-04    |    1e-04

Sphere |                          L1                                |                                L2
-------|------------------------------------------------------------|-----------------------------------------------------------
       | Iter   Reach     Pass                abs(delta)            | Iter   Reach     Pass                abs(delta)
       |      itermax  second threshold                             |      itermax  second threshold
       |
  9    | 10       Y       N        8.58e-04   3.40e-04   5.08e-04  |  4       N       Y        6.03e-08   1.30e-07   7.49e-08
 10    | 10       Y       N        1.41e-03   2.17e-03   1.57e-04  |  4       N       Y        1.29e-07   1.37e-07   5.52e-08
 11    | 10       Y       N        6.42e-04   2.26e-04   3.95e-04  |  4       N       Y        1.07e-07   3.62e-08   3.22e-08
 12    | 10       Y       N        1.99e-04   1.34e-04   6.30e-04  |  4       N       Y        9.44e-08   3.83e-08   6.93e-08
 13    | 10       Y       N        9.34e-03   3.28e-02   4.78e-02  |  7       N       Y        4.11e-08   3.52e-07   8.45e-07
 14    | 10       Y       N        1.30e-03   1.10e-03   2.57e-04  |  4       N       Y        1.22e-07   8.79e-10   1.03e-08
 15    | 10       Y       Y        9.75e-05   2.96e-05   3.81e-05  |  4       N       Y        1.72e-09   4.35e-08   5.98e-08
 16    | 10       Y       N        1.34e-03   7.01e-04   3.83e-04  |  4       N       Y        1.26e-07   2.01e-08   5.61e-08

Absolute accuracy evaluation of MMS data (continued) ---- Dataset: INDOTLoop of Asset Grade 2

            Overall results of fitting Cutlevel 2 to sphere model through estimation by L1-norm minimization

Total surface area of sphere  = 0.397 sqaure meter (coverage area of 100%)

After L1 fitting, filter the points with magnitude of fitting residual (||V||) > 1.0 cm (the outliers)

                        Sphere 9    Sphere10     Sphere11     Sphere12     Sphere13     Sphere14     Sphere15     Sphere16

# points in Cutlevel 1  2927        14156        7217         12568        89025        2748         3847         6672
# points in Cutlevel 2   230          526         393           857         1963         237          190          329
 (Cutlevel 2 obtained from Hough transform)

% CovArea BEFORE  (percentage of area on sphere covered by point clouds before removing the points those are outliers)
                        79.56        69.96        68.43        92.66        100.00       71.98        54.10        72.86


Fit by L1: (V is residual vector, ||V|| is the magnitude of residual vector)

RMSE ||V||              0.051        0.017        0.019        0.023        0.045        0.038        0.025        0.031
Smallest ||V|| (m)      0.000        0.000        0.000        0.000        0.000        0.000        0.000        0.000
Largest  ||V|| (m)      0.157        0.067        0.077        0.100        0.124        0.139        0.059        0.110

# outliers removed       180          291          226          491         1666          175          130          231
# points remain           50          235          167          366          297           62           60           98
 (Cutlevel 3)

% CovArea AFTER (percentage of area on sphere covered by point clouds after removing the points those are outliers)
                        51.66        61.82        55.99        84.90        69.53        53.56        43.45        52.22

% CovArea Removed (% CovArea BEFORE - % CovArea AFTER)
                        27.89         8.14        12.43         7.75        30.47        18.43        10.65        20.63
```

Absolute accuracy evaluation of MMS data (continued) ---- Dataset: INDOTLoop of Asset Grade 2

Detail results of fitting Cutlevel 3 to sphere model through estimation by Least Squares minimization

	Sphere 9	Sphere10	Sphere11	Sphere12	Sphere13	Sphere14	Sphere15	Sphere16
# points in Cutlevel 3	50	235	167	366	297	62	60	98
Smallest ||V|| (m) in								
Easting (E)	0.000	0.000	0.000	0.000	0.000	0.000	0.000	0.000
Northing (N)	0.000	0.000	0.000	0.000	0.000	0.000	0.000	0.000
Elevation (h)	0.000	0.000	0.000	0.000	0.000	0.000	0.000	0.000
Largest ||V|| (m) in								
Easting (E)	0.006	0.009	0.008	0.010	0.012	0.006	0.009	0.007
Northing (N)	0.007	0.010	0.008	0.009	0.013	0.009	0.008	0.010
Elevation (h)	0.010	0.009	0.008	0.008	0.012	0.009	0.006	0.010
RMSE ||V|| (m)	0.005	0.005	0.004	0.005	0.007	0.004	0.004	0.005
Smallest ||V|| (m)	0.000	0.000	0.000	0.000	0.000	0.000	0.000	0.000
Largest ||V|| (m)	0.010	0.010	0.009	0.010	0.016	0.010	0.010	0.010

Statistics of V's computed from all 8 sphere targets

Average RMSE ||V|| = 0.005 m (0.5 cm)
Min RMSE ||V|| = 0.004 m (0.4 cm), of Sphere 14
Max RMSE ||V|| = 0.007 m (0.7 cm), of Sphere 13

Smallest ||V|| = 0.000 m (0.0 cm), of Sphere 9
Largest ||V|| = 0.016 m (1.6 cm), of Sphere 13

Absolute accuracy evaluation of MMS data (continued)
Dataset: INDOTLoop of Asset Grade 2 (original data (WITHOUT Transformation))

	Sphere 9	Sphere10	Sphere11	Sphere12	Sphere13	Sphere14	Sphere15	Sphere16
Detected								
E_Det (m)	913372.343	913229.090	913109.530	912976.625	912916.904	913391.705	913483.853	913457.083
N_Det (m)	578088.233	578263.817	578464.060	578704.544	579163.335	579135.338	578742.231	578388.145
h_Det (m)	216.317	214.799	213.143	212.120	210.461	210.867	213.202	214.575
Reference								
E_Ref (m)	913372.904	913229.567	913109.996	912977.117	912917.393	913392.229	913484.352	913457.593
N_Ref (m)	578087.309	578263.011	578463.251	578703.722	579162.528	579134.455	578741.393	578387.289
h_Ref (m)	217.476	215.964	214.261	213.204	211.646	212.011	214.355	215.740
Dif (Detected-Reference)								
dE (m)	-0.561	-0.477	-0.466	-0.492	-0.489	-0.524	-0.499	-0.510
dN (m)	0.924	0.806	0.809	0.822	0.807	0.883	0.838	0.856
dh (m)	-1.159	-1.165	-1.118	-1.084	-1.185	-1.144	-1.153	-1.165
|Dif| (absolute value of Dif)								
|dE| (m)	0.561	0.477	0.466	0.492	0.489	0.524	0.499	0.510
|dN| (m)	0.924	0.806	0.809	0.822	0.807	0.883	0.838	0.856
|dh| (m)	1.159	1.165	1.118	1.084	1.185	1.144	1.153	1.165
dP (planimetric) (m)	1.081	0.936	0.934	0.959	0.944	1.026	0.976	0.996
dQ (3D) (m)	1.585	1.495	1.457	1.447	1.515	1.537	1.510	1.533

Statistics computed from all 8 sphere targets

Average dE = -0.502 m (-50.2 cm), Worst dE = 0.561 m (56.1 cm)
Average dN = 0.843 m (84.3 cm), Worst dN = 0.924 m (92.4 cm)
Average dh = -1.147 m (-114.7 cm), Worst dh = 1.185 m (118.5 cm)
Average dP (planimetric) = 0.981 m (98.1 cm), Worst dP = 1.081 m (108.1 cm)
Average dQ (3D) = 1.510 m (151.0 cm), Worst dQ = 1.585 m (158.5 cm)

RMSE E = 0.503 m (50.3 cm)
RMSE N = 0.844 m (84.4 cm)
RMSE h = 1.147 m (114.7 cm)
RMSE P (planimetric) = 0.983 m (98.3 cm)
RMSE Q (3D) = 1.510 m (151.0 cm)

Absolute accuracy evaluation of MMS data (continued)
Dataset: INDOTLoop of Asset Grade 2 (transformed data)

	Sphere 9	Sphere10	Sphere11	Sphere12	Sphere13	Sphere14	Sphere15	Sphere16
Detected								
E_Det (m)	913372.836	913229.581	913110.019	912977.110	912917.383	913392.185	913484.338	913457.573
N_Det (m)	578087.395	578262.977	578463.219	578703.702	579162.492	579134.501	578741.395	578387.308
h_Det (m)	217.431	215.926	214.282	213.274	211.631	212.009	214.327	215.691
Reference								
E_Ref (m)	913372.904	913229.567	913109.996	912977.117	912917.393	913392.229	913484.352	913457.593
N_Ref (m)	578087.309	578263.011	578463.251	578703.722	579162.528	579134.455	578741.393	578387.289
h_Ref (m)	217.476	215.964	214.261	213.204	211.646	212.011	214.355	215.740
Dif (Detected-Reference)								
dE (m)	-0.068	0.014	0.023	-0.007	-0.010	-0.044	-0.014	-0.020
dN (m)	0.086	-0.034	-0.032	-0.020	-0.036	0.046	0.002	0.019
dh (m)	-0.045	-0.038	0.021	0.070	-0.015	-0.002	-0.028	-0.049
|Dif| (absolute value of Dif)								
|dE| (m)	0.068	0.014	0.023	0.007	0.010	0.044	0.014	0.020
|dN| (m)	0.086	0.034	0.032	0.020	0.036	0.046	0.002	0.019
|dh| (m)	0.045	0.038	0.021	0.070	0.015	0.002	0.028	0.049
dP (planimetric) (m)	0.110	0.037	0.039	0.021	0.038	0.063	0.014	0.028
dQ (3D) (m)	0.119	0.053	0.044	0.074	0.040	0.063	0.032	0.056

Statistics computed from all 8 sphere targets

```
Average dE                = -0.016 m (  -1.6 cm),   Worst dE =   0.068 m (6.8 cm)
Average dN                =  0.004 m (   0.4 cm),   Worst dN =   0.086 m (8.6 cm)
Average dh                = -0.011 m (  -1.1 cm),   Worst dh =   0.070 m (7.0 cm)
Average dP (planimetric)  =  0.044 m (   4.4 cm),   Worst dP =   0.110 m (11.0 cm)
Average dQ (3D)           =  0.060 m (   6.0 cm),   Worst dQ =   0.119 m (11.9 cm)

RMSE E                =  0.032 m (3.2 cm)
RMSE N                =  0.041 m (4.1 cm)
RMSE h                =  0.039 m (3.9 cm)
RMSE P (planimetric)  =  0.052 m (5.2 cm)
RMSE Q (3D)           =  0.065 m (6.5 cm)
```

Absolute accuracy evaluation of MMS data (continued): BEFORE transformation vs. AFTER transformation
Dataset: INDOTLoop of Asset Grade 2

	Sphere 9	Sphere10	Sphere11	Sphere12	Sphere13	Sphere14	Sphere15	Sphere16
Dif BEFORE (Detected-Reference) (from originally data)								
dE (m)	-0.561	-0.477	-0.466	-0.492	-0.489	-0.524	-0.499	-0.510
dN (m)	0.924	0.806	0.809	0.822	0.807	0.883	0.838	0.856
dh (m)	-1.159	-1.165	-1.118	-1.084	-1.185	-1.144	-1.153	-1.165
Dif AFTER (Detected-Reference) (from originally data)								
dE (m)	-0.068	0.014	0.023	-0.007	-0.010	-0.044	-0.014	-0.020
dN (m)	0.086	-0.034	-0.032	-0.020	-0.036	0.046	0.002	0.019
dh (m)	-0.045	-0.038	0.021	0.070	-0.015	-0.002	-0.028	-0.049

Transformation parameters

3 Rotations				Translation (shift)
	Degree	Min	Second	
Omega = -0.001563194 degree =	-0.00000	-0.00000	-5.62750	TE (m) = 0.484
Phi = -0.003395692 degree =	-0.00000	-0.00000	-12.22449	TN (m) = -0.839
Kappa = -0.000750407 degree =	-0.00000	-0.00000	-2.70147	Th (m) = 1.143

Statistics computed from all 8 sphere targets : BEFORE transformation (origianl) vs. AFTER transformation

BEFORE transformation (original data)	AFTER transformation
Average dE = -50.2 cm, Worst dE = 56.1 cm	Average dE = -1.6 cm, Worst dE = 6.8 cm
Average dN = 84.3 cm, Worst dN = 92.4 cm	Average dN = 0.4 cm, Worst dN = 8.6 cm
Average dh = -114.7 cm, Worst dh = 118.5 cm	Average dh = -1.1 cm, Worst dh = 7.0 cm
Average dP = 98.1 cm, Worst dP = 108.1 cm	Average dP = 4.4 cm, Worst dP = 11.0 cm
Average dQ = 151.0 cm, Worst dQ = 158.5 cm	Average dQ = 6.0 cm, Worst dQ = 11.9 cm
RMSE E = 0.503 m (50.3 cm)	RMSE E = 0.032 m (3.2 cm)
RMSE N = 0.844 m (84.4 cm)	RMSE N = 0.041 m (4.1 cm)
RMSE h = 1.147 m (114.7 cm)	RMSE h = 0.039 m (3.9 cm)
RMSE P (planimetric) = 0.983 m (98.3 cm)	RMSE P (planimetric) = 0.052 m (5.2 cm)
RMSE Q (3D) = 1.510 m (151.0 cm)	RMSE Q (3D) = 0.065 m (6.5 cm)

Relative accuracy evaluation of MMS data (use the whole network of validation points)
Dataset: INDOTLoop of Asset Grade 2

	Min	Between		Max	Between	
Distance (m)	226.613	S9	S10	1167.606	S9	S13

	Min	Between		Dist (m)	Max	Between		Dist (m)
|ddE| (cm)	0.3	S12	S13	462.664	9.5	S9	S11	458.614
|ddN| (cm)	0.2	S10	S13	952.162	11.8	S9	S10	226.613
|ddh| (cm)	0.1	S10	S16	259.690	10.2	S12	S13	462.664
|ddP| (cm)	0.3	S10	S11	233.227	14.8	S9	S11	458.614
|ddQ| (cm)	0.3	S10	S11	233.227	14.9	S9	S11	458.614

RMSE |ddE| = 0.042 m (4.2 cm)
RMSE |ddN| = 0.060 m (6.0 cm)
RMSE |ddh| = 0.045 m (4.5 cm)
RMSE |ddP| (planimetric) = 0.062 m (6.2 cm)
RMSE |ddQ| (3D) = 0.062 m (6.2 cm)

Sorted distance (Ascending) (m)	Between		|ddE| (cm)	|ddN| (cm)	|ddh| (cm)	|ddP| (cm)	|ddQ| (cm)
226.613	S 9	S10	8.4	11.8	0.6	14.5	14.5
233.227	S10	S11	1.1	0.4	4.7	0.3	0.3
259.690	S10	S16	3.2	5.0	0.1	0.4	0.4
274.768	S11	S12	2.6	1.3	3.5	2.4	2.4
311.659	S 9	S16	5.2	6.8	0.7	5.2	5.2
355.100	S15	S16	1.0	1.7	1.2	1.7	1.7
355.751	S11	S16	4.4	4.6	4.7	5.2	5.3
403.769	S14	S15	2.4	4.5	1.0	4.9	4.9
458.614	S 9	S11	9.5	11.4	4.1	14.8	14.9
462.664	S12	S13	0.3	1.5	10.2	1.5	1.5
466.365	S11	S15	3.3	2.9	3.5	1.0	1.0
475.627	S13	S14	3.4	7.6	4.2	3.9	3.8
507.924	S10	S12	1.5	1.7	8.1	2.2	2.2
508.627	S12	S15	0.7	1.6	6.9	0.6	0.6
542.021	S10	S15	2.2	3.2	1.2	1.8	1.8
575.287	S12	S16	1.7	3.3	8.2	3.3	3.3
598.228	S12	S14	3.1	6.0	6.0	2.2	2.2
663.444	S 9	S15	6.2	8.6	0.6	7.4	7.4
706.235	S13	S15	1.0	3.1	3.2	2.6	2.6
725.326	S11	S13	2.3	0.2	6.7	0.4	0.4
728.177	S11	S14	5.8	7.4	2.5	4.5	4.6
732.428	S 9	S12	6.9	10.1	7.5	12.3	12.3
750.057	S14	S16	1.4	2.7	2.2	2.8	2.8
886.571	S10	S14	4.6	7.7	2.1	6.7	6.7
944.845	S13	S16	2.0	4.8	2.0	5.1	5.1
952.162	S10	S13	1.2	0.2	2.0	0.5	0.6
1047.298	S 9	S14	3.8	4.1	1.5	4.0	4.0
1167.606	S 9	S13	7.2	11.7	2.6	13.5	13.5

APPENDIX E: MOBILE TERRESTRIAL LASER SCANNER (MTLS) SPECIFCATIONS MANUAL

MOBILE TERRESTRIAL LASER SCANNER (MTLS) SPECIFCATIONS MANUAL

CONTENTS

A. PURPOSE OF THIS MANUAL

The **Mobile Terrestrial Laser Scanning (MTLS) Specifications Manual** defines standards and procedures for preparing, collecting, editing, delivering, exploiting, and archiving electronic mapping data that is produced for the Indiana Department of Transportation (INDOT). These standards apply to all projects delivered to INDOT by contracted consulting firms, or exchanged internally within INDOT.

The purpose of the standards and procedures within this manual is to obtain an optimal degree of statewide uniformity within INDOT's combined Aerial/Ground Survey process, to establish and maintain MTLS Standards for INDOT and contracted consultants, and to allow for all of the project data to be effectively managed from conception to completion. These standards apply to any MTLS technology, regardless of vendor or make.

The work that was done to support the development of this Mobile Terrestrial Laser Scanning (MTLS) Specifications Manual is described in the research report titled *Laser Mobile Mapping Standards and Applications in Transportation* (Johnson, Bethel, Supunyachotsakul, & Peterson, 2016). The work includes experiments that were done, data that was collected, analysis that was carried out, and conclusions that were drawn about the accuracy of Mobile Terrestrial Laser Scanning (MTLS) systems. The findings and knowledge obtained from this research project were essential in the development of this MTLS Specifications Manual. This is because many of the technically related numbers and values, as well as other insights presented in the MTLS Specifications Manual, are substantiated and justified through these findings.

B. GENERAL

LiDAR (Light Detection and Ranging) is a technology that uses laser scanner(s) to obtain geospatial positions and signal reflectivity of points on the objects being surveyed. The fundamental result is a point cloud that contains three dimensional position (X, Y, Z) and intensity data. The intensity data gives information about the reflectivity of the survey objects' surface at each point captured in the scanning environment.

Mobile Terrestrial Laser Scanning (MTLS) is a system that uses LiDAR scanner(s) supported by one or more digital cameras, a Global Navigation Satellite System (GNSS) receiver, an Inertial Measurement Unit (IMU), a Distance Measurement Indicator (DMI), and ancillary devices to display, process, and record the navigation and geospatial data. The system is mounted on a moving terrestrial platform. Typically vehicles including vans and trucks are used, but boats, and rail vehicles may be used as dictated by the scanning environment. The Mobile Terrestrial Laser Scanner (MTLS) is often referred to as a Mobile Laser Scanner (MLS) and the whole system that deploys MTLS technology is conventionally known as a Mobile Mapping System (MMS).

B.1 Components of Mobile Mapping System

The Mobile Mapping System (MMS) can be configured in variety of ways depending on different vendors, requirements, and makes. The performance of the MMS itself depends on the specifications of the fundamental or main components which can be itemized as follows:

- Laser Scanner (active ranging sensor with steering optics)
- Digital Cameras
- Global Navigation Satellite System (GNSS) Receivers
- Inertial Navigation System (INS) incorporating the Inertial Measurement Unit (IMU) with onboard software displaying navigation, estimation, and error propagation solutions
- Distance Measurement Indicator (DMI) or Wheel Revolution Counter
- Rigid Platform for stable geometric calibration of the components
- Ancillary Devices for solution display, system control, and data storage

Table B.1 lists selected major attributes which comprise the specifications of the laser scanner, digital cameras, GNSS receivers, and INS which directly relate to the overall performance of a Mobile Mapping System.

It should be noted that the units listed in Table B.1 are the conventionally used units; there may be variability in the specifications listed by different vendors and manufacturers.

B.2 Working Scheme of the Mobile Mapping System (MMS)

In general, there are two different technologies that laser scanners use to determine the range to the scanned targets, *time of flight* and *phase* technology. The time of flight technology scanners typically have a longer range compared to those using the phase technology; however, the phase technology is generally faster than the time of flight technology.

The laser scanner in a Mobile Mapping System uses the time-of-flight technology to determine the range to the scanned targets. The rotating laser scanner also measures the angular direction of the range line using high resolution angle encoders. With range and angular direction measurements to the targets, the coordinates of scanned points are then computed in the scanner reference coordinate frame.

The point cloud coordinates in the scanner frame can be transformed to the IMU body frame if the rotation parameters and the translation parameters are known by calibration. The so-called "boresight angles" are the orientations of the scanner frame with respect to the IMU body frame and the "lever arm offsets" are the three dimensional offsets from the scanner frame origin to the IMU body frame origin.

The Inertial Measurement Unit (IMU) instantaneously reports the orientations of the IMU body frame (roll, pitch and heading) with respect to a reference frame known as "Instantaneous Local Level Frame" that has the origin aligned with IMU body's origin.

TABLE B.1
Examples of some major specifications of laser scanner, digital cameras, GNSS receivers, and INS.

MMS Main Components	Major Specifications
Laser Scanner	• Point Repetition Rate (PRR) (measurements/sec or Hz) • Line Scan Speed (LSS) (lines/sec or rotation rate) • (PRP and LSS determine the overall measurement rate) • Range • Accuracy (length unit, mm for absolute comparison) • Precision (length unit, mm for repeatability) • Least Count of Angle Measuring Device
Digital Camera	• Resolution (pixels per frame) • Frame Rate (frames/sec) • Exposure (micro sec or sec) • Field of View (deg in H x deg in V) • Degree of Compression
Global Navigation Satellite System (GNSS) Receivers	• Data Rate (Hz) • Tracking (GPS, GPS & GLONASS) • Reacquisition (sec) • Kinematic processing with multiple base station
Inertial Navigation System (INS)	• IMU Data Rate (Hz) • IMU Drift Rate (deg/hr) • Gyro Bias (deg/h) • Accelerometer Bias (μg or mg)

The coordinates measured and transformed into the IMU body frame can be then transformed to the Instantaneous Local Level Frame.

The GNSS receiver mounted on the vehicle is continuously collecting time-tagged data for the Instantaneous Local Level Frame's position. The GNSS data logs obtained from the GNSS receiver mounted on the MMS vehicle and the data from receivers occupying a project base station(s) are then post-processed to arrive at the instantaneous position of the Instantaneous Local Level Frame with respect to an Earth-centered-earth-fixed (ECEF) project datum frame. The point cloud data in the Instantaneous Local Level Frame can then be transformed to the ECEF frame (georeferenced).

B.3 Mobile Mapping System (MMS) Error Sources

The errors present in a Mobile Mapping System can be categorized into two main sources: instrumental errors and operational errors.

B.3.1 Instrumental Errors

The physical components of a MMS and the calibrated relationships among them contribute to the instrumental errors of the MMS itself. The following is a summary of error sources in the principal components of an MMS.

Laser Scanner Errors. The laser scanner of an MMS uses time-of-flight technology to determine the range to the scanned points. The laser scanner also makes angular readings to the points using angle encoders. With range and angular measurements to the targets, the locations of scanned points are then determined. The errors in range and angular measurements are a contributing cause of the uncertainty in locating the actual positions of the scanned objects.

Global Navigation Satellite System (GNSS) Errors. GNSS error sources include the satellite and receiver clock errors, orbit errors, the atmospheric delays, and random noise. These errors may be modeled in the GNSS solution or compensated by differencing techniques relative to fixed control stations. The GNSS solution determines the project datum coordinate system of the scanned object points. Residual GNSS errors contribute to the relative positional errors between points and the absolute positional errors in the final coordinate system.

IMU Attitude Errors. The principal role of the IMU is to provide angular velocity observations which can be integrated into angular position information (roll, pitch, and heading) of the IMU body frame with respect to the Instantaneous Local Level Frame. Together with position data, this enables the point data in the Instantaneous Local Level Frame to be transformed into the ECEF frame. Thus all points in the point cloud are brought into a common reference frame. Knowledge of the sensor attitude with respect to the local level frame, via IMU data, affects every point. Therefore any uncompensated errors from the IMU will have direct impact on the geometric quality of the point cloud.

Boresight Alignment Errors (body frame / scanner frame angles and offsets). The orientation of the scanner frame with respect to the IMU body frame is expressed through boresight angles and lever arm offsets. The boresight angles cannot be observed by direct measurements, therefore these values are obtained indirectly through a calibration process. There are inevitable residual adjustment errors present in the alignment estimates.

The lever arm offset values can be obtained either though calibration or by measurements or both. Note that the values required are vector components, not just lengths, so some realization of the relevant coordinate systems is necessary.

B.3.2 Operational Errors

In addition to the errors from the MMS's instruments that directly contribute to overall errors, the way the system is operated also plays a vital role in the resulting MMS error budget. System operation procedures also affect the completeness and the quality of the scanned data.

GNSS Signal Multipath. The structures in the vicinity of the GNSS receiver can cause multipath interferences of GNSS signals resulting in decreased accuracy of the positions. The multipath effect can be quite severe especially in urban areas (urban canyons) where there are many tall building structures.

GNSS Signal Obstruction. The structures or objects in the vicinity of the GNSS receiver can cause an obstruction between the GNSS receiver and some or all satellites. This forces the receiver to estimate position with fewer satellites available in the viewing window resulting in geometrically weaker positioning solutions of the MMS. The obstruction effect is quite severe especially in urban areas (urban canyons) where there are many tall building structures.

Loss of GNSS Signal Lock. Closely related to signal obstruction is "momentary obstruction" resulting in loss of lock, or discontinuities in signal tracking. It differs from the obstructions mentioned above, in that it is momentary rather than persistent. The loss of GNSS signal lock greatly affects the positioning of the MMS. The loss of GNSS signal lock is mainly caused by obstruction features such as trees, bridges, vehicles, etc.

Traffic Conditions. A heavy traffic conditions during the MMS data collection causes vehicle and pedestrian shadows or occlusions in the resulting point cloud. Note that some of these conditions can be mitigated by having the MMS vehicle make multiple passes.

Weather Conditions. Rain or snow during the MMS data collection process can be very detrimental to the data quality due to the fact that the rain droplets or snowflakes themselves behave as scatterers with unpredictable corruption of the point cloud. Recent rain can be an issue if there are significant puddles or standing water, as these will cause specular reflections of the laser energy. This has two deleterious effects: it prevents properly detecting the ground surface under the puddle, and it may introduce spurious points via the reflection (we could also call this multipath of the scanner itself).

B.4 Factors Affecting the Selection of Mobile Mapping as Survey Method

There are many factors to be considered in deciding if MMS is the appropriate technology for data collection for a project. Below is a list of the major factors to be considered:

- Size of the project; in terms of area and length
- Nature of the project area (urban area, flat open area, mountainous area, etc.—i.e., is it easily accessible via smooth roads or smooth surfaces which will support the vehicle?)
- Safety
  - Accessibility
  - Environmental issues in the project area (severe weather zone, extreme temperature, extreme condition (wind, visibility issue), etc.)
  - The laser scanner must be operated in a way to ensure the eye safety of the travelling public, pedestrians and animals
- Availability of unobstructed GNSS signals, for example interior of a parking garage would present difficulties.
- Desired products (deliverables) of the project.
- Project time constraints
- Project budgets
- Could the project be achieved at lower cost by static scanning, photogrammetry, or conventional surveying or kinematic GPS?

C. DATA AND METADATA

A Mobile Mapping System (MMS) produces a great deal of data in addition to the fundamental object point cloud. Users should be familiar with the data that may be available as an aid in quality acceptance and control and in developing additional applications using the data set. This chapter will cover characteristics of the data obtained from a Mobile Mapping System (MMS), conventional formats, and accompanying Metadata or support data.

C.1 Data Obtained from Mobile Mapping System (MMS)

C.1.1 Raw Sensor Data

The raw sensor data obtained from a Mobile Mapping System (MMS) can be varied and is typically stored in a proprietary format which depends on the sensors and components of the MMS used in data

acquisition process. If any of these data are wanted, then prior negotiations with the vendor for tools or translators will be necessary.

The raw sensor data typically includes the following:

- Readings from each laser scanner—the angles and ranges for a pulsed laser scanner or the angles and phases readings from a full waveform scanners
- Digital images taken from digital cameras and/or video files from a video recording system
- Distance readings from DMI
- GNSS readings which are the positioning data obtained from the GPS receiver
- IMU readings

To be useful, it is important that the raw sensor data listed is appropriately time-tagged.

C.1.2 Raw Point Cloud and Imagery

The aforementioned raw sensor data must be integrated and processed to arrive at a point cloud and imagery in an arbitrary reference frame of convenience. The point cloud at this stage is conventionally known as a raw point clouds. Because raw point clouds have not undergone any correction procedure though the use of project control points or reconciliation with overlapping point clouds, users may easily detect or visualize separations (misalignments or mismatches) between clouds from different scanning paths. Users are likely to also be able to visualize misalignment between raw point clouds and raw images.

C.1.3 Corrected Point Cloud and Imagery

The corrected or controlled point clouds are the raw point clouds that have been corrected through the use of project control points, and/or other overlapping point clouds. Assuming that raw point clouds and raw images have been properly corrected, the separations between point clouds from different scanning paths will be greatly reduced and the images will be consistent with each other and with the corresponding point clouds. The point clouds and images that have been projected through the use of project control points into an established project coordinate system are known as the registered, geo-referenced, or corrected point clouds and images.

C.1.4 Trajectory Files

The post-processing of the GNSS position data combined with IMU trajectory data and distance readings from the DMI results in the final trajectory of each MMS vehicle pass. The data sets and results of the trajectory determination are often collected into a trajectory file. For users of Applanix navigation equipment this file has a standard, proprietary format known as "Smoothed Best Estimate of Trajectory (SBET)."

C.1.5 Value-Added Products (Derived Products)

For particular applications with unique objectives, a variety of filters and processors can be applied to the point cloud. For example, object classification, vegetation removal, vehicle removal, feature extraction, terrain modeling, etc. may be applied to point clouds to produce specific types of value-added products. These are referred to as derived datasets or extracted features or dimensions. Examples of such derived datasets include cross sections, profiles, contours, utility locations, and bridge clearances.

Derived datasets can be obtained not only from manipulations applied to the point cloud data itself, but they can also be obtained through the manipulations of point clouds and other relevant information such as registered imagery.

C.2 Auxiliary Information for Mobile Mapping System (MMS) Data

Along with the data itself, several types of auxiliary data is usually provided as well. This can include a Project Narrative, and also Metadata or support data needed to fully exploit the point cloud. It is important to stress that the Project Narrative and the Metadata are not the same thing and should not be considered interchangeable. The Metadata is the data about the MMS data itself. This might include format specifications, unit descriptions, trajectory data, index files, or information about the imagery.

The Project Narrative report itself should provide the general information about the data collection. This could include notes taken at the time of the collection regarding date, time, weather, traffic, personnel, condition of roadway, condition of targets, etc. It may also include narratives about processing steps, GNSS adjustments, fitting of overlapping point clouds to one another, or fitting of point clouds to targeted project control points. Depending on organization details of the Narrative Report, there may be supplementary reports about some specific topics.

C.3 Conventional File Formats for Mobile Mapping System (MMS) Data

Conventional file formats for MMS data are listed in Table C.1. Users typically will be dealing with the point clouds, imagery, and derived data (value-added products) in common, open formats. Therefore, these conventional formats are listed in the table. In some projects, the raw sensor data may be part of the required deliverables and some typical formats of proprietary, raw sensor data obtained from a Mobile Mapping System (MMS) are included; however, raw data are system dependent and are stored in the hardware-specific formats. Some typical file formats of value-added products are included, but the list is not exhaustive.

TABLE C.1
Conventional file formats of mobile mapping system data.

MMS Data	Conventional File Format	Remarks (ASCII /Binary)	Commonly Used Software to Read and/or Process
The Raw Sensor Data			
GNSS Data	RINEX	ASCII	Text Editor (Notepad, WordPad)
Digital Images	TIFF, JPEG, PNG	Binary	Photoshop
Digital Video	AVI, MOV, MPG	Binary	Media Player, Quicktime
Point Cloud and Imagery			
Raw Point Clouds	LAS, PTX, XYZ	LAS: binary standard, PTX, XYZ ASCII open	TopoDot, Terrasolid, Pointools, Leica Cyclone, Faro Scene, Scene LT
Raw Digital Images	TIFF, JPEG, PNG	Binary	Photoshop
Corrected Point Clouds	LAS, PTX, XYZ	LAS: binary standard, PTX, XYZ ASCII open	TopoDot, Terrasolid, Pointools, Leica Cyclone, Faro Scene, Scene LT
Corrected Digital Images	TIFF, JPEG, PNG	Binary	Photoshop
Trajectory File	SBET, SHP KMZ, TXT	Binary ASCII	Text Editor for ASCII
The Derived Dataset			
Cross sections, contours, bridge clearances	CAD formats (e.g., DGN, DXF, DWG)	Binary, ASCII	MicroStation, AutoCAD

D. ACCURACY, RESOLUTION, AND COMPLETENESS OF MMS DATA

The accuracy of an MMS dataset depends on several factors which can be categorized into the groups as follows:

- Hardware and specifications of the Mobile Mapping System used
- Usage of the control points, and the quality and distribution of control points
- Data collection parameters (range, incident angles, speed of vehicle, etc.)
- Data collection environment (the nature of the scanning area (urban area or open area, weather, temperature, traffic conditions, etc.)
- Data processing techniques

The horizontal accuracy and vertical accuracy are handled separately as they often have different accuracy requirements; however, they are of course geometrically related. The horizontal accuracy of MMS data is tested by comparing the planimetric coordinates of well-defined validation points extracted from the MMS dataset against the coordinates of the same points obtained independently from a higher accuracy ground survey. Similar to the case of horizontal accuracy testing, the vertical accuracy testing compares the elevations at validation points and independently surveyed elevations.

D.1 Accuracy Specifications

There are two types of MMS dataset accuracies that must be addressed: (1) the absolute accuracy, sometimes referred to as the network accuracy, and (2) the relative accuracy, sometimes referred to as the local accuracy.

D.1.1 Absolute Accuracy (Network Accuracy)

The absolute accuracy is a value that represents the uncertainty in the planimetric coordinates (horizontal position) and the elevation (vertical position) of a point in the point cloud. The absolute accuracy is evaluated by testing horizontal and vertical position discrepancies at project validation points. Project control points should be referenced to the National Spatial Reference System (NSRS) which is defined, maintained and published by the National Geodetic Survey (NGS). NAD 83(2007) is the geodetic datum recommended for horizontal control. NGVD 88 and orthometric (sea level) heights is recommended for vertical control. In a case where ellipsoid heights are used, the former horizontal datum suffices for both horizontal and vertical accuracy.

D.1.2 Relative Accuracy (Local Accuracy)

Relative accuracy is a value that represents the uncertainty in the *difference* in the planimetric coordinates (horizontal position) and elevation (vertical position) between points in the point cloud. Experience has shown that for MMS data, since it is continuously registered to the absolute coordinate reference system during collection, relative accuracy computed for a set of validation points distributed throughout the point cloud is the same as absolute accuracy. Therefore, we do not tabulate a relative accuracy specification for the validation points. A specification for the vertical difference between closely spaced adjacent points is tabulated. For some applications such as design and construction work high absolute accuracy is critical, in contrast, for some applications such as bridge clearance measurement, a high relative accuracy is sufficient.

D.2 Accuracy Reporting Standard

MMS data accuracy reporting should conform to the following items:

- Use root-mean-square error (RMSE) to compute the positional accuracy of a dataset
- Positional accuracy (both horizontal and vertical) shall be reported at the 95% confidence level
- Positional accuracy (both horizontal and vertical) shall be reported in ground units
- The unit shall be the same as the unit of the MMS dataset coordinates
- The number of digits to the right of the decimal point for reported accuracy shall be equal to the number of digits to the right of the decimal point for the MMS dataset coordinates

For more details about how the root-mean-square error (RMSE) and the 95% confidence level are computed to represent the positional accuracy of the dataset, see Appendix A.

D.3 Accuracy Requirements

TABLE D.1
95% critical values for testing MMS absolute results.

Absolute Accuracy	Design	Asset
Horizontal	95% of tested points <8 cm discrepancy from reference position	95% of tested points <18 cm discrepancy from reference position
Vertical	95% of tested points <5 cm discrepancy from reference elevation	95% of tested points <24 cm discrepancy from reference elevation

TABLE D.2
95% critical values for testing MMS relative vertical results.

Relative Accuracy	Design	Asset
Vertical difference between closely space points	95% of tested dV <5 cm discrepancy from reference dV	95% of tested dV <6 cm discrepancy from reference dV

D.4 Range Effect

The range between the laser scanner and the target objects or terrain plays a vital role in the positional accuracy of the scanned points. Although the accuracy of the range itself may be largely independent of range, the coordinate values of the scanned points depend on both measured length and the measured direction of the range line. It is the latter angular solution that makes point coordinate accuracies range dependent. It is important to not only specify the required accuracy for the delivered point cloud but to also specify the required accuracy within a required range (e.g. the delivered point clouds shall have the accuracy of X.X cm within 20 m range)

Since accuracy of the point coordinates degrades when the range between the laser scanner and the point increases, some vendors may specify an effective range or a range limit and exclude all the points that get scanned beyond the specified range to ensure a consistent level of accuracy.

D.5 Resolution (Point Density) of MMS Dataset

The resolution of the MMS dataset is characterized in terms of point density which is the number of points in a given unit area (points/m^2 or points/ft^2). The point density varies within the point cloud and is affected by the following project factors:

- Scanner specifications (Point Repetition Rate and Line Scan Speed)
- Nominal distance from the scanner
- Vehicle speed
- Number of scanning passes
- Obstructions

A point density value by itself is not a complete piece of information. It is important that the point density information be accompanied by the distance from the scanner and the location where it was evaluated (e.g., the point density of 1000 points/m^2 evaluated on the (horizontal) pavement surface at 3 meters away from the scanner, the point density of 100 points/m^2 evaluated on the (vertical) building wall at 20 meters away from the scanner).

Point density plays an important role in feature extraction from scanned point clouds. A contractor shall ensure that the point density within a point cloud is sufficient to permit the extraction of features of interest (e.g., lines, spheres, cylinders, planes, poles, etc.) at the specified level of accuracy within the specified distance from scanner.

Scanning the scene using the maximum sampling rate of the laser scanner to achieve point clouds with maximum possible density often seems to be the best practice. However, some vendors have commented that using the maximum scan rate may produce noisy point clouds for some specific features. Discussions with the vendor prior to scanning can be useful here.

D.6 Multiple Scan Passes and Overlapping Scans

The same scene (roads, buildings, etc.) is often scanned with multiple scanning passes to ensure high quality of the scanned point cloud (increase point density, fill the shadow gaps, create good geometry of scanned points on the feature of interests for feature extraction) or to cover larger areas with side overlapping scans. There is no specific rule about the minimum percentage of point cloud overlap. Disregarding costs, more overlap means more redundancy

which is beneficial. A practical rule would be that every point in the scene should be seen by at least 2 scan heads on different passes. In general, looking at consistency or non-consistency (gaps) between data on the same feature from separate passes is an ideal way to judge many aspects of the whole post processing effort (multiple cloud reconciliation, enforcement of control point positions, etc.).

E. CONTROL AND VALIDATION SURVEY

MMS service providers and vendors should be responsible for any control surveys that are needed. Often they subcontract this activity to local surveying firms, working to their specifications. Vendors may have the control survey and target placement done by INDOT. INDOT must consider the responsibility and liability for control accuracy affecting the delivered products.

On the other hand, INDOT may very well wish to take responsibility for validation surveys, as this gives them a way to quantitatively evaluate the quality of the delivered products against requirements for accuracy. Checkpoints or validation points and off-road targets provide a way to implement such a validation survey, in which the control values are withheld from the MMS vendors, and are only used by INDOT to check the delivered data quality.

E.1 GNSS Base Stations

GNSS observations at fixed base receiver(s) and the receiver mounted on vehicle are used in the kinematic post-processing of the GNSS data to reference the point cloud to the project coordinate system. Vendors typically set up their own GNSS base stations for a project to ensure that the baselines to the vehicle are short and hence will not degrade the post-processing kinematic solutions. INDOT may share knowledge of network ground control points in the proximity of the project. INDOT may occupy the control points and supply the raw GNSS data streams to the vendor.

Considerations for setting up project GNSS base stations include the following:

- Keep baselines from base receiver to vehicle receiver short for the differential GNSS solution. A single base receiver station, centrally located, may be sufficient for small project areas.
- Multiple GNSS base station receivers may be distributed over large project areas. For linear roadway projects, a minimum is to place at least one GNSS base station at the beginning and one at the end of the project.
- Multiple GNSS base station receivers increase redundancy in case of an accident, receiver error, human error in setting base stations, or other possible error.
- The GNSS base stations must conform to Chapter 25, GPS Survey Control Network of the INDOT Design Manual.

E.2 Project Control and Validation Points

The raw MMS dataset must be adjusted to the project control coordinate datum. Project control points are used to solve for the parameters of a coordinate transformation from the raw dataset coordinate system to the project coordinate datum. Validation points are established to make an independent evaluation of accuracy of the delivered products. Validation point coordinates should be withheld from the solution and not used in post processing. Project control points and validation points are the well-defined points and their coordinates are independently surveyed from a higher accuracy surveying method.

Project control points are often designed by the vendor, and they are typically placed within the road right of way. Validation points are often established by the client and may be in the roadway or adjacent to the roadway. The points must be identifiable in the point cloud. This is accomplished by placing reflective targets on the roadway (crosses, squares, chevron) or placing reflective objects (sphere for example) plumbed over points off the roadway. The target position on the surveyed point is established by processing the intensity signal from shapes on the roadway or by processing the geometry of points on the target object.

Considerations for establishing project control and validation points include the following:

- Control and validation points must be independently surveyed to a higher accuracy than the MMS data.
- Control points can either be a point in the permanent local control network or they can be connected to the local control network and placed for a specific project
- Control and validation points must be uniquely identifiable and visible in the point cloud. When control points are targeted, consider target size, shape, and reflectivity in the final point cloud.
- The control points should be placed over the scanned area in a well distributed manner and at a spacing adequate to meet the accuracy requirement of the final point cloud.
- Validation points should be placed at locations approximately midway between adjacent control points.
- If the scans include roadways, the control points should be placed on both sides of the roadway as well as on the centerline or median area (without safety being compromised) in a well distributed manner.
- The control points which are set by using GPS must conform to Chapter 25, GPS Survey Control Network of the INDOT Design Manual.

F. QUALITY MANAGEMENT

Quality management involves tasks performed before and during MMS data acquisition and data processing to proactively monitor and ensure the quality of the MMS datasets. The planned tasks are documented in what is known as Quality Management Plan (QMP) and the major tasks in quality management can be categorized into quality assurance (QA) and quality control (QC) tasks.

F.1 Quality Assurance (QA)

Quality assurance (QA) refers to the planning of the tasks *prior to any collection activity* to manage the overall quality of the project. The QA program is planned by the vendor to ensure quality in the data collection and data processing activities. The QA report should be included in the project deliverables. Examples of QA activities will include: recent system calibrations, planning for multiple passes, planning for any special driving maneuvers at corners, planning for project control, planning optimal vehicle velocities and settable parameters, monitoring expected weather, etc.

F.2 Quality Control (QC)

Quality control (QC) refers to the check procedures and evaluations performed during stages of the project to detect any problems. QC may indicate needed corrections for ensuring the quality of products in intermediate stages and the quality of the final products. The QC report should be included in the project deliverables. Examples of QC activity include: monitoring PDOP metrics for the GNSS constellation, monitoring unexpected obstructions which may require re-executing the pass, monitoring adjustment statistics when merging overlapping point clouds, monitoring adjustment statistics (discrepancies) when fitting point cloud to project control, carrying out any independent validation point evaluation, etc.

The quality control planned tasks shall include but not be limited to the procedures described in Part F.2.1 through F.2.4.

F.2.1 Alignment Evaluation of Overlapping Point Clouds from Different Passes

In general, the overlapping scanned point clouds from different scanning passes are not well aligned without an adjustment through the use of project control points and/or cloud-to-cloud registration algorithms. These adjustment processes can dramatically improve the alignment between overlapping clouds from different passes. The misalignments between scanning passes are visualized through the vertical separations (difference in elevation data) between clouds. Note that horizontal misalignments (in non-horizontal planar data) also manifest themselves as vertical separations. The proposed procedures for comparing the elevation data (vertical separation) of overlapping point clouds from different passes must be documented and included in the Quality Management Plan (QMP).

F.2.2 Adjustment of the Raw MMS Dataset

The raw MMS dataset is adjusted and registered to the project control points through a coordinate transformation adjustment. The descriptions of the proposed type of transformation (i.e. the mathematical model, rigid body, seven parameter, rigid body without scale, etc.) to be used and the selected control points to be used must be documented and included in the Quality Management Plan (QMP).

F.2.3 Accuracy Evaluation of Corrected Point Clouds

As previously discussed in Part D, the accuracy evaluation of the MMS corrected point clouds is performed by comparing the coordinates of project validation points from the MMS dataset against the coordinates of the same points obtained independently from a higher accuracy survey. Validation points cannot have been used in the previously mentioned transformations. The descriptions of the proposed accuracy evaluation process of corrected point clouds must be documented and included in the Quality Management Plan (QMP). INDOT may decide whether to require the vendor to make a validation check or do it themselves independently.

F.2.4 Accuracy Evaluation of Other Derived Products

Besides the accuracy evaluation performed directly on the corrected point clouds, the accuracy of any required derived dataset or derived products must also be evaluated. A suitable method of evaluating the accuracy of a derived product is dependent on the type of product. The description details of the proposed method used in the accuracy evaluation process of the derived products must be documented and included in the Quality Management Plan (QMP).

F.3 Quality Management Plan (QMP)

The quality management plan (QMP) shall include the description of the proposed QA and QC plans, and it shall be submitted for review and approval before the start of the project. During the QMP review, INDOT may request some amendments applied to the QMP before approving the plan. The suggested contents of QMP are discussed in Part G.1.4.

G. DELIVERABLES AND DOCUMENTATIONS

The deliverables and documentation of projects depend on the type of projects and their associated workflows or procedures to arrive at the final products. It is not feasible to list deliverables and documentation for each specific type of project; therefore, minimum required deliverables and documentation for all MMS projects will be summarized and the optional deliverables that may be considered for specific applications must be agreed upon in the contract.

G.1 Fundamental Deliverables and Documentation

The following deliverables and documentation should be delivered for all projects. The recommended

formats of Fundamental Deliverables and Documentation are listed in Table G.1.

G.1.1 Point Clouds, Imagery and Videos

- Corrected point cloud
- Corrected imagery and videos

The point cloud data, imagery and videos must be delivered in agreed upon project reference coordinate system. It is desirable to also require the delivery of raw point cloud data and imagery in order to monitor the extent of the correction and refinement steps. However INDOT may choose to not make this mandatory.

The delivered data should be clean and free from the erroneous points caused by signal scattering, signal processing, and background reflections.

G.1.2 Derived Data (Value-Added Products/Modeled Point Clouds)

The required delivered products are not limited to only observed point clouds and imagery; the derived datasets are project dependent and vary among types of projects. The point cloud may be classified into different types of features of interest such as the cross sections or profiles of roads, the clearance of surveyed bridges, the extracted drainage lines, the locations of utilities, the modeling/extraction of power lines are examples of possible derived products for some projects. The required deliverable data for each project must be specified in the agreement.

The required file formats of the delivered data are to be clearly specified in the contract agreement. For some common products, unless specified otherwise in the contract agreement recommended files formats can be found in Table C.1.

G.1.3 System Calibration Report

A system calibration report provides verification of recent/current calibration of the geometric relationship between the laser scanner and INS unit (boresight calibration, lever arm offsets calibrations), camera calibration (parameters of every camera used in the system to obtain images), and other ancillary device calibration. As a minimum, the report must describe the date, extent, and result summary for any relevant calibration processes. The report should also include some statements about the authority and qualifications of the individuals or service providers who have made the calibration. It is desirable to include the calibration results and their associated statistics in detail, although this may be considered proprietary information by some vendors.

G.1.4 Quality Management Plan Report

Quality management plan (QMP) must include the description of the proposed QA and QC plans. The Quality management plan should include, but not be limited to the following:

- Descriptions and map of control points (same contents as Control Survey Report)
- Proposed procedures to be used in alignment evaluation of overlapping point clouds from different passes
- Proposed procedures to be used in the adjustment process of the raw MMS dataset
- Proposed procedures to be used for the accuracy evaluation of corrected point clouds
- GNSS PDOP values during data acquisition
- Descriptions and map of validation points
- Summaries of statistical and adjustment results for data merging, registration, and validation

Sections G.1.5 through G.1.8 summarize reports that are associated with the fundamental data processing procedures. Starting from the first step of the data acquisition process, until the production of deliverable products as specified in the project contract, many data processing and evaluation steps must occur. These steps should be summarized including basic procedures and results to complete the project documentation. If there are additional steps not itemized here, they should also be summarized in the same way.

G.1.5 Trajectory Analysis Report

The trajectory analysis report shall document the steps used for processing the GNSS and IMU readings in order to obtain the final trajectory of the MMS vehicle, typically expressed as the Smoothed Best Estimate of Trajectory (SBET file, or equivalent). The results and related statistics shall be documented in the trajectory analysis report.

G.1.6 Report of the Alignment Evaluation of Overlapping Point Clouds from Different Passes

The results from the process of comparing the elevation data (vertical separation) of overlapping point clouds from different passes and the results with their associated statistics as well as any other the related information must be documented and reported in detail. The results of this vertical separation analysis shall be reported whenever it occurs, both before and after fitting to control points.

G.1.7 Report of the Adjustment of the Raw MMS Data to Control Points

The statistical results from the adjustment process of fitting raw MMS data to project control points (transformation process) including related, supplementary information must be documented and reported in detail.

G.1.8 Modeled Dataset Report

The modeled dataset report should provide detailed information on how the final deliverables derived from

the point clouds were obtained. The underlying information includes the name of the software or analytical tools used to produce the deliverable, the steps or procedures, and any related statistics of the results. For example, if a Digital Terrain Model (DTM) is a required final product, this report should cover the name of the software packages and whatever is known about the algorithms employed. It should also briefly mention the workflow used to arrive at the final DTM. Additionally, it should also provide the information about the values of any adopted parameters used in DTM computations as well as the associated statistics of the result.

G.1.9 Report of the Corrected Point Clouds Accuracy Evaluations

The statistical results of the accuracy evaluation processes applied to the corrected point clouds as well as any related information must be documented and reported in detail.

G.1.10 Report of the Derived Products' Accuracy Evaluations

The statistical results of the accuracy evaluation processes applied to any derived products as well as any related information must be documented and reported in detail.

G.1.11 Project Narrative Report

The project narrative report should include the following information:

- Project name and location identifier
- Survey date, time, weather conditions, limits, purpose, personnel involved, contacts with customer personnel, log of activities with relevant details such as velocities, scan rates, etc.
- Project datum, epoch and units
- Survey control points found, held and set (see Control Survey Report)
- Personnel, equipment, and surveying methodology employed
- Problems encountered, if any
- Other supporting survey information such as GNSS observation logs
- Dated signature and seal (if licensure is required) of the surveyor\engineer in charge

G.1.12 Control Survey Report

Include a listing and map of project control point locations and type of signalization with relevant statistics from any adjustment procedures used to arrive at final project control coordinates. Specify the horizontal and vertical coordinate datum used for the final project control.

G.1.13 Metadata Files

As a minimum, include the adjusted trajectory file with information about how the adjustment was done.

G.1.14 Final Project Report

Include all of the items listed in this chapter G, organized in a readable fashion.

G.2 Optional Deliverables and Documentation

Besides the aforementioned fundamental deliverables and documentation, there may be other required deliverables and their related documentations based on the agreement of client and vendor. Table G.1 summarizes the list of deliverables below:

TABLE G.1
Deliverables list.

Fundamental Deliverables and Documentations	Point clouds, imagery and videos Derived data (modeled point clouds/value-added products) System calibration report Quality management plan report Fundamental Data Processing Documentations and Reports • Trajectory Analysis Report • Report of the Alignment Evaluation of Overlapping Point Clouds from Different Passes • Report of the Adjustment of the Raw MMS Data to CP's • Modeled / Derived Data Report Report of the Corrected Point Clouds Accuracy Evaluation Report of the Derived Products Accuracy Evaluation Project narrative report Control Survey Report Metadata Files Final Project Report
Optional Deliverables and Documentation	As specified in the contract

H. APPLICATIONS OF MOBILE TERRESTRIAL LASER SCANNING

The applications for mobile terrestrial laser scanning is a dynamic list as users refine existing applications and continue to develop new applications. Table H.1 incorporates the information in the paper by Williams, Olsen, Roe, and Glennie (2013) and then adds and/or modifies a number of the listed applications into the format shown. Of course there are overlaps with what could be accomplished using static terrestrial scanners or airborne scanners. Users must select the best method based on available equipment and resources and needs for accuracy, density, redundancy, and completeness.

TABLE H.1
General and related specific applications.

General Activity	Specific Application
Project Planning	Roadway Analysis Topographic Mapping, Digital Terrain Modeling Environmental Studies Surveying, Other Measurements Intersection Upgrade/Rehab Drainage Analysis Urban Feature Modeling/City Modeling/GIS
Project Development	3D Design, Clashes, Interferences Feature Extraction for CAD, Baseline Data
Construction	Progress Monitoring As-Built/Repair Documentation Machine Control and Construction Automation Post Construction QA/QC Pavement Smoothness Assessment Earthwork Quantities ADA Compliance
Maintenance	Bridge Inspection Pavement Inspection Power Line Clearance Above Ground Utility Inspection Vegetation Management Drainage/Flooding Assessment
Operations	Traffic Congestion/Parking Utilization Land Use/Zoning Compliance Tax Assessment Building Information Modeling (BIM) Bridge Information Modeling (BrIM) Emergency Response Clearances, Vertical & Horizontal (Bridges, Signs, Guardrails, …)
Safety	Extraction of Geometric Properties & Features (Sightlines, Obstructions) Accident Investigation/Forensic Investigations Railroad Grad Crossing Inspection Facilitate Cooperative Operations with Trolleys, Trains, Light Rail, Aviation, Bikes, Pedestrians Driver Assistance, Autonomous Navigation
Asset Management	Inventory Mapping Modeling and Inspection Automated/Semi-Automated Sign Extraction Billboard Management Signals, Pavement Markings, Bike/Pedestrian Amenities
Tourism	Virtual Tour of Region Attractions Integration with Turn by Turn Driving Instructions Historical Baseline Survey & Preservation
Research	Unstable Slope Detection Landslide Assessment Coastal Erosion Useful Integrations of Point Cloud and Image Data Extraction of CAD Model from Point Cloud Use of Point Cloud Features to Control Imagery Virtual Reality (VR) interaction with Point Cloud Data Planning Drone Waypoints and Trajectories

It should also be recognized that the real value from mobile laser scanning is the registered point cloud. As imaging and computer vision capabilities advance, comparable point clouds can in some cases be generated from imagery. This certainly is an area of active research. Some of the listed applications can best be accomplished by simply viewing

the point cloud or viewing an integrated display of the point cloud with associated imagery. Other applications may be best accomplished using software aids for automated or semi-automated extraction of features or dimensions. One of the exciting opportunities offered by laser scanning data is that multiple departments may be able to make use of the same data for quite different purposes. The data itself becomes a significant asset.

I. REFERENCES

Federal Geographic Data Committee (FGDC). (1998). *Geospatial positioning accuracy standards, Part 3: National standard for spatial data accuracy* (Document No. FGDC-STD-007.3-1998). Reston, VA: Federal Geographic Data Committee.

Johnson, S. D., Bethel, J. S., Supunyachotsakul, C., & Peterson, S. (2016). *Laser mobile mapping standards and applications in transportation* (Joint Transportation Research Program Publication No. FHWA/IN/JTRP-2016/01). West Lafayette, IN: Purdue University. http://dx.doi.org/10.5703/1288284316164

Williams, K., Olsen, M. J., Roe, G. V., & Glennie, C. (2013). Synthesis of transportation applications of mobile LiDAR. *Remote Sensing*, *5*(9), 4652–4692. http://dx.doi.org/10.3390/rs5094652

APPENDIX: ROOT MEAN SQUARE ERROR (RMSE) CALCULATION FOR REPRESENTING THE POSITIONAL ACCURACY OF A DATASET

This section illustrates the details of how the root mean square error (RMSE) is computed to represent the positional accuracy of the MMS dataset. The positional accuracy is evaluated by analyzing the coordinate discrepancies at validation checkpoints distributed throughout the point cloud.

Refer to the surveyed reference coordinates in Easting, Northing and Elevation of the i-th validation point as $(E_{Ref}, N_{Ref}, h_{Ref})_i$. and the observed coordinates of the same validation point obtained from the MMS dataset as $(E_{Det}, N_{Det}, h_{Det})_i$. Calculate the discrepancies in coordinates at each validation point. The coordinate discrepancy values are denoted dE_i, dN_i, and dh_i are the difference calculation shown in Equation A.1.

$$\begin{bmatrix} dE \\ dN \\ dh \end{bmatrix}_i = \begin{bmatrix} E_{Det} \\ N_{Det} \\ h_{Det} \end{bmatrix}_i - \begin{bmatrix} E_{Ref} \\ N_{Ref} \\ h_{Ref} \end{bmatrix}_i \quad (A.1)$$

For the i-th validation point the discrepancy, dP_i, in planimetric 2D position is calculated as shown in Equation A.2.

$$dP_i = \sqrt{dE_i^2 + dN_i^2} \quad (A.2)$$

For the i-th validation point the discrepancy, dQ_i, in 3D position is calculated as shown in Equation A.3.

$$dQ_i = \sqrt{dE_i^2 + dN_i^2 + dh_i^2} \quad (A.3)$$

Then the Root Mean Square Error in Easting, Northing, and Elevation of the MMS dataset can be computed using the coordinate discrepancy in of all n validation points as shown in Equations A.4, A.5 and A.6 respectively.

$$RMSE_E = \sqrt{\frac{\sum_{i=1}^{n} dE_i^2}{n}} \quad (A.4)$$

$$RMSE_N = \sqrt{\frac{\sum_{i=1}^{n} dN_i^2}{n}} \quad (A.5)$$

$$RMSE_h = \sqrt{\frac{\sum_{i=1}^{n} dh_i^2}{n}} \quad (A.6)$$

The Root Mean Square Error in planimetric 2D position can be computed from the Root Mean Square Error in the Easting and Northing coordinates as shown in Equation A.7.

$$RMSE_P = \sqrt{(RMSE_E)^2 + (RMSE_N)^2} \quad (A.7)$$

The Root Mean Square Error in 3D position can be computed from the Root Mean Square Error in Easting, Northing, and Elevation coordinates as shown in Equation A.8.

$$RMSE_Q = \sqrt{(RMSE_E)^2 + (RMSE_N)^2 + (RMSE_h)^2} \quad (A.8)$$

The RMSE computed values may be scaled to the 95% confidence range as shown below.

$$Error_{P-95} = RMSE_P \times 1.7308 \quad (A.9)$$

and

$$Error_{h-95} = RMSE_h \times 1.9600 \quad (A.10)$$

In general the accuracy of the dataset is separated into horizontal accuracy and vertical accuracy which are computed as RMSE values and then scaled to a 95% confidence range (see pages 10 and 11 in FGDC (1998)).

About the Joint Transportation Research Program (JTRP)

On March 11, 1937, the Indiana Legislature passed an act which authorized the Indiana State Highway Commission to cooperate with and assist Purdue University in developing the best methods of improving and maintaining the highways of the state and the respective counties thereof. That collaborative effort was called the Joint Highway Research Project (JHRP). In 1997 the collaborative venture was renamed as the Joint Transportation Research Program (JTRP) to reflect the state and national efforts to integrate the management and operation of various transportation modes.

The first studies of JHRP were concerned with Test Road No. 1—evaluation of the weathering characteristics of stabilized materials. After World War II, the JHRP program grew substantially and was regularly producing technical reports. Over 1,500 technical reports are now available, published as part of the JHRP and subsequently JTRP collaborative venture between Purdue University and what is now the Indiana Department of Transportation.

Free online access to all reports is provided through a unique collaboration between JTRP and Purdue Libraries. These are available at: http://docs.lib.purdue.edu/jtrp

Further information about JTRP and its current research program is available at: http://www.purdue.edu/jtrp

About This Report

An open access version of this publication is available online. This can be most easily located using the Digital Object Identifier (doi) listed below. Pre-2011 publications that include color illustrations are available online in color but are printed only in grayscale.

The recommended citation for this publication is:

Johnson, S. D., Bethel, J. S., Supunyachotsakul, C., & Peterson, S. (2016). *Laser mobile mapping standards and applications in transportation* (Joint Transportation Research Program Publication No. FHWA/IN/JTRP-2016/01). West Lafayette, IN: Purdue University. http://dx.doi.org/10.5703/1288284316164